ABSTRACT

Unique Fragmentation of Pentafluorobenzylic Alcohols and the Use of Modified Injection Port Liners in the Gas Chromatographic-based Screening for Catalytic Activity

Henry C. Fisher

Mentor: Charles M. Garner, Ph.D.

An unprecedented reaction, the base-catalyzed fragmentation of pentafluorobenzylic alcohols, was investigated. Studies on a variety of C_6F_5-derived alcohols show that a dual reaction pathway occurs in mixed solvent systems such as DMSO and methanol. ^{19}F NMR and GC-MS analyses have been used to examine the mechanism of the fragmentation. Other reaction variables, which involved changing the base and/or solvent conditions, have been studied to determine their effect on fragmentation. The relative rates of reactivity of a variety of pentafluorobenzylic alcohols were determined.

A new technique to screen potential metal catalysts rapidly via GC-MS using modified injection port liners has been developed. A variety of interesting reactions of organic molecules catalyzed by metal salts in the gas phase have been discovered. This technique has also been applied to the fragmentation reactions above.

The Unique Fragmentation of Pentaflurobenzylic Alcohols and the Use of Modified Injection Port Liners in the Gas Chromatographic-Based Screening for Catalytic Activity

by

Henry C. Fisher, B.A.

A Thesis

Approved by the Department of Chemistry and Biochemistry:

Marianna A. Busch, Ph.D., Chairperson

Submitted to the Graduate Faculty of
Baylor University in Partial Fulfillment of the
Requirements for the Degree
of
Master of Science

Approved by the Thesis Committee:

Charles M. Garner, Ph.D., Chairperson

Jesse W. Jones, Ph.D.

Kenneth W. Busch, Ph.D.

Charles A. Weaver III, Ph.D.

Accepted by the Graduate School
December 2005

J. Larry Lyon, Ph.D., Dean

TABLE OF CONTENTS

LIST OF FIGURES

LIST OF TABLES

LIST OF SCHEMES

ACKNOWLEDGMENTS

First and foremost, I want to thank Professor Charles Garner for taking a chance on me, and for giving me an opportunity to continue my studies in chemistry here at Baylor. I did not fully realize the joys and excitement of organic chemistry until I took his Advanced Organic Laboratory in my final semester as an undergrad, and I will be eternally grateful that he saw potential in me beyond all of my past academic hardships. I want to thank Dr. Garner for pressing me to present my research, even though I was always hesitant. Through these experiences I have grown more confident in myself. I want to especially thank him for his assistance in the tireless preparation of posters, presentations and this document, and for making my words more "efficient." Lastly, I want to thank him for being a wonderful and patient adviser and mentor these last two and half years.

I want to thank my family, specifically my mother and brothers for their emotional and financial support through all of these years in school. Although they did not necessarily understand what I studied, they were always encouraging. Thank you mom for all of your prayers and for your faith.

I want to thank my thesis committee members, Professors Kenneth Busch, Jesse Jones, and Charles Weaver for donating their time to review my work and for being flexible. I have to acknowledge Dr. Jones for he put off a state congressional committee meeting for my defense.

I want to acknowledge Professor Carlos Manzanares for allowing me to join this graduate program, and for giving me that first and very crucial year to prove myself.

I want to thank Dr. Jim Karban for taking his time out whenever I had an NMR question, and for teaching me some neat tricks on the Varian 500 MHz NMR even though I never got a chance to use that instrument in my research. I also want to thank Dr. Kevin Klausmeyer for acquiring my X-ray structure.

To the "backbone" of this department, Nancy Kallus, Adonna Cook, and Barbara Rauls, thank you all for your assistance and support over the years. I want to thank Nancy for always patiently listening to every concern I had, whether it be with coursework or other matters. Barbara, I have sincerely enjoyed our conversations over the last couple of years. You cannot imagine how many times I left your office feeling uplifted after a bad day.

To the Garner Group of the past whose ranks I soon join: Kimberly Brien, Dr. Keith Monk, and Lacy Coker. They were the ones who greeted me with open arms into the Garner Group and I thank all of them for showing me the ropes in the lab. I want to thank Kim for being a "kindred spirit" in the department for the first year and a half. It was uncanny how many of our academic experiences overlapped, and it was nice to know someone else went through many of the same frustrations. We also had the honor of being the first two Garner Group members who had the priviledge of moving into our new digs in the Baylor Sciences Building. Was that not loads of fun or what? I want to thank Keith for setting the bar high in regards to work ethic. Although it was his last year in the department, I wanted to work just as hard as he did on research. I have to acknowledge Lacy Coker for being the best and most bubbly lab mate anyone could ask for. Her presence, whether in lab or in meetings was enough to "get excited!" about chemistry. She also really set a high standard for all of the undergraduate researchers

who followed her. I have to thank Kem Amadi for all of her assistance on the GC liner project, and for her agreeable and patient spirit throughout the process.

To the Garner Group of the present: Nathan Duncan, Tiffany Turner, and Sheree Allen. It has been a pleasure getting to know all of you this past semester. You are all so talented and will take this research group to new depths. I pass the baton onto you guys.

To my friends or I should say “my family”: Jody Harvey, Chris Davis, Tricia Diamond, Jason Dee, Vanessa Castleberry, and most recent additions Tiffany Turner and Sheree Allen. I cannot imagine making it through this program without you all. Each of you have uplifted me and enriched my life in so many ways. You truly are and will always be my Baylor family. To the friends in the department that I have not specifically mentioned, I want to thank you all for your kind words of encouragement and support over the years.

Finally, I want to thank all of the professors who have expanded my knowledge and who have challenged me to be a better researcher and student. I have to thank Baylor University for all of the financial support, as well as the Welch Foundation whose grant supported both my research and me for the last year or so. This experience has truly been one of great challenges and rewards. I came into this program two and a half years ago in broken spirits and very unsure of what I could accomplish. Now, I am can say that I leave sure of the path before me, and knowing that I did the best that I could to accomplish my goals here at Baylor.

CHAPTER ONE

Base-Catalyzed Carbon-Carbon Bond Cleaving Reactions and Rapid Screening of Potential Metal Catalysts

Introduction

Carbon-carbon (C-C) bonds are relatively strong (~ 78.5-90 kcal/mol) and mechanisms by which such bonds can be broken are limited.[1] For double and triple carbon-carbon bonds, energies may be as high as ~ 150 kcal/mol and 200 kcal/mol, respectively.[2] This accounts in part for the incredible variety of organic molecules that are not only possible but also stable. Reactions that result in cleavage (fragmentation) of C-C bonds under basic conditions are quite rare, especially under circumstances where a carbon acts as an anionic (negatively charged) leaving group. A major portion of this chapter will focus on fragmentation reactions involving stabilized carbanions that can be specifically categorized under what are known as heterolytic carbon-carbon bond cleavages.[2]

While the first part of this thesis will focus on base-catalyzed heterolytic C-C bond cleavages, the second part will be a study of a new technique for rapidly screening potential catalysts using gas chromatography (GC). Metal catalysis is poorly enough understood that catalysts are discovered at least as often as they are designed. Therefore, a rapid method for evaluating these materials is necessary. The second part of this chapter will describe the foundations for our rapid screening technique.

Background

Many carbon-carbon bond cleavages are facilitated by the "increasing stability of the carbanion leaving group."[3] Carbanions can be stabilized if surrounded by electron-withdrawing groups or atoms, such as the halogens. One such reaction is the *haloform reaction*, where trihalogenated methyl ketones may be cleaved under basic conditions. For example, 2,2,2-trichloro-1-arylethanones (**1**) may undergo C-C bond cleavage in mildly acidic to highly basic aqueous solution *via* corresponding tetrahedral intermediate (**2**) and exhibit first-order rate laws (Scheme 1.1).[4] The trichloromethyl anion (**3**) is stabilized by the three electronegative chlorines surrounding the carbon. The conjugate acid, chloroform, has a pK_a value in H_2O of 13.6, is indicating the stability of this anion.[5]

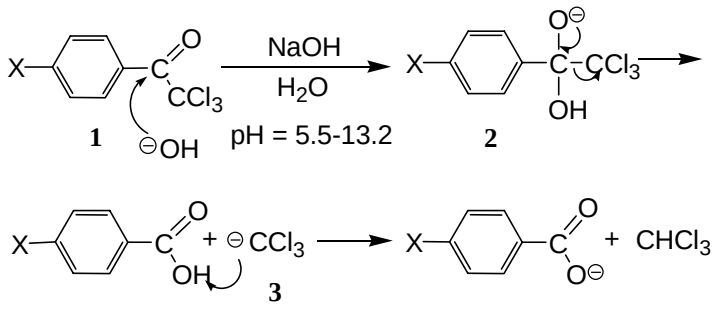

Where X = H, OMe, or Cl

Scheme 1.1. Haloform reaction of 2, 2, 2-trichloro-1-arylethanones.

Electon-attracting aryl substituents stabilize carbanion formation, especially if alkyl groups surrounding a quaternary carbon are attached to electron-withdrawing groups such as an ester or nitro group. In the study of unsubstituted and *para*-substituted benzoates of 3-dimethylamino-2,2-*bis*(*p*-nitrophenyl)propanol (**4a-d**), reversible decomposition occurs in ethanol to form 1,1-*bis*(*p*-nitrophenyl)ethylene (**7**) via a carbanion intermediate (**6**) and the iminium ion (**5**) (Scheme 1.2). It should be noted that this reaction does not occur if the phenyl groups lack electron-withdrawing nitro groups.[6]

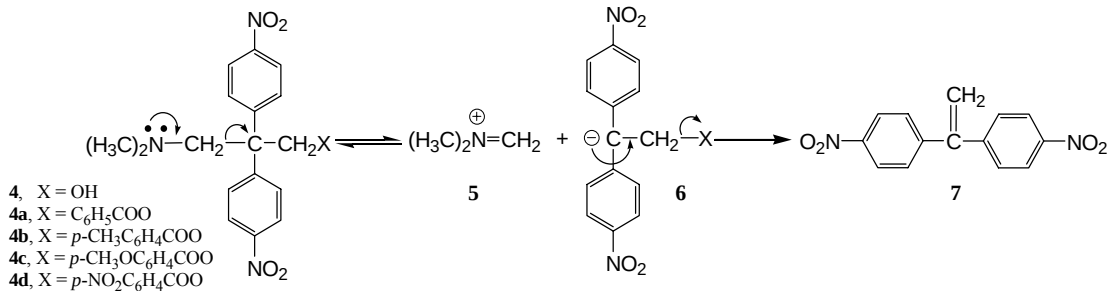

Scheme. 1.2. Reversible carbanion formation of benzoate derivatives of 3-dimethylamino-2,2-*bis*(*p*-nitrophenyl)propanol (**4**).[6]

An explanation of increased propensity to form a carbanion due to the addition of nitro groups can be explained in the comparison of acidities between diphenylmethane and *bis*(*para*-nitrophenyl)methane (compounds that are comparable to species **6** in Scheme 1.2) with pKa values (DMSO) of 32.3 and 15.2, respectively.[7, 8] The addition of nitro groups onto the phenyl ring drastically increases acidity, suggesting ease of carbanion formation through deprotonation is most probable.

Alkyl nitriles (R-CN) are an important source of C-C bond cleavages, especially in regards to forming stable carbanion leaving groups. A variety of secondary nitriles, for example, may undergo oxidative decyanation to ketones, during which cyanide is a leaving group. Many secondary nitrile derivatives were studied, and compounds with at least one aryl group directly attached to the α-carbon (a carbon adjacent to an electrophilic sight in a molecule) produced higher isolated yield ketone than derivatives without. In a specific example, 2-(4-fluorophenyl)propionitrile (**8**) was deprotonated with lithium diisopropylamide to form the carbanion (**9**) (Scheme 1.3). This intermediate species was than "trapped" with gaseous oxygen at -78° C to form the peroxy intermediate (**10**). Hydroperoxynitrile (**11a**) or acetoperoxynitrile (**11b**) were formed when intermediate (**10**) was treated with either aqueous acid or acetyl chloride, respectively, and these compounds were readily reduced to the cyanohydrin (**12**) on

treatment with stannous chloride solution. Reaction of the cyanohydrin with aqueous sodium hydroxide resulted in the formation of ketone product (**13**).

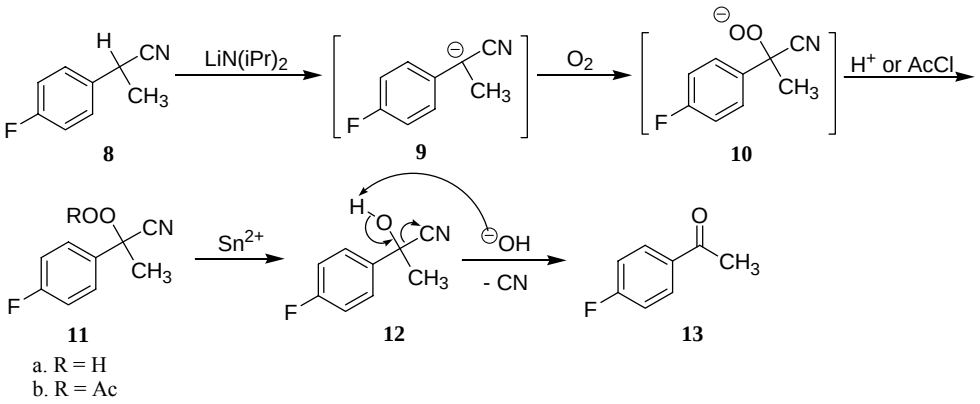

Scheme 1.3. Oxidative decyanation of secondary alkyl nitriles.[9]

Reductive decyanation of α-amino nitriles occurs readily using borane under mild conditions to give a good yield of amine product (Scheme 1.4). In this process, the nitrile group is stabilized to leave by forming a complex with borane, and an iminium intermediate (**15**) is formed. The cyanoborohydride ion supplies a hydride to the iminium

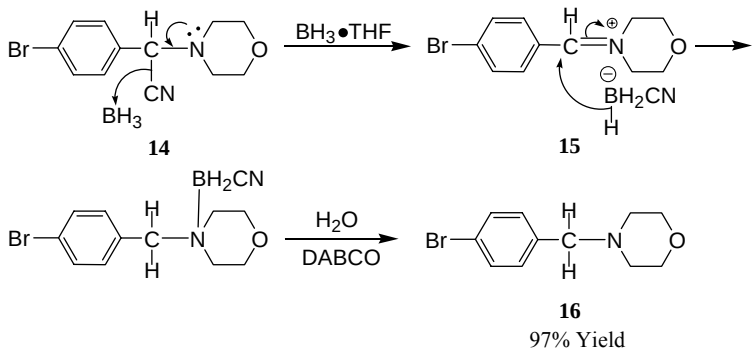

Scheme 1.4. Reductive decyanation of α-amino nitriles.[10]

carbon, forming the amine product (**16**). Several equivalents of 1, 4-diazabicyclo-[2.2.2]octane (DABCO) were used as a decomposing agent, effectively removing borane from the amine product.[10]

Non-enolizable ketones may cleave their α-carbon-carbon bonds under basic conditions using sodium amide in liquid ammonia in what is known as the *Haller-Bauer* reaction.[11] In one example, (2-fluorophenyl)-phenylmethanone (**17**) cleaves rapidly to form fluorobenzene (**19**) and benzamide (**18**) (Scheme 1.5).

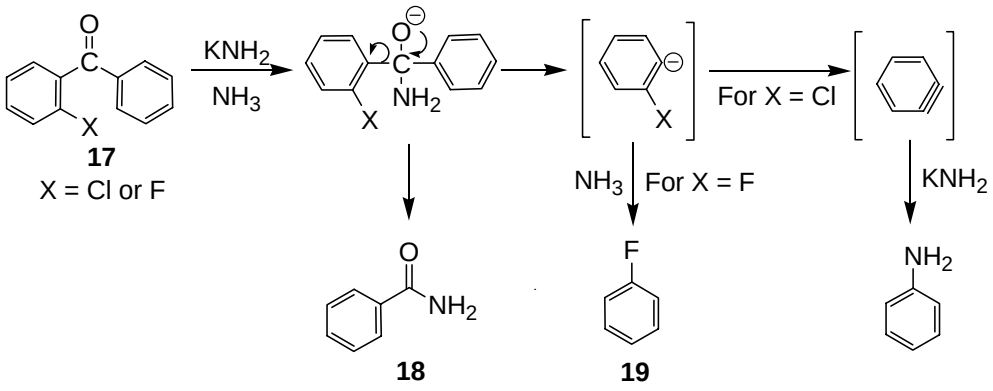

Scheme 1.5. *Haller-Bauer Reaction* of 2-(halophenyl)-phenylmethanones. The fluorinated compound reacted through a different pathway.[11]

This reaction did not proceed using pure benzophenone, nor did it proceed with *meta*- or *para*-chlorinated benzophenones.[11] Note that none of the chlorinated benzophenone derivatives examined showed any formation of halobenzene, as observed with the *ortho*-fluorobenzophenone. Also, aniline was a prevalent product in several of the studies, suggesting a benzyne mechanism was involved. Halogens, especially fluorine, on the *ortho* position relative to the ketone, add to the stabilization of the phenyl carbanion due to an inductive effect.

Reverse (retrograde or "retro-") condensation reactions, such as those related to the aldol, Claisen, or Michael reactions are also examples of carbon-carbon bonds cleaved through carbanion intermediates. Aldol products may revert to the original carbonyl compounds under base catalysis (Scheme 1.6). In this particular example,

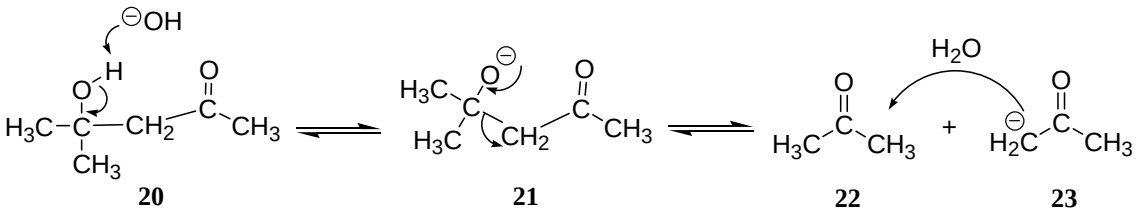

Scheme 1.6. Retro-aldol reaction of 4-hydroxy-4-methyl-2-pentanone.[1]

the starting aldol compound (**20**) derived from two molecules of acetone (**22**) reverts back easily. Aldols prepared from ketones are especially susceptible to retro-aldol reactions. In fact, the aldol condensation is unfavorable in these cases unless the reaction is driven by dehydration of the product. The remaining enolate (**23**) hydrolyzes quickly in aqueous solution.[1]

Another classic example of carbon-carbon cleavage is the retro-Claisen condensation. Under the same conditions as the forward Claisen reaction, it is possible to revert to starting materials (Scheme 1.7). Sodium ethoxide attacks the ketone carbonyl of

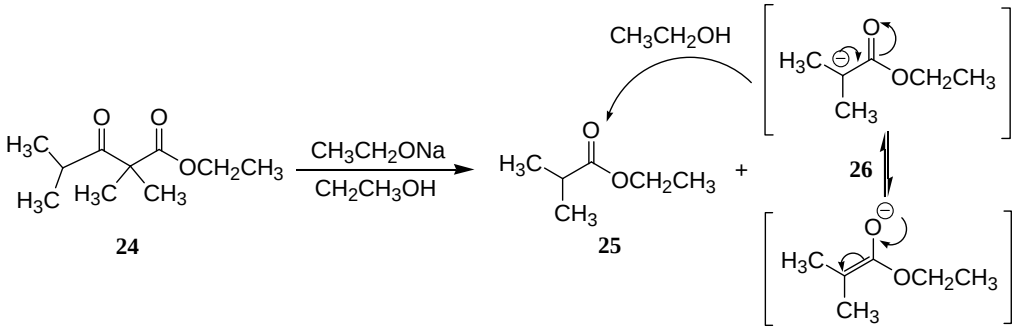

Scheme 1.7. An example of a retro-Claisen Condensation.[1]

a β-keto ester (**24**), and this can catalyze a carbon-carbon cleavage to form a molecule of ethyl isobutyrate (**25**) and its enolate (**26**). However, for the reaction to be reversible there must be a lack of hydrogens on the α-carbon between the two carbonyl groups of

the β-keto ester (**24**). Otherwise, this relatively acidic proton (pK_a ~10) is simply removed with no further reaction occurring.

Similarly, the Michael reaction may also undergo reversal under catalytic base conditions (Scheme 1.8). In the forward Michael reaction, benzylacetone (**27**) and nitrostilbene (**28**) react at or below ambient temperature to form 5-nitro-3,4,5-triphenyl-pentan-2-one (**29**). This product may undergo reversal when treated with more base and heated.[12] Unlike the examples given for the retro-aldol and Claisen reactions, products from retro-Michael reaction or other retro-type reactions do not always revert to the original starting reagents. Under these conditions, the nitro-triphenylketone (**28**) expels a nitro-stabilized carbanion, whose conjugate acid has a pKa of 12.2 (DMSO).[13] This intermediate was protonated by water leading to compound (**30**). A comparison of group electronegativities between a nitro and methyl keto-carbonyl group (4.08 and 2.93, respectively) show that a negative charge would be better stabilized by the more electronegative nitro group.[14]

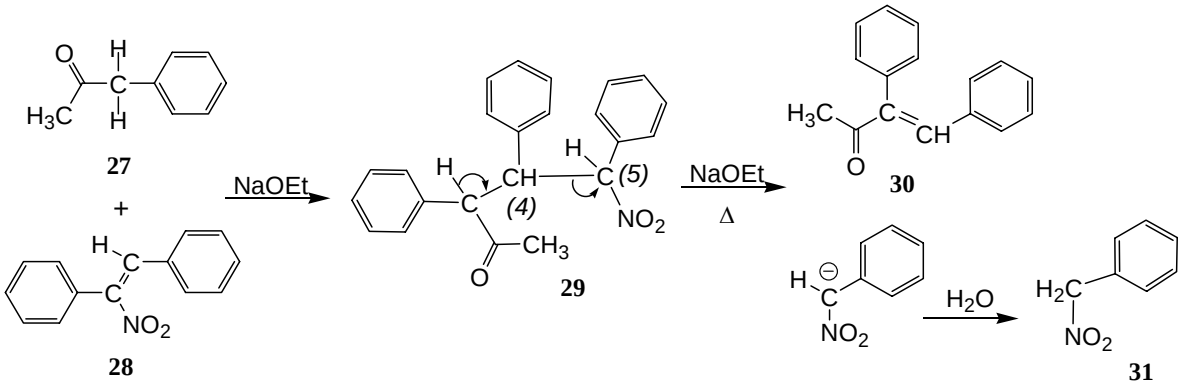

Scheme 1.8. An example of a retro-Michael reaction.[12]

The addition of certain Grignard and organolithium reagents to ketones is also known to be reversible. Benkeser and associates have studied this phenomenon on a

variety of sterically hindered allylic alcohols. The corresponding alkoxides (**33**) were generated by treating the allylic alcohol (**32**) with *n*-butyllithium or methylmagnesium bromide (Scheme 1.9).[15] The magnesium alkoxides were allowed to react at room

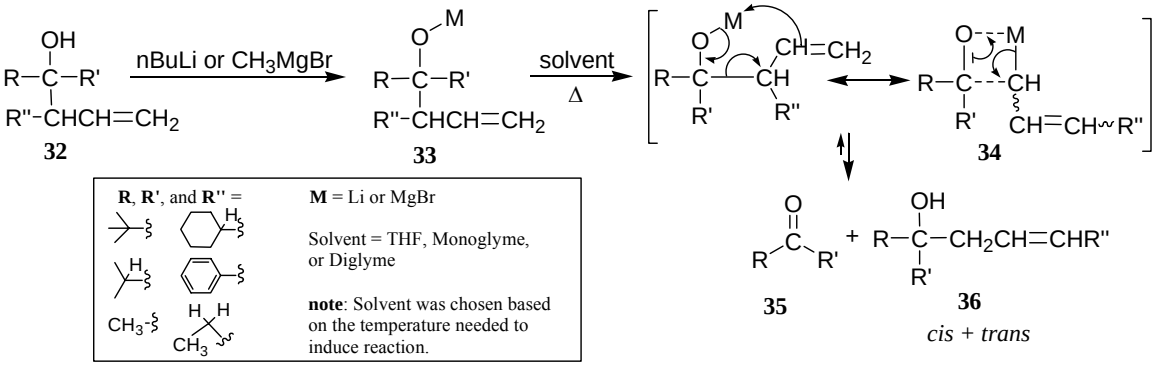

Scheme 1.9. Reversible Grignard and organolithium reaction. [15]

temperature in tetrahydrofuran (THF), and generally formed high yields of carbinols (**36**) as a mixture of *cis* and *trans* isomers. Small amounts of ketone (**35**) were also formed. This ketone formation depended on whether alkyl groups (**R** and **R'**), such as ethyl, isopropyl, and cyclohexyl, attached had enolizable hydrogens on their α-carbons. Derviatives of lithium alkoxides were studied more extensively and required higher temperatures (25 ºC to 162 ºC) in various solvents determined by the temperature needed to complete the reaction. Ultimately, the formation of "reversal" products (**36**) may be attributed to a four-center transition state (**34**), where a concerted movement of electrons temporarily forms a ketone fragment and a metalated allyl fragment (a carbanion). The allylic carbanion may re-attack the keto-carbonyl at either end of the allyl system, not only reforming a new alkoxide but also forming a new secondary carbon attachment. Again, substantial ketone product formation (**35**) may be possible if the ketone tends to enolize.

The decarboxylation of carboxylic acid derivatives is another commontype of carbon-carbon cleavage that should be noted, although a carbanion mechanism is not always directly involved. The decarboxylation of benzisoxazole-3-carboxylic acids have been studied extensively by Kemp, et. al. (Scheme 1.10).[16,17,18] The 3-carboxybenzioxole

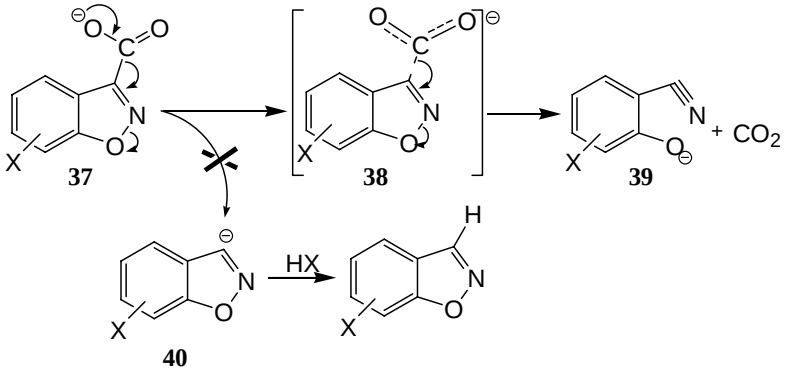

Scheme 1.10. The decarboxylation of benzisoxazole-3-carboxylic acids.[16,17,18]

(**37**) may undergo decarboxylation when treated with tetramethylguanidine or tetrabutylammonium acetate to form the salicylonitrile product (**39**). The mechanism by which the carboxyl group group cleaves is concerted, simultaneously cleaving both a carbon-carbon bond and a nitrogen-oxygen bond (**38**). Experiments to prove a carbanion pathway were not conclusive, and attempts to "trap" the carbanion (**40**) at low pH were not successful. The rate of decarboxylation was highly solvent dependent, where polar aprotic solvents (DMSO, DMF) tended to give accelerated reactions relative to reactions in polar protic (water, MeOH) or non-polar solvents (CCl_4, C_6H_6).

Decarboxylation, however, may produce stable carbanions as observed with nitro-substituted arylmethyl carboxylate salts in aprotic media (THF, DME, DMSO). Using UV-vis spectroscopy to observe relative decay of absorption spectra with time, relative stabilities of 2,4,6-trinitrobenzyl (**42**), 2,4-dinitrobenzyl (**44**), and 4-nitrobenzyl (**46**)

carbanions were determined (Scheme 1.11).[19] As expected, the trinitrobenzyl anion is the most stable relative to the dinitrobenzyl and the *p*-nitrobenzyl anions due to the ability of *ortho* and *para* nitro groups to stabilize a carbanion. As depicted in the scheme below, every carbon on the trinitrobenzyl anion (**42**) where a negative charge can resonate is supported by an electron withdrawing group, thus stabilizing that negative charge. The respective pKa values of 2,4,6-trinitrotoluene (pKa =10.5, DMSO); 2,4-dinitrotoluene (pKa = 23, H_2O:DMSO); and 4-nitrotoluene (pKa = 42, H_2O:DMSO) confirms that with greater acidity comes a greater affinity to deprotonate and form a stabilized carbanion.[20] It should be noted that 18-crown-6 ether (**47**) was used as a catalyst where THF was the solvent. The crown ether dramatically accelerated this reaction; approximately one equivalent increased the rate of decarboxylation by a factor of 13- to 500.[19]

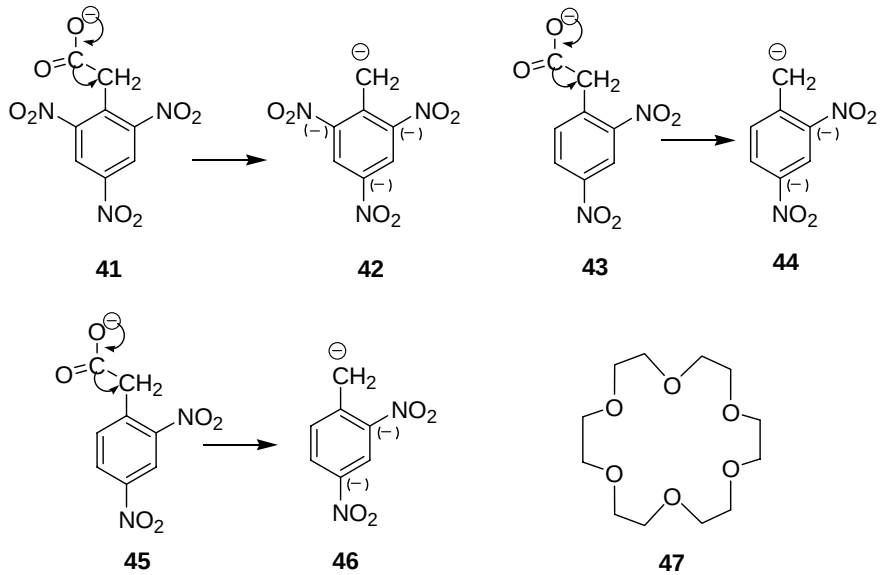

Scheme 1.11. Decarboxylation of several nitrophenyl acetates.[19]

Decarboxylations may be exploited for an efficient one-step synthesis of a variety of β-keto esters (Scheme 1.12).[21] The formation of dicarbonyl-stabilized anions are good leaving groups for carbon-carbon bond cleavage. For example, monoethyl malonate (**48**)

treated with two equivalents of n-butyllithium forms a dilithio dianion species, in which the α-carbanion can readily react with an acid chloride to form the intermediate species (**49**). A concomintant loss of carbon dioxide is followed by a formation of an α-keto ester enolate, which in turn is protonated to form the ketoester product (**50**). Keto-ester conjugate acids such as compound **50** have an estimated pKa value of 11.[22]

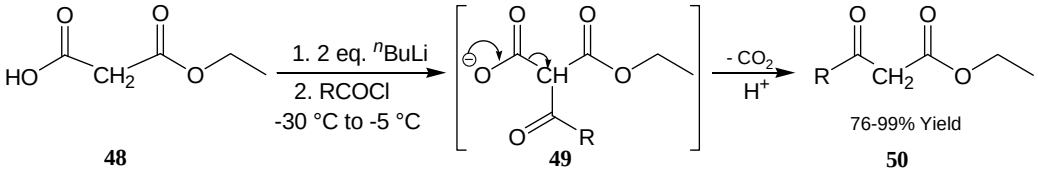

Scheme 1.12. One-step synthesis of β-keto esters from monoethyl malonate.[21]

An important source of potential carbon-carbon bond cleaving reactions can be attributed to the rearrangement of electrons in alkoxides, which are formed from alcohols under strongly basic conditions. Again, whether C-C bond cleavages occur is determined by the "environment" around the carbon of attack. Aryl alkynyl alcohols, for example, represent a group of alcohols that are susceptible to carbon-carbon bond cleavage.

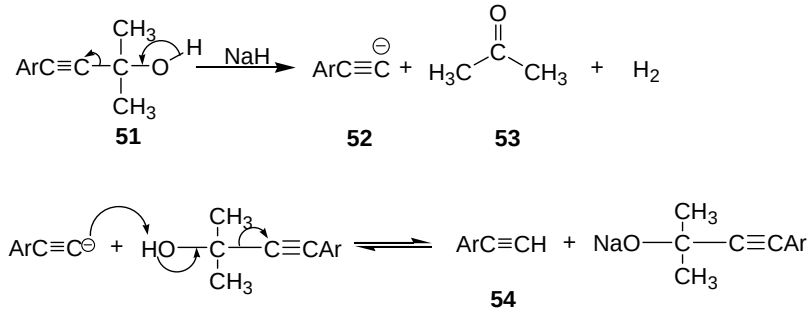

Scheme 1.13. Formation of arylacetylenes from arylacetylenic alcohols.[23]

Arylacetylenes may be prepared in an efficient two-step process, where in the first step the derived acetylenic alcohol (**51**) may be cleaved by sodium hydride to form the

acetylenic carbanion (**52**), 2-propanone (**53**), and hydrogen gas. The desired acetylene product (**54**) forms in the second step when it is protonated by additional alcohol in the reaction (Scheme 1.13.).[23] Formation of an acetylenic carbanion may be rationalized by comparing the pKa values of phenyl acetylene and acetylene, which are 18.5 and 25 (H_2O), respectively.[22]

The formation of carbanions is not always the result of direct cleavage of a C-C bond, as shown by the previous examples. Base-induced formations of carbanions on one part of a molecule may induce C-C bond cleavage in other parts if the conditions are optimal. For instance, *trans*-8-bromocamphor hydrazones (**56**), prepared from trans-π-bromocamphor (**55**) and hydrazine, can fragment to limonene (**59**) under Wolff-Kishner reduction conditions (Scheme 1.14).[24]

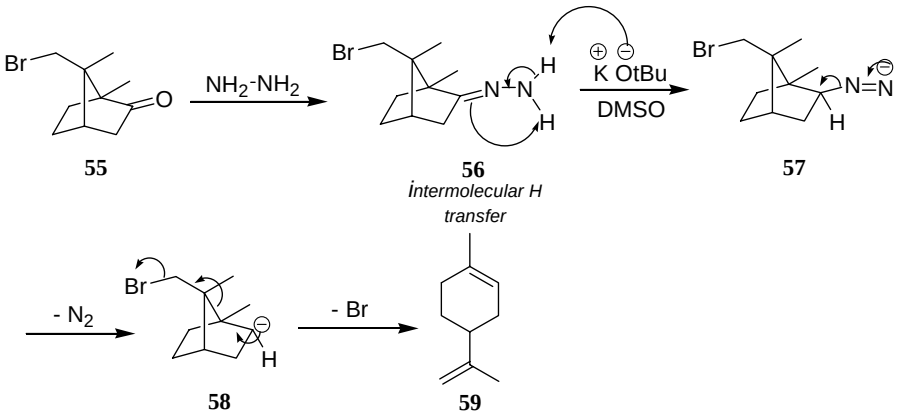

Scheme 1.14. Fragmentation of trans-π-bromocamphor (**55**) to limonene (**59**).[24]

Cyclic ylides have been reported to fragment via a C-C bond breaking mechanism. When five-membered cyclic 1,1-dimethylpyrrolidinium (**60**) and 1-methyltetrahydro-thiophenium (**64**) are treated with phenyllithium, the ylides (**61**) and (**65**), respectively, are formed (Scheme 1.15). Rearrangement of the negative charge

under electrophilic conditions caused fragmentation in both molecules to form ethylene (**62**) and either the dimethylvinylamine (**63**) or the methylvinylsulfide (**66**).[25, 26]

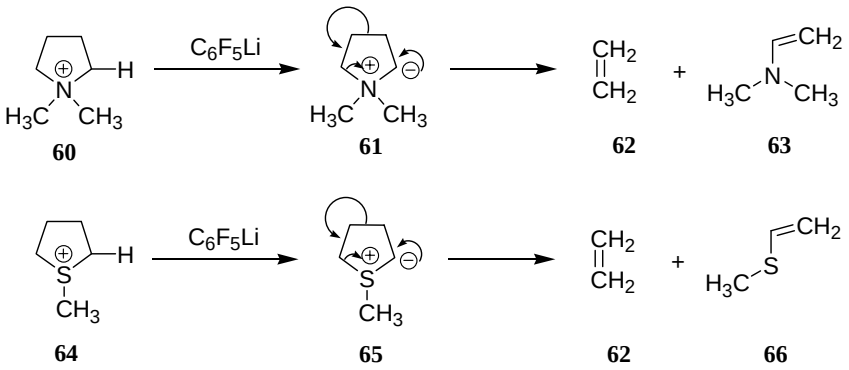

Scheme 1.15. Fragmentation of cyclic ammonium (**61**) and sulfonium (**64**) ylides upon treatment with phenyllithium.[25, 26]

Keto-imines, when tosyl-substituted on the nitrogen, undergos base catalyzed fragmentation to form unsaturated keto nitriles (Scheme 1.16). This occurs when compound **67** is treated with potassium *tert*-butoxide. The α-proton (pKa ~ 28, DMSO) is removed by the base and a carbanion is formed. A cascade flow of electrons effectively breaks the C-C bond between the imine carbon and adjacent tertiary carbon forming the nitrile moiety (**69**).[27]

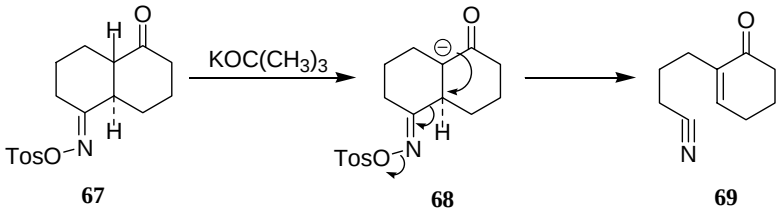

Scheme 1.16. Fragmentation of a keto-imine compound (**67**) to a nitrile (**69**).[27]

Molecules with strained ring systems are more prone to cleave C-C bonds even if there is an unstabilized leaving group. For example, fenchone (**70**) may be treated with sodium amide in toluene and refluxed at 80° C for about 16 hours to form the ring-

opened "fencholyl amide" (**71**) (Scheme 1.17).[28] This reaction can occur when the nucleophilic amide attacks the carbonyl, forming a tetrahedral intermediate with negatively charged oxygen. The carbonyl reforms by cleaving the adjacent C-C bond to to form a tertiary carbanion, a very poor leaving group.

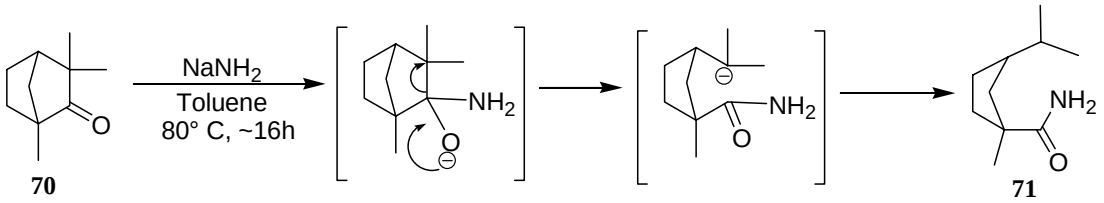

70 **71**

Scheme 1.17. C-C bond cleavage during the formation of fencholyl amide (**71**).[28]

Unstabilized carbanion leaving groups have also been observed at high temperatures. Camphor (**72**), for instance, may be reacted with neat potassium hydroxide pellets at 250-300° C to induce a C-C bond cleavage (Scheme 1.18).[28] The camphor

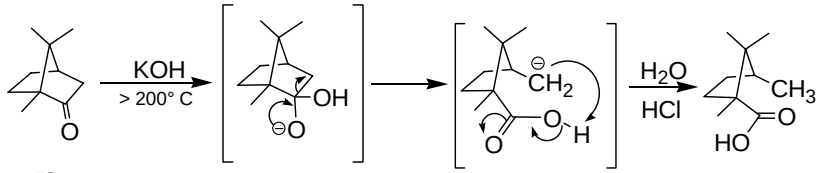

72 **73**

Scheme 1.18. Camphor (**72**) treated with potassium hydroxide and high temperature can cleave a C-C bond to form campholic acid (**73**).

carbonyl is attacked by hydroxide to form a tetrahedral intermediate, and reformation of the carbonyl group occurs with formation of a primary carbanion. This highly unstable and basic carbanion is protonated by the carboxylic acid, and campholic acid (**73**) is formed upon treatment with acid.

Molecules in sterically strained environments have tendencies to break C-C bonds under certain conditions. Tri-*tert*-butyl carbinol (**74**), a sterically hindered molecule, was fragmented using potassium dimsylate (**75**) at 25° C (Scheme 1.19). Although not

proven at the time, release of a *tert*-butyl carbanion was suggested as the most probable route of reactivity with di-*tert*-butyl ketone (**77**), and isobutane (**78**) recovered from the completed reaction.[29]

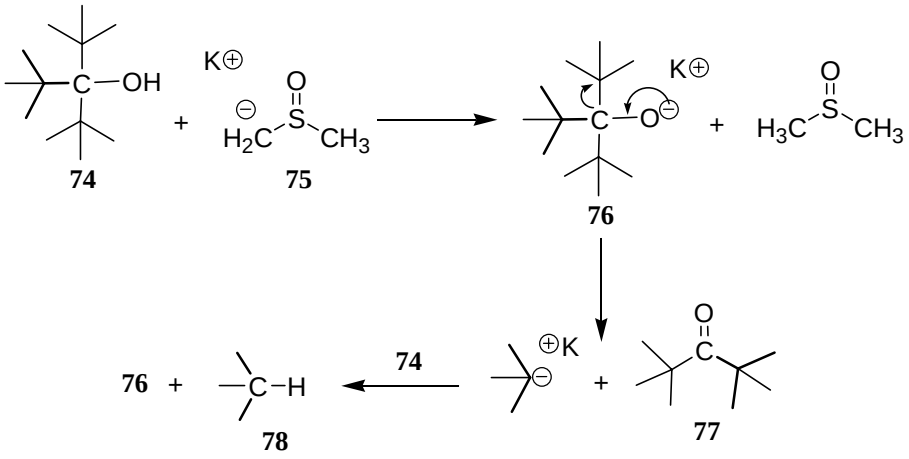

Scheme 1.19. Fragmenation of tri-*tert*-butyl carbinol (**74**) using potassium dimsylate (**75**).[29]

The influence of the positive metal counterion, such as lithium, sodium, potassium, or even magnesium halide may effect the stabilization of a carbanion.[30] Zook, March, and Smith studied cation effect on the "ease of cleavage" for potassium, sodium, and lithium alkoxides of 3-isopropyl-2,4,4-trimethyl-3-pentanol (**79**). Cleavage of the alkoxides were initiated by heating and each alkoxide cleaved at varying temperature ranges (Figure 1.1).[31] The potassium alkoxide cleaved between a temperature range of 160 to 182° C to form ketones **80** and **81** in a 95% total yield with no presence of alcohol. Cleavage of the sodium alkoxide occurred at a temperature range of 199 to 215° C with slightly less formation of ketones **80** and **81** and a small amount of alcohol (**79**) remained. The lithium alkoxide differed drastically over the other two alkali studied, where marginal amounts of ketone product formed even at a temperature range of 213 to 320° C.[31] The authors concluded that the nature of bonds between ions become more covalent

and less ionic as electronegativity increases, which would explain the lack of reactivity for the lithium alkoxide in comparison to the others. Stability of alkoxides was evident in decreasing order by alkali metal, where Li > Na > K.[31] Conductivity of lithium, sodium, potassium and cesium salts of dimethylsulfoxide (dimsyl anions) confirm the results gathered by Zook, et. al., where basicity of corresponding alkoxides after titration with *tert*-butanol increased by the order Li < Na< K < Cs.[32]

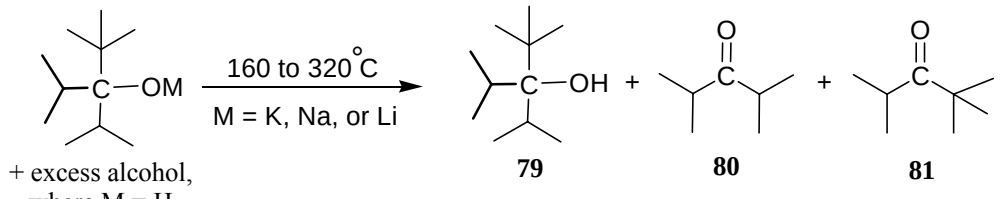

79 **80** **81**

mole % of product formation

K:	0	60	35
Na:	7	52	32
Li:	24	35	25

Figure 1.1. Comparison of alkoxide cleavage based on cationic interations.[31]

The choice of solvent can play an active role in the enhancement of anionic C-C bond cleavages, especially if the solvent can increase overall basicity and when the target molecule is strained enough to cleave. A study was conducted on several derivatives of highly strained tri-alkyl carbinols synthesized with different combinations of *tert*-butyl, 1-bicyclo[2.2.2]octyl, 1-norbornyl, and 1-adamantyl groups; the last three alkyl groups being multicyclic and also bulky (Scheme 1.20). Compounds **82**, **83**, **84**, and **85** were all reported to be stable to deprotonation with lithium dimsylate (Li^+DMSO^-), a highly basic nucleophile. The conjugate alkoxides, however, formed when the trialkylcarbinols were treated with n-butyllithium and fragmented upon addition of hexamethylphosphotriamide (HMPT).[33] Surprisingly, more than one type of fragmentation occurred with some of the

carbinols studied. For compound **82**, isobutane was reported to have formed in a 97.4% yield. Compound **84**, functionalized with all three types of bridgehead alkyl groups, formed a mixture of three alkanes. Percent yields of the alkanes were 38.3, 50.2, and 11.5% for adamantane, bicycle[2.2.2]octane, and norbornane, respectively.[33]

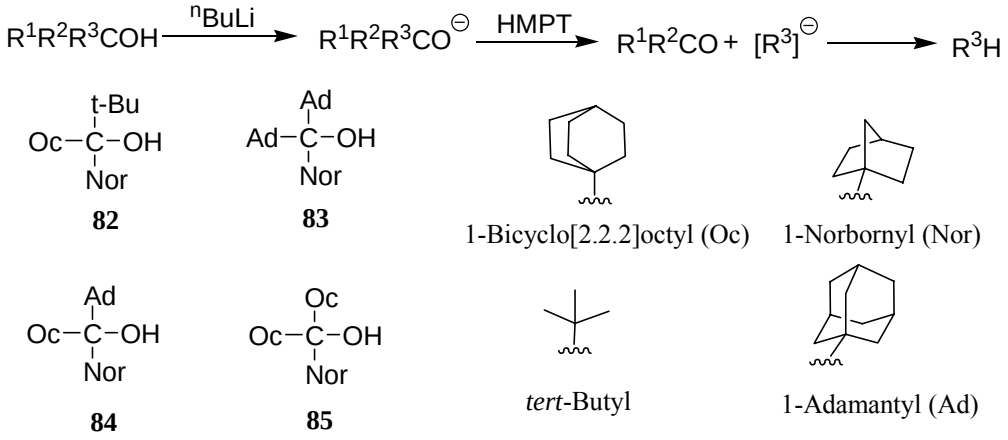

Scheme 1.20. Solvent-dependent fragmentation study of varying trialkyl carbinols.[33]

To summarize, several types of conditions promote the heterolytic fragmentation of C-C bonds, generally forming stabilized carbanions as intermediates. Only certain kinds of molecules with certain kinds of stabilized anionic leaving groups undergo C-C cleavage reactions. Strong bases, such as hydroxides, alkoxides, amide salts, hydrides, organolithium and Grignard reagents are always the initiators of anionic fragmentation reactions. Molecules undergoing fragmentation in most of the examples presented have slightly acidic hydrogens, which is usually enhanced by adjacent electrophilic sites on or adjacent to the point of attack. If these groups are not directly attacked by a base, then they are efficiently electron-withdrawing to activate other parts of the molecule (i.e. α-methylene or methine carbon next to a carbonyl). The fragmentation of the ammonium and sulfonium ylides are an exception to many of the examples presented thus far, since

the positive nitrogen and sulfur give neutral leaving groups (Scheme 1.15). In nearly all of the examples presented, the carbon leaving groups have been stabilized by the attached substituents (excluding the trialkyl carbinols in Scheme 1.18 and any bicyclic example where internal cleavage occurs). Substituents such as electronegative halogens, nitro and aromatic groups readily pull electron density away from a carbon center. This, in essence, allows stabilized carbanion formation. The cyanide ion is a useful leaving group under the right conditions. Its conjugate acid, hydrogen cyanide (HCN) has a pKa value of 9.1(H_2O), which indicates that the formation of its anion readily occurs in basic solution.[22] Alkynyl groups fragment under basic conditions, but resulting carbanion formations are only stable if they are tethered by an aryl or electron-withdrawing group (see Scheme 1.13). The steric hindrance of alkyl groups surrounding an alkoxide greatly influences whether fragmentation occurs, since a release in strain energy between large groups (i.e. adjacent *tert*-butyl groups) is favorable. Finally, choice of solvent can play a major role in promoting C-C bond fragmentation by enhancing the basicity of the environment around the molecule of attack and further stabilizing the carbanion leaving group.

Fragmentation of Pentafluorobenzylic Alcohols: An Overview
Gellation of Organic Liquids and Incidental Observation of Fragmentation Behavior

Garner, et al., (1998) reported that a variety of non-polar organic liquids can be reversibly immobilized using of 4-*tert*-butyl-1-arylcyclohexanol derivatives. Several derivatives were synthesized by modifying the aryl functionality, but only the phenyl (**86**) and fluorinated aryl derivatives (**87** and **88**) were active organogelators. Also, positioning of the substituents is important; the aryl group must be in the 1-axial position (*trans* diastereomer) and the *tert*-butyl substituent in the 4-position of the cyclohexane ring.[34]

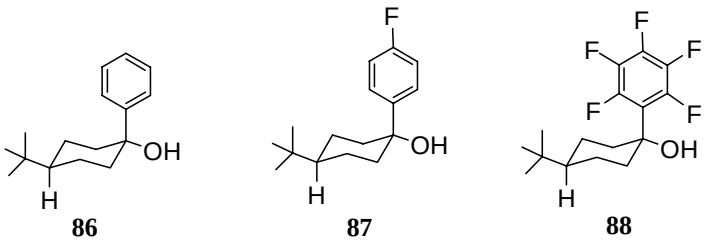

86 **87** **88**

Figure 1.2: Three derivatives of *trans*-4-*tert*-butyl-1arylcyclohexanol: Active gelators of organic solvents. [34]

A study comparing gel melting points relative to the weight percent of gelling agent present in a variety of organic solvents (i.e. heptane, toluene, dichloromethane, ethyl acetate, and ether) clearly showed that solvent polarity and concentration of the gelling agent strictly determine the melting point of a gel (Figure 1.3). Heptane, the most non-polar solvent in this study, required only 0.7 wt. % of gelling agent (**86**) to be immobilized at room temperature.[34]

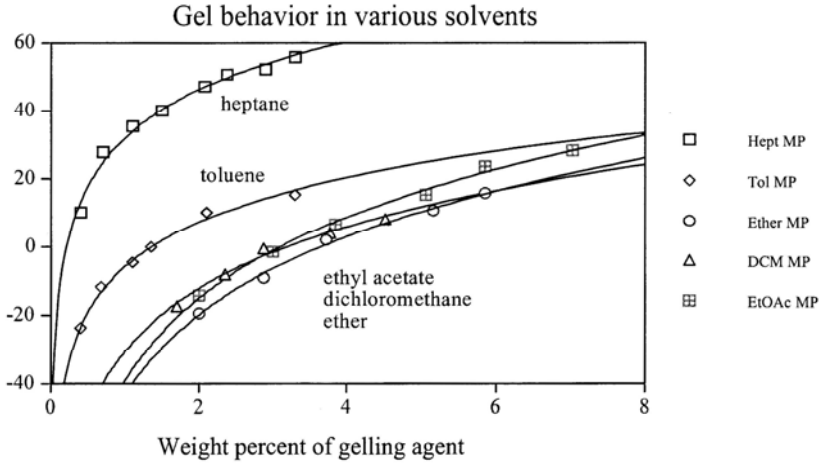

Figure 1.3. A chart comparing the melting point versus concentration of gelling agent (**86**) on a variety of solvents of differing polarities.

One possible application of these materials would be the gellation of perfluorinated solvents. Perfluorinated solvents are immiscible in both organic solvents and water unless heated or put under extreme pressure. The development of new

applications using biphasic solvent systems is promising, especially in catalysis chemistry where conservation of expensive reagents is an issue. The main drawback of these solvents is that they have a higher density than most common organic solvents that is, they form a layer below the organic. Also, reagents used in the fluorous phase have to be modified to be soluble, usually involving ultrafluorinating a molecule or the addition of large fluorinated alkyl chain "tags." This, unfortunately, can destroy the functionality of the reagent, and render the technique useless. The gellation of fluorinated solvents is a desirable goal that has been accomplished only recently.

In the gelling studies involving a fluorous solvent such as perfluoromethyl-cyclohexane (PFMC), all three gelling agents (**86-88**) were of very low solubility even in hot PFMC. However, *trans*-4-tert-butyl-1-(pentafluorophenyl)cyclohexanol (**88**), being partly fluorinated, was considered the most compatible. Using C_6F_5 gelling agent (**88**), PFMC *could* be gelled at very low concentrations (~0.1 wt.%) of gelling agent, but only transiently (for a few seconds). Crystallization of the gelling agent occurred rapidly, unlike in other non-polar organic solvents. Next, synthetic modifications to the gelling agent were considered to enhance gellation of the PFMC. One idea was to increase solubility and possilbly decrease crystallinity of the gelling agent by introducing a large, highly fluorinated alkoxy chain (as in **89**) to the aryl ring. Given the propensity of polyfluorinated aryl rings to undergo nucleophilic aromatic substitution, we hoped to accomplish this through an addition/elimination mechanism. This, however, did not work, with ketone (**90**) and ether (**91**) products being observed instead (Scheme 1.21). Although not the desired result, this fragmentation appeared to involve a $C_6F_5^-$ leaving group. To our knowledge, this is the first instance of a C_6F_5 group acting as a good leaving group. Chapter Two of this thesis will further detail the mechanism and reaction

conditions that promote the fragmentation of 4-*tert*-butyl-1-(pentafluorophenyl)-1-cyclohexanol, as well as other pentafluorobenzylic alcohols.

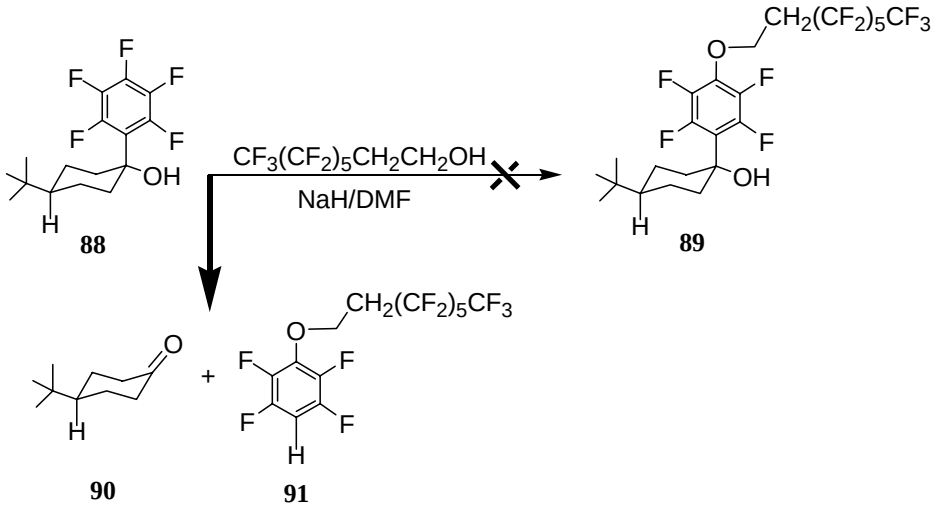

Scheme 1.21. Treatment of the pentafluorobenzylic alcohol (**88**) with highly fluorinated octanol and sodium hydride in DMF did not proceed to desired product (**89**). Products **90** and **91** were unexpectedly formed.

The Use of Modified Injection Port Liners in the Gas Chromatography-based Screening for Catalytic Activity: An Introduction and Background

Capillary gas chromatography is one of the most powerful and efficient analytical tools for analyzing reactivity of organic compounds. The resolving power of capillary GC is extremely good, displaying a separating powers of 50,000 to 200,000 theoretical plates.[35] Capillary GC analysis, however, is limited by the volatility and thermal stability of the analytes, and this usually limits the size of the molecules analyzed to about 500 mass units or less. During GC analysis, the sample is rapidly vaporized in a high temperature injection port and swept through the column with an inert carrier gas such as helium, hydrogen, or argon. The GC can be coupled with many different types of detectors, but commonly flame ionization detectors (FID) and mass spectrometry (MS) detectors are used.

Despite the high temperatures used to vaporize the sample (around 250° C), decomposition reactions are rare because the environment (the GC injection port and column) is rather inert. During analysis, samples come in contact only with a glass-lined injection port and the thin stationary phase of the fused silica column. In particular, samples usually never come in contact with hot metal surfaces within the GC. However, contamination of the injection port can lead to undesirable reactivity. After observing several cases of unexpected reactivity of this sort, we conceived that *intentional* contamination of the GC injection port with various metal salts could be a way of rapidly screening such materials for catalytic activity. Metal salts placed in solution may be coated onto a solid support, such as Celite™, and dried. This material is placed within an injection port liner, which acts as the reaction vessel. These liners must be conditioned at high temperature for a length of time to remove any volatiles that may harm the stationary phase of the column. Once these careful preparations are accomplished, a large range of organic molecules with differing functionalities may be injected and analyzed rapidly for reactivity.

Relatively few studies using GC injection ports to study reactivity have been reported in the literature, and these have been inelegant approaches not necessarily using the capillary gas chromatographic technique. In an early example of catalytic reactions using injection ports in gas chromatography, Kokes, Tobin and Emmett used a packed column instrument to analyze the breakdown of simple hydrocarbons.[36] In this experiment, a branched hydrocarbon, 2,3-dimethylbutane (**92**), was passed through a Houdry M-46, silica-alumina based cracking catalyst using hydrogen (H_2) carrier gas at 400° C. Based on the chromatogram, 2,3-dimethylbutane decomposed to smaller

hydrocarbons and even dehydrogenated to double bonded species, though not all observed GC peaks were identified (Figure 1.4).

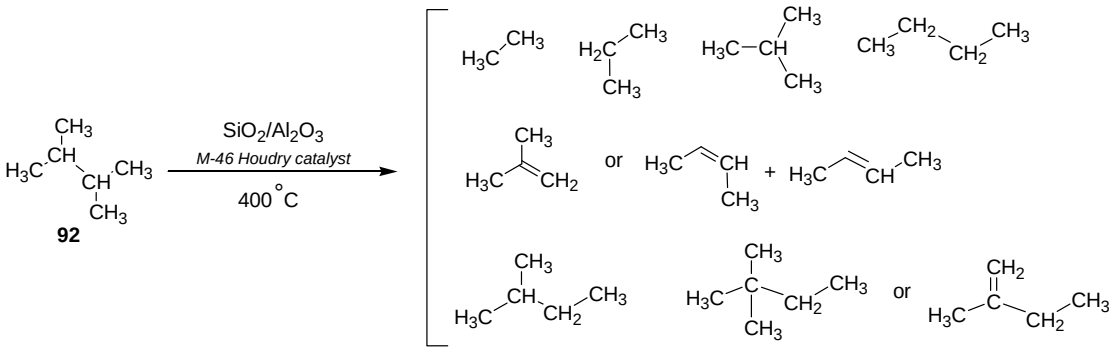

Figure 1.4. Decomposition of 2,3-dimethylbutane (**92**) passed through Houdry M-46 liner at 400° C.[36]

In a later experiment, Hall and Emmett discussed an improved a microcatalytic technique for the kinetic study of catalytic hydrogenation of ethylene.[37] The technique utilized a mixture of gaseous hydrogen and ethylene (in a 60:40 ratio) passed through a reactor tube containing a copper-nickel alloy catalyst. The "slugs" of hydrogen and ethylene gas were carried using pure helium through a homemade packed column lined with charcoal as the stationary phase, and the formation of reduction product was recorded by a thermal conductivity detector at the end of the column (Figure 1.5).[37]

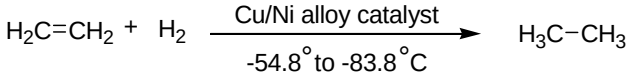

Figure 1.5. Kinetic study of the reduction of gaseous ethylene, treated with hydrogen gas, and passed over a copper/nickel prepared reactor tube.[37]

More recently, Schiffino and Merrill used a microcatalytic reactor (injection port) attached directly to a mass spectrometer to study the dehydration of methanol over a γ-alumina (Al_2O_3) catalyst.[38] Although GC was not used as the primary analytical tool in

this instance, the application of using a packed alumina injection port liner to promote catalytic activity on a molecule is still relevant. In this experiment, the methanol was studied over a temperature range of 230 to 350° C, and any dimethyl ether and water were pushed through the system using helium or argon as the carrier gases (Figure 1.6). The formation of products were observed coninually by mass spectrometry over a 20 second period for several different reaction conditions.[38]

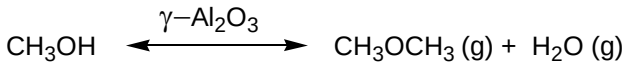

Figure 1.6. Kinetic study of the catalytic dehydration of methanol using γ-alumina in a microcatalytic reactor and monitored by mass spectrometry.[38]

The dehydration of alcohols was studied further using a cobalt(II) sulfate promoted γ-alumina catalyst inside a GC injection port. In this particular work, the investigators studied the activation energy of the dehydration of 2-butanol (Figure 1.7).[39] Other alcohols such as 1-propanol, 2-propanol, 1-butanol, 2-butanol, *tert*-butanol, and 1-hexanol and 2-ethyl-1-hexanol were also examined for dehydration. As in the previous examples, a glass injection port was used as the primary reaction vessel. Skrdla and Robertson were exceptionally particular about the preparation of their cobalt sulfate-alumina liners, which were conditioned at 350° C for 1 hour, and primed using several blank injections of analyte and dichloromethane. The dehydration kinetics for all of the alcohols were studied under isothermal conditions with the only the injection port temperature being varied at 50° C intervals. The reaction rates of the various alcohols dehydrated were directly dependent on the injection port temperature. During the investigation, the dehydration of 2-butanol follows pseudo-first order kinetics, and had an activation energy of 83 kJ/mol.

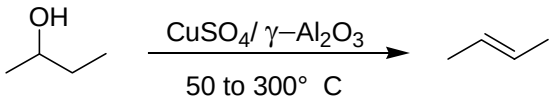

Figure 1.7. The kinetics of $CuSO_4$/ γ-Al_2O_3 catalyzed dehydration of 2-butanol were studied using the GC injection port as the main reaction vessel.[39]

Though crudely demonstrated in the last few examples, the use of the GC injection port as a reaction vessel offers many different possible applications. GC injection port experiments are versatile for several reasons: injection port temperatures can be varied easily, many types of reagents can be placed within an injection port and tested for catalytic activity, and analysis occurs immediately thereafter. Today's modern GC's, as mentioned previously, may be equipped with MS detectors that include spectral matching software making it easier to identify new compounds. The use of an auto-injector/auto-sampler apparatus also enhances the convenience of this analytical technique. In our methodology, we have been able to study a large number of reactivities rapidly. Furthermore, we have been able to confirm that the base-catalyzed fragmentation of 4-*tert*-butyl-1-(pentafluorophenyl)-1-cyclohexanol not only occurs rapidly in solution using DMSO, but under high temperature gas-phase conditions as well. Chapter Three of this thesis will detail the rapid analyses of several classes of organic molecules, and their reactivities towards a variety of metal catalysts. Experimentation of this sort was accomplished with the expectation of finding unique reactions, and with the hope that these new-found reactivities can be duplicated in solution.

CHAPTER TWO

Fragmentation Studies of Pentafluorobenzylic Alcohols

Results and Discussion

Initial Experiments

The initial experiments centered on replicating the fragmentation of pentafluorobenzylic alcohols, and determining the exact conditions and parameters that needed to be studied. Based on the initial observations made of the fragmentation behavior as outlined in Chapter One, Scheme 1.19, it was quickly determined that an alkoxide salt, such as sodium methoxide, in a polar aprotic solvent (i.e., DMSO) rapidly induced the fragmentation of a pentafluorophenyl group from an alcohol such as *cis*-4-*tert*-butyl-1-(pentafluorophenyl)-1-cyclohexanol (**93**). The *cis* isomer was chosen as the first molecule of study due to its ample availability, though ultimately we compared its reactivity to that of the *trans* isomer. Prior to this, it had not been known whether fragmentation was an isomer-specific consequence limited to only the *trans* (organogelating) isomer (**88**).

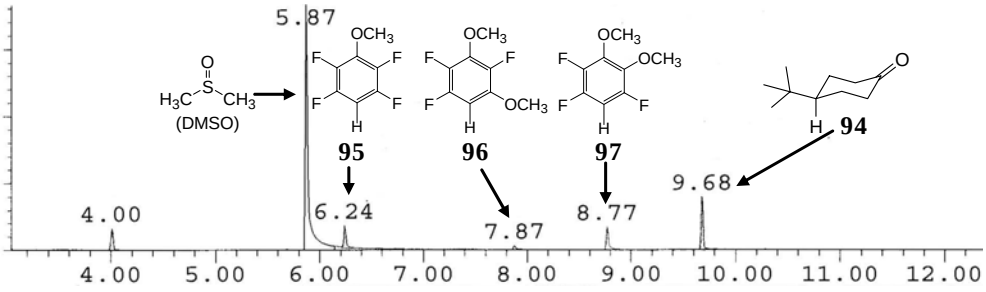

Figure 2.1. GC-MS analysis of the fragmentation of cis-C_6F_5 alcohol (**93**).

From the initial GC-MS studies (Figure 2.1), it was immediately apparent that fragmentation occurred rapidly using one equivalent of sodium methoxide (4.37 M in methanol) in DMSO solvent to form tetrafluoroanisole (**95**), 4-*tert*-butylcyclohexanone (**94**), and if left long enough with excess base two trifluorodimethoxybenzene compounds (**96**, **97**), although the dimethoxy species were not identified until later on in this project (Figure 2.2). This reaction, though, occurred far too rapidly (< 2 min) to observe formation of intermediate species, and therefore a specific mechanism could not be suggested.

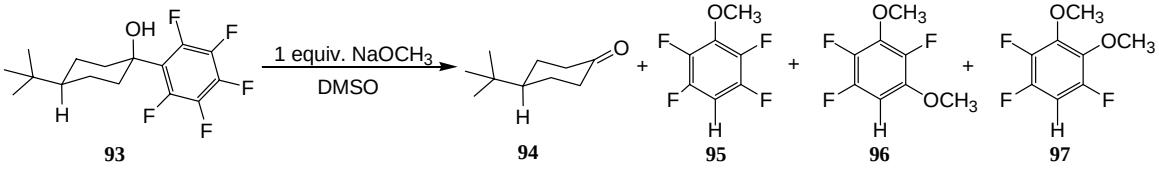

Figure 2.2. Reaction of **93** and resultant products.

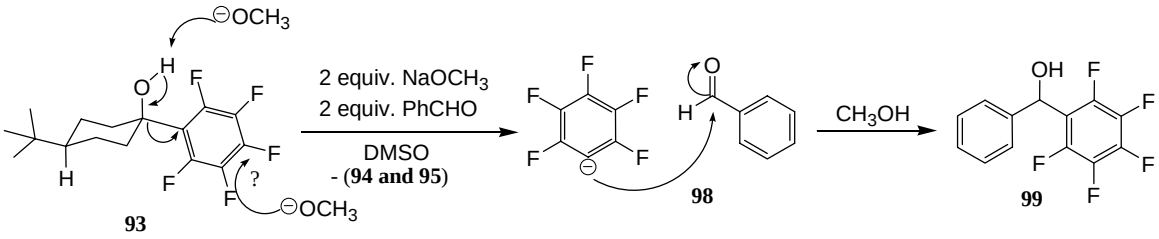

Scheme 2.1. Reaction of *cis*-C_6F_5 alcohol (**93**) that proved the formation of $C_6F_5^-$ occurs.

To probe whether the formation of the pentafluorophenyl anion occurred during fragmentation, benzaldehyde (**98**) was added in an attempt to "trap" the anion. The addition of two equivalents of both sodium methoxide and benzaldehyde to the *cis*-C_6F_5 alcohol (**93**) in DMSO (Scheme 2.1) did generate some (pentafluorophenyl)-phenyl methanol (**99**) (Figure 2.3). The formation of this product could only have occurred if pentafluorophenyl anion was generated in the fragmentation and attacked the

benzaldehyde in solution. It was still unknown whether tetrafluoroanisole (**95**), a major product, was produced by nucleophilic aromatic substitution at the aryl ring followed by fragmentation, or if fragmentation preceded substitution.

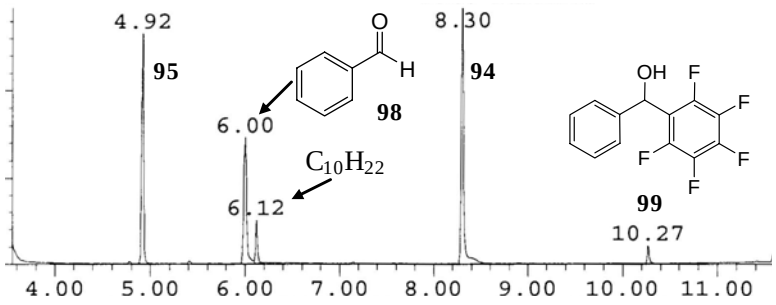

Figure 2.3. GC-MS analysis of benzaldehyde "trapping" reaction of C_6F_5 anion. Note: Decane ($C_{10}H_{22}$) was used as an internal standard for this analysis.

To study the specific mechanism of fragmentation, it was necessary to find a solvent system that would slow the reaction down enough to observe formation of intermediate compounds. Methanol was the first solvent studied in a reaction using the *cis*-C_6F_5 alcohol. Reaction occurred very slowly, with only a minimal amount of product forming after four days (Figure 2.4). The small amount of product that did form,

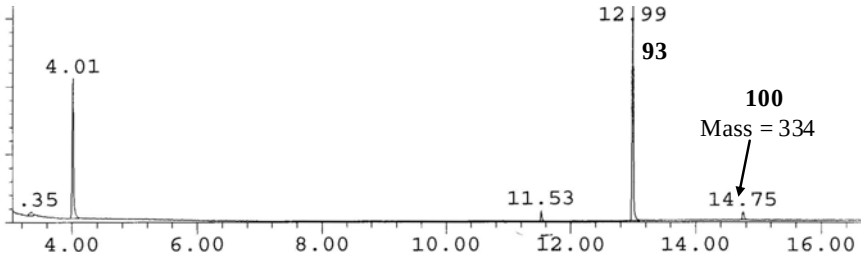

Figure 2.4. GC-MS analysis of **93** treated with sodium methoxide and methanol at t = 4 days.

however, had a longer retention time and higher mass (M = 334) than the starting alcohol (M = 322). We were able to deduce that the mass of 334 resulted from a substitution of fluorine (M = 19) by a methoxy group (O-CH_3, M = 31), which can occur when

methoxide directly substitutes on the phenyl ring in an addition/elimination reaction (Figure 2.5).

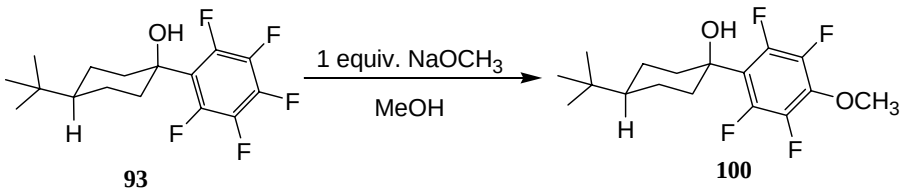

93 **100**

Figure 2.5. Nucleophilic aromatic substitution of **93** occurred using methanol as the solvent to form *cis*-4-*tert*-butyl-1-(2,3,5,6-tetrafluoro-4-methoxy-phenyl)-cyclohexanol (**100**).

To accelerate the reaction, the same methanol reaction described above was heated. Originally, the reaction mixture was to be heated at 60° C for several days, but the solution was also overheated to well above 100° C at the start of the reaction. A GC-MS of this solution showed complete fragmentation of the *cis*-C_6F_5 alcohol (**93**) to the ketone (**94**) (Figure 2.6). This was our first indication that heat may also play a role in the fragmentation of C_6F_5.

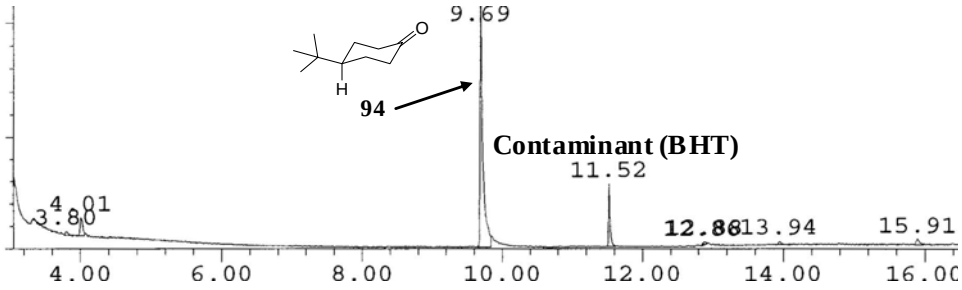

Figure 2.6. Heating of methanol reaction above 100° C led to complete fragmentation of *cis*-alcohol (**93**).

Because the reactivity in pure methanol was so low, we then studied reactions using mixtures of methanol and DMSO. With this idea in mind, three experiments involving the variation of solvent ratios were conducted using the same amounts of *cis*-

alcohol (**93**), equivalents of sodium methoxide, volume of solvent, and length of reaction time. Reaction mixtures with 25:75, 50:50, and 75:25 volumetric percentages of DMSO to methanol were allowed to react for 10 minutes and worked up immediately. No reactivity was observed for the 25:75 reaction within the 10 minute window, and only 2.8% (GC peak area %) of substitution product (**100**) was observed for the 50:50 mixture, similar to what was observed for the pure methanol reaction in Figure 2.4. The 75:25 reaction showed a drastic difference in reactivity, with both fragmentation and substitution products observed in the GC-MS analysis (Figure 2.7). Of the 50% starting alcohol that reacted in a time period of 10 minutes, about 40% became substituted product (**100**) versus only about 10% fragmentation product (**94**). Clearly, the presence of methanol tends to slow fragmentation and favor substitution.

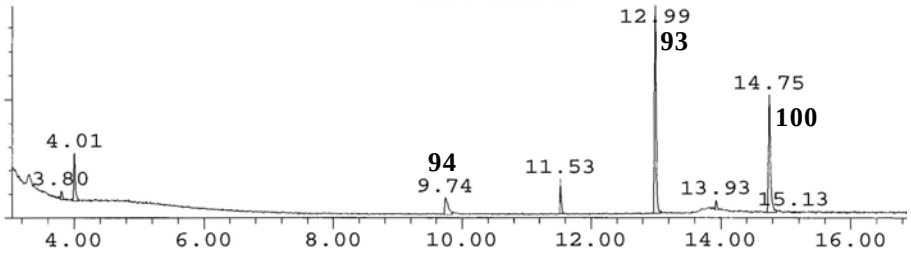

Figure 2.7. GC-MS analysis displaying the increased substitution and decreased fragmentation of *cis*-alcohol (**93**) using 75:25 (v/v) % of DMSO to methanol.

The general conditions of fragmentation presented thus far were solely determined using GC-MS analyses. Time dependent studies can become tedious, with this particular analytical technique due to the water-organic phase work-ups needed before analysis. The risk of contamination is increased and the loss of more volatile products such as pentafluorobenzene and tetrafluoroanisole is possible upon rotary evaporation. Therefore, a consistent analytical technique was needed to monitor the real-time reaction kinetics of the C_6F_5 fragmentation. Proton nuclear magnetic resonance (^{1}H

NMR) appeared to be a good choice; however, a mixed solvent system that included methanol was problematic, giving a particularly large singlet resonance around 3.2 ppm. This large solvent peak in the middle of our spectral window dwarfed all other resonances, effectively making it hard to observe the formation of other species. Fluorine-19 (^{19}F) NMR presented a much better option in analyzing the reaction of our pentafluorobenzyl alcohols, as most of the intermediate species predicted are fluorinated and the solvents are entirely invisible. The rest of this chapter will discuss the use of ^{19}F NMR in the determination of the mechanism of fragmentation as well as other conditions studied.

Mechanisms of Fragmentation/Substitution

At the start of this project, three mechanisms were hypothesized to explain step-wise how the fragmentation reaction might occur and the types of intermediate products that could be formed. In the first mechanism, it was proposed that fragmentation occurs by a simultaneous substitution/fragmentation process (Scheme 2.2). In the first step of

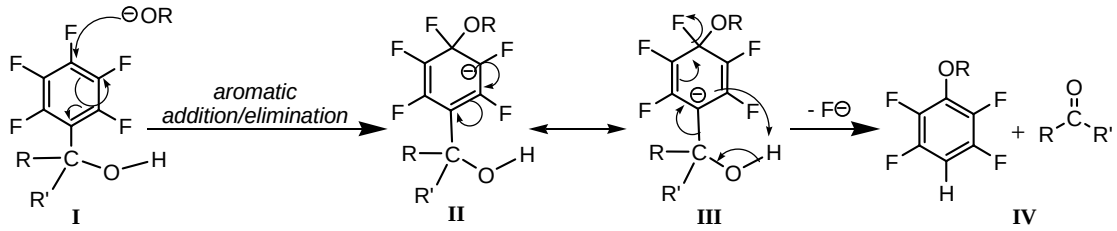

Scheme 2.2. Suggested simultaneous substitution/fragmentation mechanism.

this mechanism, the C_6F_5 ring is attacked by the nucleophilic alkoxide in the *para* position (**I**) and delocalization of the resulting negative charge around the ring can occur (**II**). The partial negative charge localized at the tertiary carbon position (**III**) could attack the hydroxyl proton followed by an immediate rearrangement of electrons causing

fragmentation of the molecule to form a tetrafluoroanisole and a ketone (**IV**). Note that this mechanism never involves a pentafluorophenyl anion.

Another possibility is that nucleophilic aromatic substitution could occur by attacking the proton on the hydroxyl group directly (Scheme 2.3). After deprotonation, a loss of ketone and formation of an alkoxy tetrafluorophenyl anion occurs (**VI**), and the anion protonates readily in a polar protic solvent such as methanol.

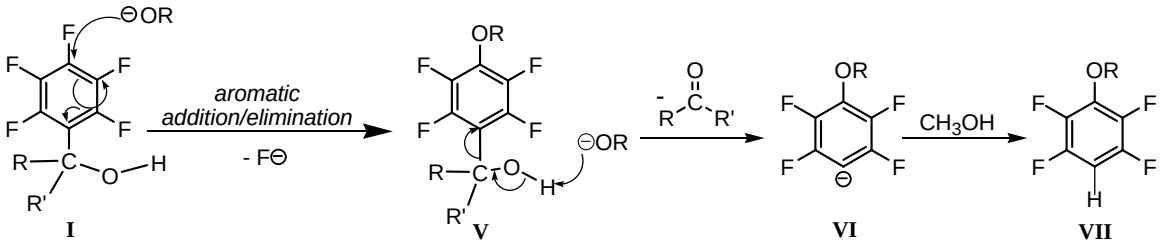

Scheme 2.3. Two step aromatic substitution/alcohol deprotonation mechanism.

In the third mechanism (Scheme 2.4), the alcohol is first deprotonated by the alkoxide, putting a negative charge onto the oxygen (**VIII**). This species can rearrange to form a ketone, breaking the C-C bond to form the C_6F_5 carbanion (**IX**). The carbanion is protonated by any alcohol present in the reaction to form pentafluorobenzene (**X**).

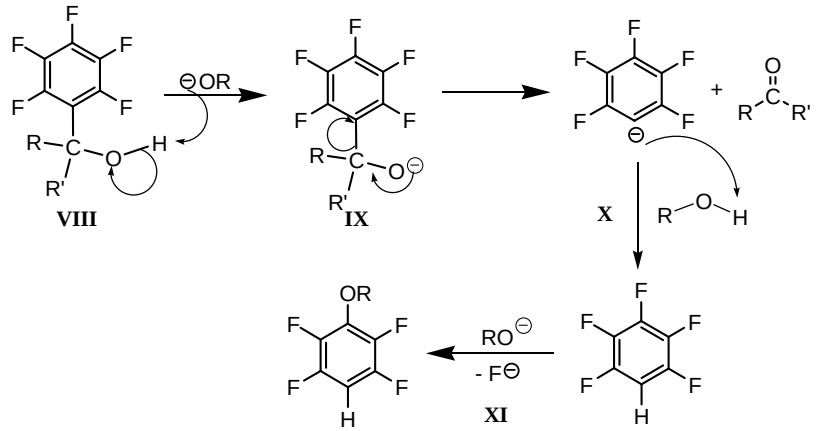

Scheme 2.4. In this mechanism, the alcohol is deprotonated first and the anion rearranges to form ketone and $C_6F_5^-$.

If excess alkoxide remains in the reaction, it can further react with pentafluorobenzene via a nucleophilic aromatic substitution to form tetrafluoroanisole (**XI**).

In our intitial ^{19}F NMR studies, we sought to determine which mechanism might be operative. The experiment was conducted such that we could observe the reaction as it was occurring. In an NMR tube reaction, *cis*-C_6F_5 alcohol (**93**) dissolved in 75:25 (v/v) % of deuterated DMSO (DMSO-d_6) and methanol, and was treated with 4 equivalents of sodium methoxide (4.37 M in CH_3OH, 25 wt.% solution). A new spectrum was collected at 2 minute intervals for about the first 20 minutes of the reaction, with scans every five minutes thereafter. In Figure 2.8, spectra taken from the first 12 minutes are stacked for comparison. Comparison and assignment of resonances was facilitated using ^{19}F reference spectra taken of stock solutions of predicted intermediates and products prior to experimentation. Furthermore, all chemical shifts were calibrated using fluorobenzene (C_6H_5F, -113.26 ppm, singlet) as an inert reference compound. Although reaction was completed 20 minutes after the addition of sodium methoxide, all predicted intermediates and products from the second and third mechanisms were observed. One interesting aspect of the spectra was the formation and eventual consumption of pentafluorobenzene (**F**), which appeared to be at its maximum at t = 4 minutes and no longer observable at t = 12 minutes. Like the reaction studied with GC-MS analysis in Figure 2.7, substitution product (**S**) readily formed, although tetrafluoroanisole (**FS**), in this case, was the major product formed by t = 12 minutes. This second major product formation was possible due to the excess of sodium methoxide in solution.

Though this first ^{19}F NMR kinetic run gave more insight into the mechanism of C_6F_5 fragmentation, it was still unknown whether the formation of tetrafluoroanisole came solely from the substitution of pentafluorobenzene, or if the methoxy substituted

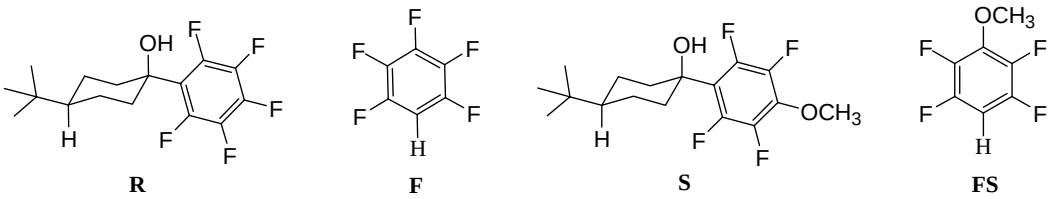

R = Reactant
S = Substitution Product
F = Fragmentation Product
FS = Fragmentation followed by Substitution

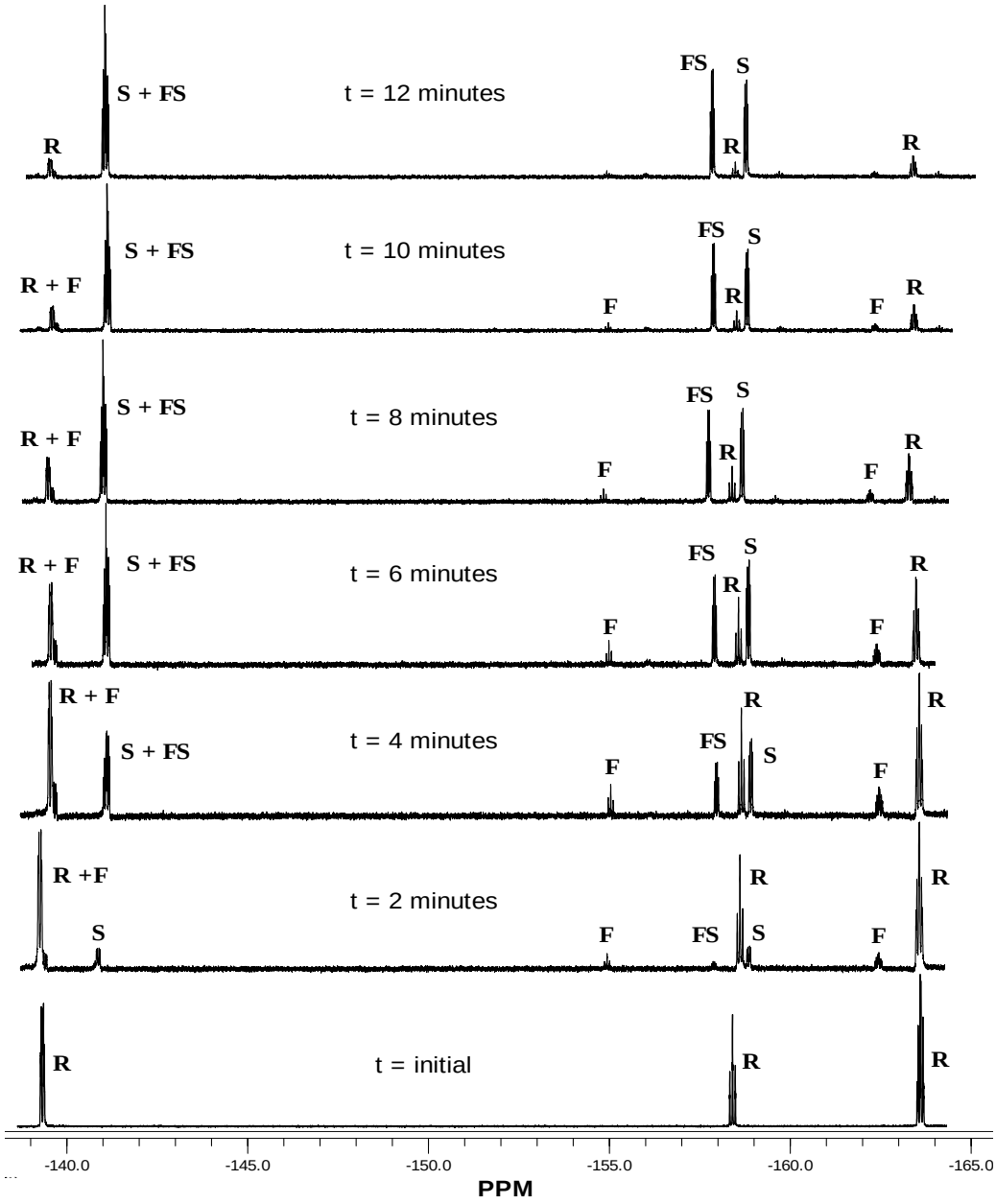

Figure 2.8. Stacked ^{19}F NMR spectra corresponding to the reaction of *cis*-C_6F_5 alcohol (**93**) treated with 4 equivalents of $NaOCH_3$ in 75:25 (v/v) % of DMSO-d_6:CH_3OH.

cis-C_6F_5 alcohol could fragment itself once treated with sodium methoxide as suggested in the second mechanism in Scheme 2.3. Therefore, in a second ^{19}F NMR kinetic study, isolated methoxy-substituted *cis* alcohol (**100**), was treated with 1 equivalent of sodium methoxide in 75:25 (v/v) % of DMSO-d_6 to methanol. The reaction was monitored at five minute intervals for a period of one hour. As presented in the stacked plot in Figure 2.9, reactivity was very low even after 45 minutes, reflecting the significantly lower reactivity of the *cis* isomer.

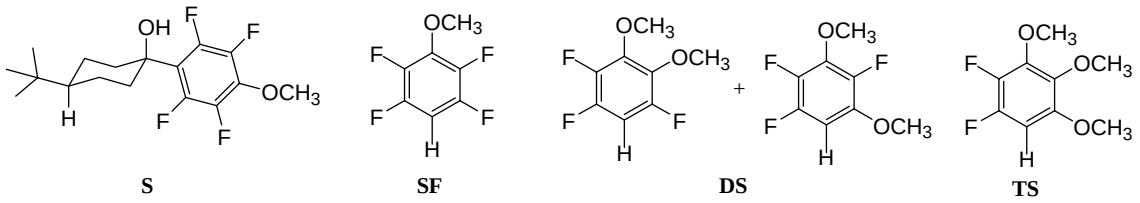

S = Starting Alcohol
SF = Substitution followed by fragmentation
DS = Disubstitued Products
TS = Trisubstituted Product

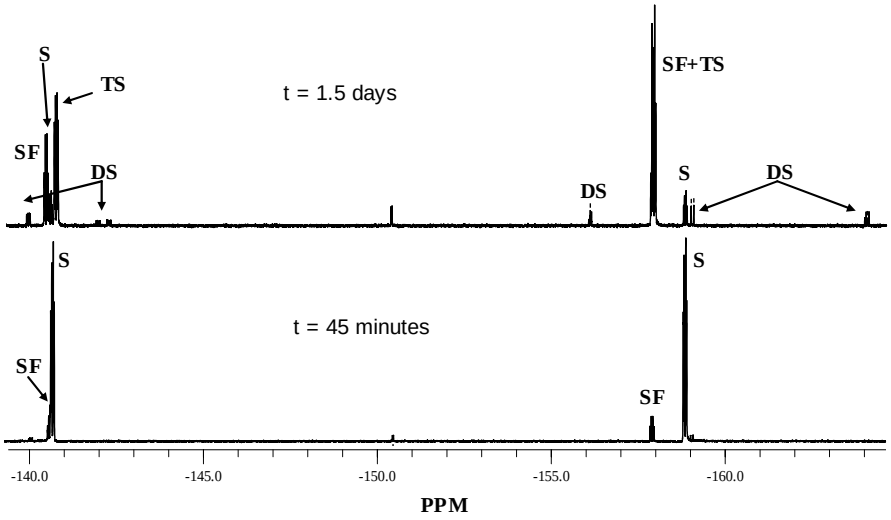

Figure 2.9. ^{19}F NMR observation of methoxy substituted *cis*-C_6F_5 alcohol (**100**).

However, the substituted alcohol (**S**) did fragment into tetrafluoroanisole (**SF**). The reaction continued for a total of 1.5 days before being analyzed again. The substituted product had completely fragmented and the resulting tetrafluoroanisole

continued to substitute to form dimethoxy (**DS**) and even trimethoxy (**TS**) species. From this experiment, we were able to confirm that the source of tetrafluoroanisole was not only due to direct substitution of pentafluorobenzene but also fragmentation of the substituted product itself.

For comparison, a GC-MS and ^{19}F NMR study of *trans*-4-tert-butyl-1-(pentafluorophenyl)cyclohexanol (**88**) was conducted. It was predicted that the *trans* alcohol would have a tendency to fragment at a faster rate than the *cis* alcohol due to the axial position of the aryl ring and the increased steric strain from 1,3-diaxial interactions (Figure 2.10). Initially, GC-MS analyses were used to compare relative rates of reactivity

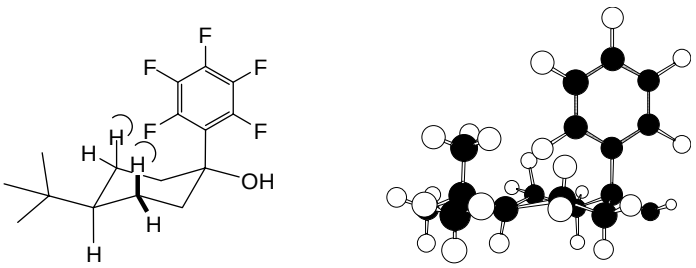

Figure 2.10. 2-D and 3-D representations of the *trans*-alcohol (**88**) depicting the steric strain between the aryl ring and the axial hydrogens at the 1,3 positions.

between the *cis* and *trans* alcohols. Again, all experiments varied the ratio of DMSO-d_6 to methanol, while keeping concentrations of starting alcohol and equivalents of sodium methoxide the same. In separate reactions using 50:50 (v/v) % of DMSO-d_6:CH_3OH, both *trans* and *cis* alcohols (**88**, **93**) were treated with 2 equivalents of sodium methoxide and allowed to react for one day. It was again evident by GC-MS analysis (Figure 2.11) that the *trans*-isomer clearly has the faster rate of reactivity, with much of the product being substitution and not fragmentation of the alcohol. We have observed that though

substitution product readily forms with the *trans* isomer, fragmentation of this alcohol is more prevalent.

Because substitution and fragmentation of the *trans* alcohol were much more rapid than the *cis* alcohol, reactions with lower solvent ratios of DMSO-d_6 to methanol were attempted. When the solvent ratio was lowered to 25:75 (v/v) %, the *trans* alcohol was observed to react about the same rate as the *cis* alcohol in 50:50 solution, with 38.4% (GC area %) of starting reagent remaining after one day of reactivity. As expected, reactivity of the *cis* alcohol was lower in the 25:75 solvent (Figure 2.12).

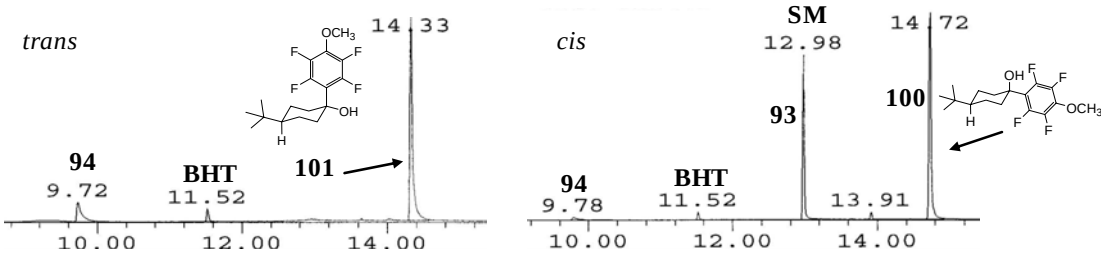

Figure 2.11. A comparison of reactivity between *cis* and *trans* alcohols in 50:50 (v:v) solvent ratio of DMSO-d_6 to methanol.

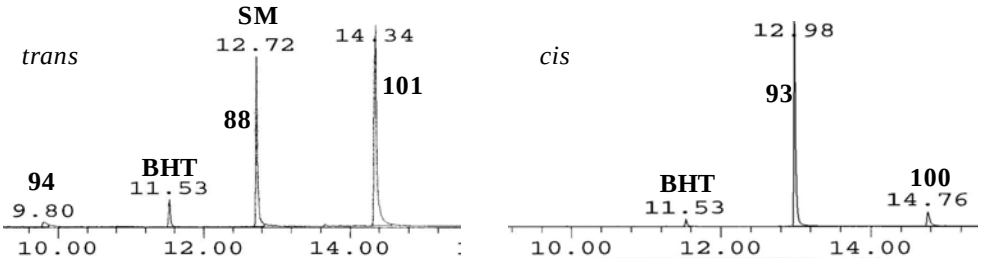

Figure 2.12. A comparison of reactivity between *cis* and *trans* alcohols in 25:75 (v:v) solvent ratio of DMSO-d_6 to methanol.

With the GC-MS data presented above, we were able to estimate the appropriate solvent ratio needed to conveniently study fragmentation of *trans* alcohol **88** by ^{19}F NMR, which was determined to be about 35:65 (v/v) % of DMSO-d_6 to methanol. In particular, this solvent ratio allowed for a longer period of reactivity. The equivalents of

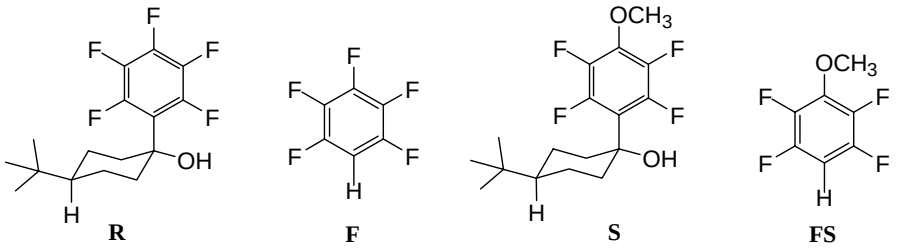

R = Reactant
S = Substitution Product
F = Fragmentation Product
FS = Fragmentation followed by Substitution

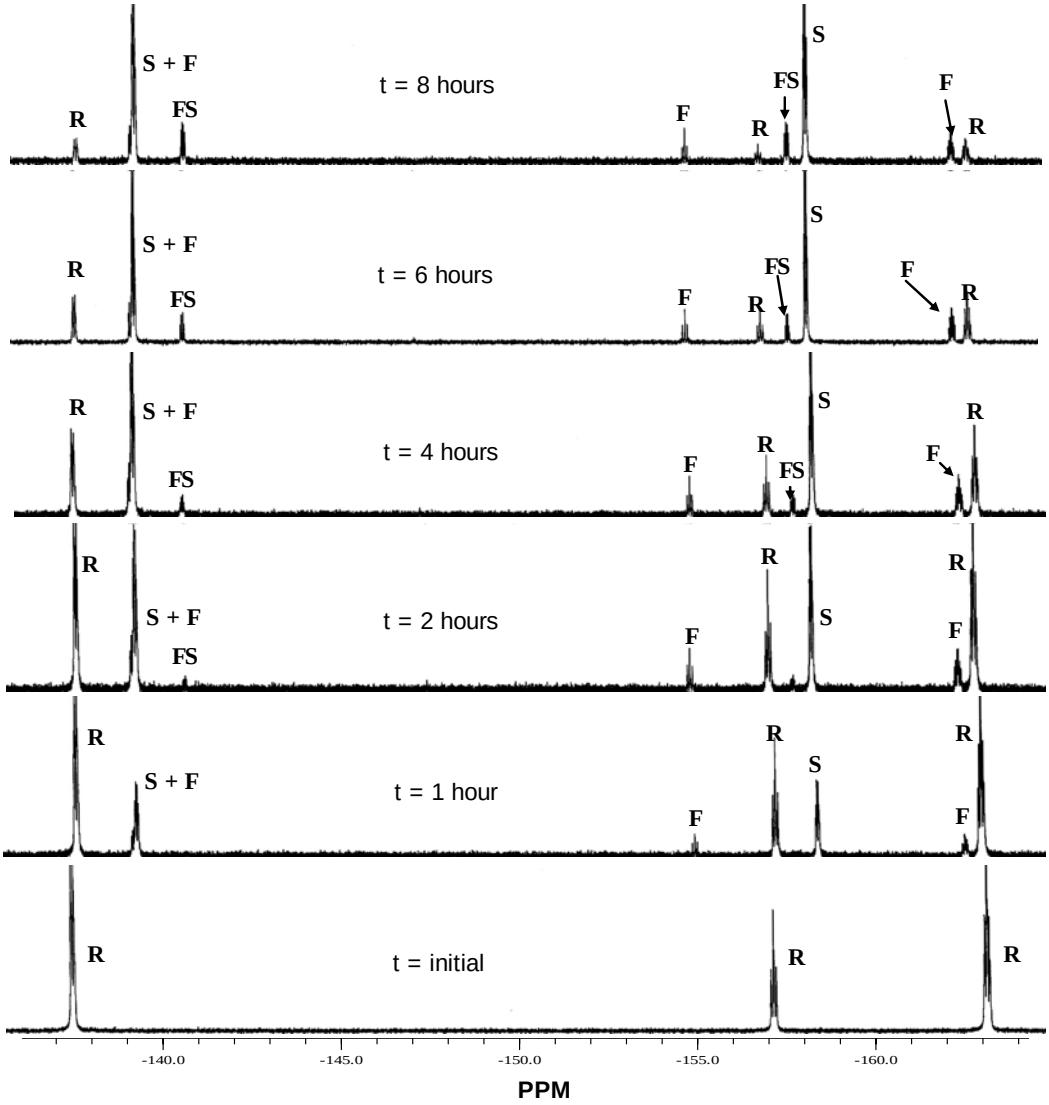

Figure 2.13. Stacked ^{19}F NMR spectra corresponding to the reaction of *trans*-C_6F_5 alcohol (**88**) with 2 equivalents of $NaOCH_3$ in 35:65 (v/v) % of DMSO-d_6:CH_3OH.

sodium methoxide were reduced by half (2 equiv.) to further slow rate of reaction. In another NMR tube reaction, the *trans* alcohol was monitored for a period of 11 hours. The time intervals between scans continued to increase as reactivity slowed with a one hour intervals between the eighth and eleventh hours. Figure 2.13 shows selected spectra from respective time intervals. The reaction was not complete even at the eleventh hour (specta not shown) with a small amount of starting alcohol (**R**) and pentafluorobenzene (**F**) remaining.

A unique property of the methoxy-substituted *trans* product (**101**) was observed while studying solvent ratio effect on fragmentation. A reaction using 15:85 (v:v) % of DMSO-d_6 to methanol was attempted, but was deemed too slow for the purposes of observing fragmentation, with only 18% (GC area %) of substituted product forming after 1 day. The reaction vessel and contents were placed on a shelf to be analyzed at a later time period (i.e., 2-5 days). However, the flask, sealed with a rubber septum, was

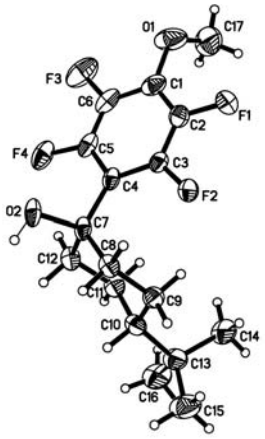

Figure 2.14. X-ray diffraction study of *trans*-4-tert-butyl-(2,3,5,6-tetrafluoro-4-methoxy-phenyl)-cyclohexanol (**101**).

neglected on the shelf for several months, and during this time period the methanol slowly evaporated from the flask. What formed, quite unexpectedly, were large clear

needle-like crystals. An X-ray diffraction study of the crystals (Figure 2.14) showed that the *trans*-methoxy-substituted alcohol had crystallized from the predominantly methanol solution. It has been reported that the *trans* alcohol (**88**), an organogelator, does not crystallize but rather forms a fibrous solid.[34] From this X-ray study we were able to demonstrate that *para*-methoxy substitution induces crystallization of the *trans* isomer as well, which destroys any gelling ability.

From all of the GC-MS and ^{19}F NMR studies conducted on the *cis*- and *trans*-alcohols (**88** and **93**), we were able to make a general assertion about the mechanism of the fragmentation of $C_6F_5^-$ that is summarized in Scheme 2.5 below:

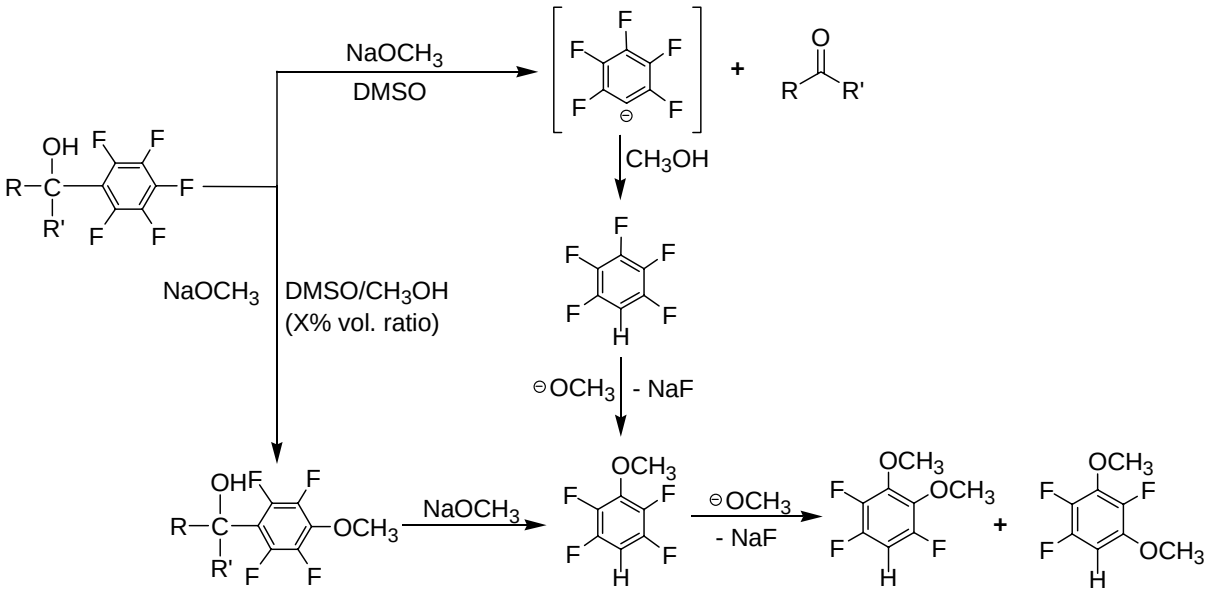

Scheme 2.5. Summary of C_6F_5 fragmentation based on studies conducted thus far.

From the reactivities observed thus far, we can demonstrate that fragmentation occurs by a combination of the second and third mechanisms hypothesized. No indication has been given that a simultaneous substitution/fragmentation process could occur (Mechanism I, Scheme 2.2). Nevertheless, the two different modes of reactivity

(fragmentation vs. substitution) may be controlled by varying the volume of methanol relative to DMSO. With the addition of methanol, direct substitution is primarily favored, but some direct fragmentation of the starting alcohol is still observed. Secondary modes of reactivity have been reported, with the formation of tetrafluoroanisole occurring by two pathways: direct substitution of pentafluorobenzene and fragmentation of substituted *cis*-alcohol. Tetrafluoroanisole, in the presence of excess methoxide, can continue to substitute to a mixture of dimethoxy species.

Structural Variations of Pentafluorobenzylic Alcohols: Effect on Fragmentation

At this point, studies of fragmentation have been focused mainly on *cis*- and *trans*-4-*tert*-butyl-1-(pentafluorophenyl)-cyclohexanol. It was not known if fragmentation was specific to the two alcohols mentioned earlier or if this reactivity would be observed in other structurally different pentafluorobenzylic alcohols. Therefore, a variety of different C_6F_5-substituted alcohols were synthesized to test the effect of structural variation on fragmentation (Figure 2.15).

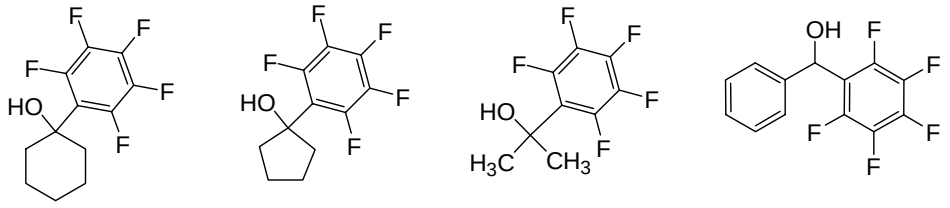

102 **103** **104** **105**

Figure 2.15. Other derivatives of pentafluorobenzylic alcohols studied for fragmentation.

The structural variations consisted of moderate structural changes in the alkyl portion of the molecule. Compared with the 4-*tert*-butyl-cyclohexanols, we explored the loss of *tert*-butyl group (**102**), smaller ring size (**103**), lack of cyclic nature (**104**), and the

addition of aromatic groups (**105**). Preparations of these alcohols are discussed in Chapter Four of this thesis.

All of the alcohols were analyzed for fragmentation in separate reactions treated with 2 equivalents of sodium methoxide in DMSO and allowed to react for 1 hour. Based on GC-MS analyses, all alcohols completely fragmented as evident by the formation of tetrafluoroanisole (**94**) (Figure 2.16). The formation of ketones and aldehydes, precursors used to prepare all C_6F_5 alcohols studied in this project, were only observed by GC-MS in alcohols **102** and **105** probably because the ketone fragments of the other two ketones (cyclopentanone and acetone) are too low boiling. Although GC-MS analyses showed no structural constraint on fragmentation, a ^{19}F NMR study was also conducted for comparison.

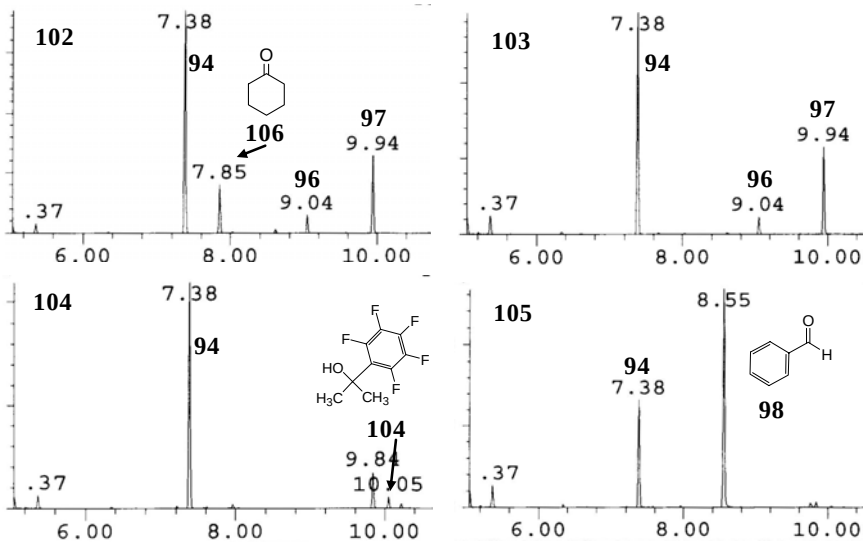

Figure 2.16. GC-MS studies to determine the occurrence of fragmentation on structurally variant pentafluorobenzylic alcohols (**102**-**105**).

For ^{19}F NMR studies of the structurally variant C_6F_5 alcohols, reaction conditions were strictly replicated from one sample to the next with respect to sample concentrations and equivalents of sodium methoxide used. Upon addition of sodium methoxide, all of

the samples were scanned at 2, 5, and 10 minute intervals for a period of 1 hour. Since DMSO-d_6 was used as the primary solvent, rapid fragmentation (t_{rxn} < 4 minutes) was observed for all of the alcohols. Figure 2.17 shows the stacked plot of the reaction with 1-(pentafluorophenyl)cyclohexanol (**102**) 4 minutes after the addition of base and at 1 hour.

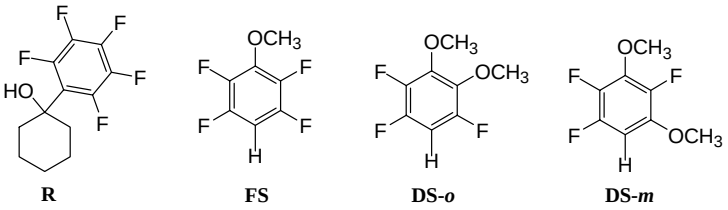

R = Reactant
DS-*o* = *Ortho*-disubstituted Product
FS = Fragmentation followed by substitution
DS-*m* = *Meta*-disubstituted Product

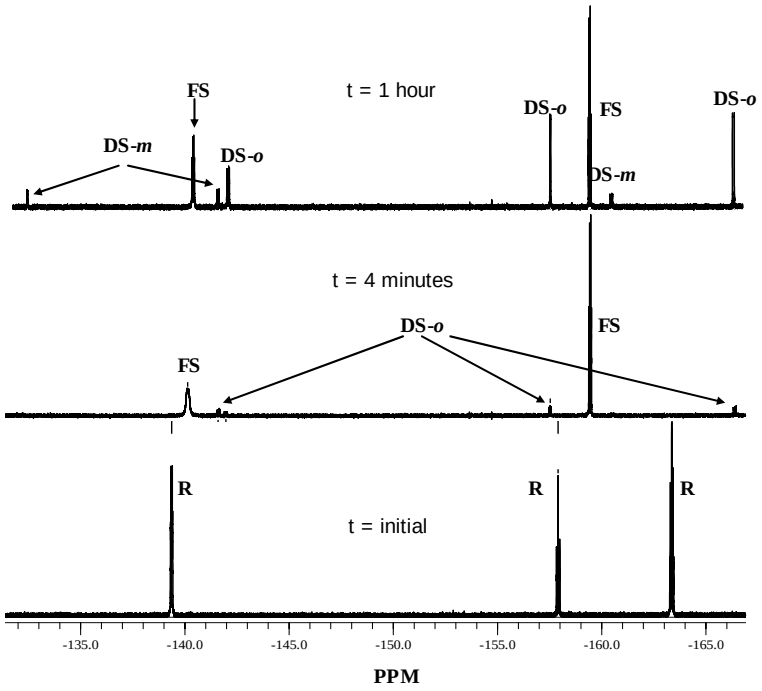

Figure 2.17. Real time stacked ^{19}F NMR specta showing fragmentation of C_6F_5-cyclohexanol (**102**) and formation of trifluorodimethoxybenzenes.

All other alcohols showed identical reactivity, therefore those plots are not shown here (Representative plots of all of the runs are located in Appendix A.). The formation of

trifluorodimethoxybenzenes (**DS-*o***, **DS-*m***) was first identified in these experiments with two sets of resonances of equal intensities observed. With tetrafluoroanisole (**FS**) as the primary product at t = 4 minutes, excess methoxide may substitute the aryl ring via two modes of attack: methoxide can substitute a fluorine either in the *ortho*-position (adjacent C-F bond) relative to *para*-methoxy group or the *meta*-position (one C-F bond away). We have rationalized that the *ortho*-dimethoxy species is the more favored species to form versus the *meta*-dimethoxy species, since localization of electrons occurs at carbons with an electron withdrawing group (-F or $–OCH_3$) (Scheme 2.6). Localization of electrons for the *meta*-product includes placement of electrons on a carbon with only hydrogen, which is not favored. However, despite this discrepancy in charge transfer from one bond to the next, the *meta*-product still forms slowly.

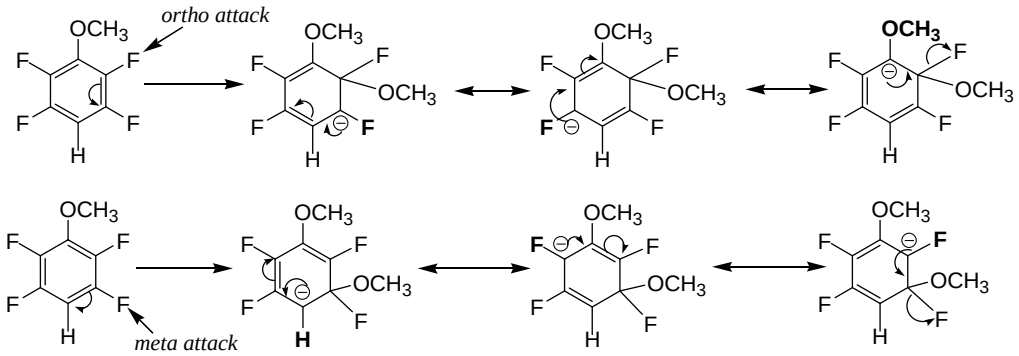

Scheme 2.6. Preferential formation of 1,2,5-trifluoro-3,4-dimethoxybenzene (**97**) by *ortho* methoxide attack versus the formation of 1,2,4-trifluoro-3,5-dimethoxybenzene (**96**) by *meta* attack.

Specific Molecular Conditions: Fragmentation with Insufficiency of Fluorines?

As recently presented, fragmentation of pentafluorobenzylic alcohols does not appear to have any structural constraints. It is this generality of fragmentation that led us to focus on the stability of the C_6F_5 anion itself, specifically to what extent fluorine stabilizes that particular anionic leaving group. In a GC-MS experiment, gelling agents

trans-4-*tert*-butyl-1-phenylcyclohexanol (**86**) and *trans*-4-*tert*-butyl-(4-fluorophenyl)-cyclohexanol (**87**) were reacted with 2 equivalents of sodium methoxide in 100% DMSO to see if fragmentation would still occur even with the lack of fluorines. Both reactions were sampled at 15 minute, 1 and 3 hour intervals with no reactivity observed. These reactions were heated at 60° C overnight, and at the beginning of both reactions temperatures accidentally exceeded 100° C before stabilizing. Even with overnight heating, no fragmentation reactivity of either alcohol was observed (Figure 2.18).

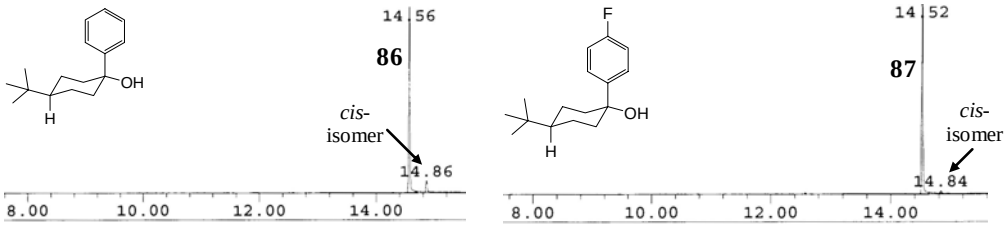

Figure 2.18. GC-MS analysis of **86** and **87**: heating did not promote fragmentation.

As demonstrated in the GC-MS analyses in Figure 2.18, the lack of fluorines on the aromatic ring of 4-*tert*-butyl-1-arylcyclohexanol clearly inhibited the fragmentation. A single fluorine in the *para* position of the phenyl ring was also not enough to support fragmentation. With this result, we had one question: How many fluorines does it take to for fragmentation to occur? With previous observations, aryl groups with four fluorines were stable enough to fragment as evidenced by the study of methoxy-substituted *cis*-alcohol (**100**). At this point, we synthesized and study fragmentation of trifluorobenzyl alcohols, which appeared to be a good intermediate number of fluorines to try. The first target that we attempted to synthesize was 4-*tert*-butyl-1-(2,4,6-trifluorophenyl)cyclohexanol (**107**). We tried to prepare this molecule, as with the C_6F_5-alcohols, using a Grignard reaction to couple the trifluorophenyl group (**109**) with the

ketone to form the resulting alcohol (**107**) (Scheme 2.7). Although new product formation was observed by GC-MS analysis, none of the products matched the mass of

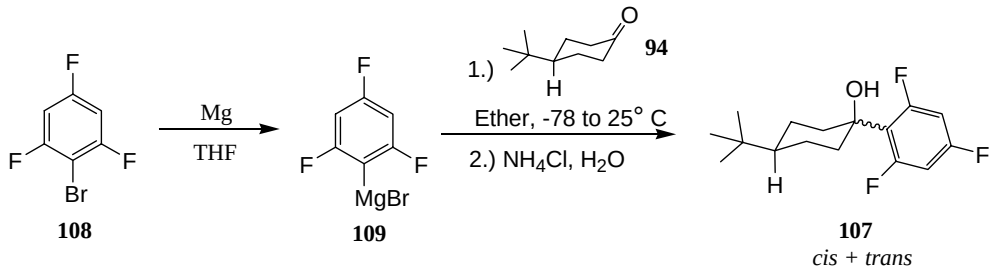

Scheme 2.7. Unsuccessful preparation of 4-*tert*-butyl-1-(2,4,6trifluorophenyl)-cyclohexanol (**107**) via the Grignard Reaction.

the target alcohol (M = 286). Alternate synthetic routes were attempted, specifically using organolithium reagents to lithiate 2-bromo-1,3,5-trifluorobenzene (**108**), and subsequently treat with 4-*tert*-butylcyclohexanone (**94**). This preparation, however, was also not successful.

It was at this point that we decided to synthesize a completely different trifluoroaryl target: Diphenyl-(2,4,6-trifluorophenyl)methanol (**110**). Not only was the synthetic route more feasible, but we could also test the effect steric crowding of the phenyl rings has on promoting fragmentation. We prepared the diphenyltrifluorophenyl methanol (**110**) based the reactions presented in Scheme 2.8. Trifluorobenzonitrile (**111**)

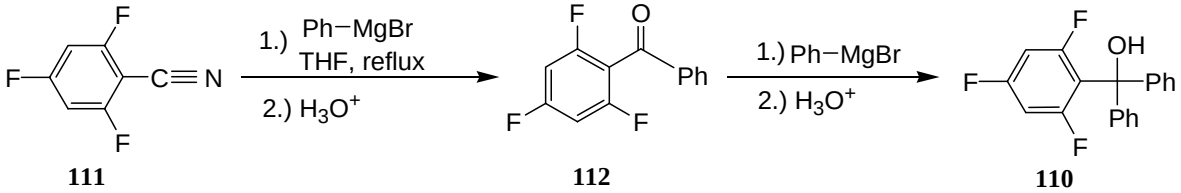

Scheme 2.8. Preparation of Diphenyl-(2,4,6-trifluorophenyl)methanol (**110**).

was treated with phenylmagnesium bromide in tetrahydrofuran (THF) under reflux conditions. After treatment with acidic aqueous solution, phenyl-(2,4,6-trifluorophenyl)methanone (**112**) was formed. This ketone, after purification, was treated with phenylmagnesium bromide in a second reaction to form the alcohol (**110**). Although column purification proved to be tedious, involving the removal of a number of unwanted byproducts, we were able to isolate about 200 mg of relatively pure alcohol (Figure 2.19).

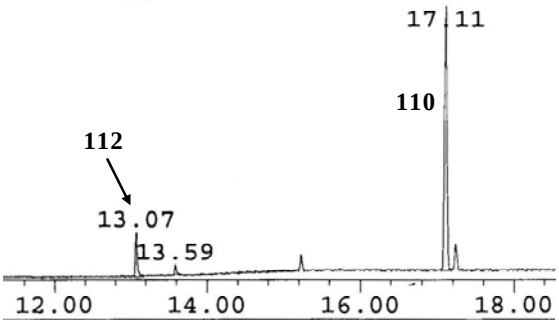

Figure 2.19. GC-MS analysis of alcohol **110**. Small amount of ketone (**112**) was not removed by column purification.

Although the alcohol (**110**) was not entirely pure, and in particular contained some ketone (**112**), a ^{19}F NMR and subsequent GC-MS analysis was conducted to see if fragmentation would occur. As with previous experiments, initial reactions were conducted using only DMSO as the primary solvent. Upon treatment with 2 equivalents of sodium methoxide, scans were taken over a period of one hour at increasing intervals of 2, 5, and 10 minutes. Selected spectra have been shown in stacked plots (Figure 2.20).

At this time, structures corresponding to product or intermediate formation have not been fully elucidated, although we know from GC-MS analysis (Figure 2.21) of this sample that the (trifluorophenyl)-diphenylmethanol (**110**) undergoes fragmentation to form a trifluoroaryl species and benzophenone (**113**). Scheme 2.9 (pg. 49) summarizes this reaction.

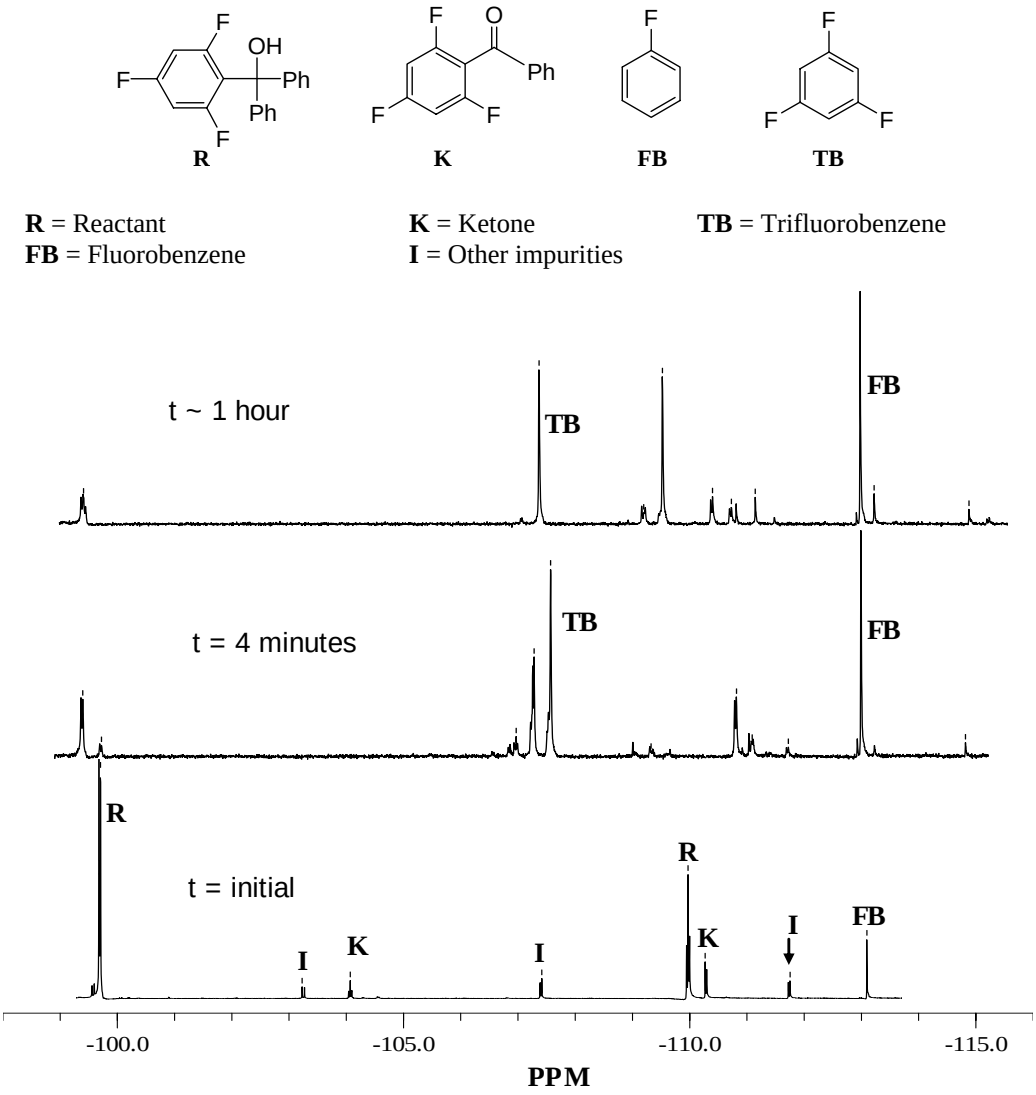

Figure 2.20. Stacked ^{19}F NMR specta showing fragmentation of Diphenyl-(2,4,6-trifluorophenyl)methanol (**110**).

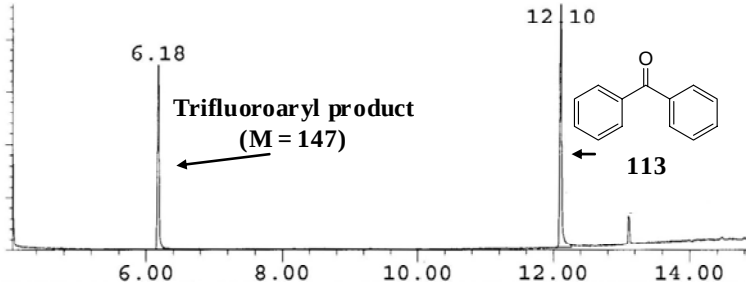

Figure 2.21. GC-MS analysis showing fragmentation of Diphenyl-(2,4,6-trifluorophenyl)methanol (**110**).

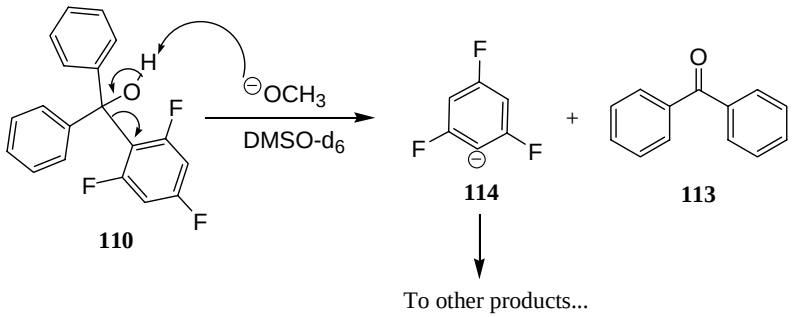

Scheme 2.9. Summary of the observed fragmention of Diphenyl-(2,4,6-trifluorophenyl)methanol (**110**).

Solvent Interactions: Effect on Fragmentation

As discussed earlier in this chapter, the solvent system had a profound effect on the reactivity of pentafluorobenzylic alcohols. In revisiting the solvent ratio studies performed on the *cis*- and *trans*-C_6F_5 alcohols (**88**, **93**), it was interesting to observe rapid fragmentation as the sole reaction in pure DMSO, while introduction of methanol drastically changed the reactivity to mostly substitution. We have noted that this drastic change in reactivity may be due to interactions of the base used. Sodium methoxide, the main base used in this project, tends to get trapped by polar protic solvents such as methanol. Figure 2.22 depicts this concept, where sodium methoxide is being held in a lattice of hydrogen-bonding, which presumably causes loss of basicity. In DMSO, the opposite is depicted, where more methoxy anions are released due to the solvation of sodium.

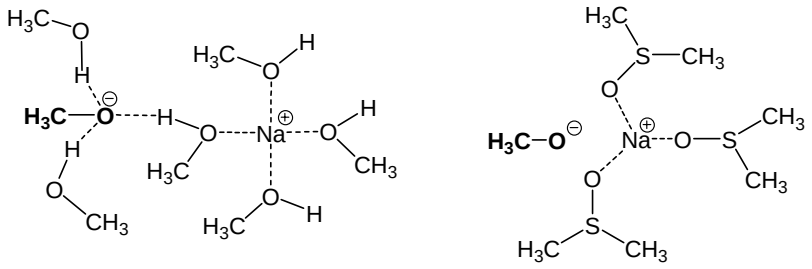

Figure 2.22. Interaction of sodium methoxide within methanol versus DMSO.

Focusing primarily on the fragmentation, though, we wanted to know specifically what types of other solvents either promote or hinder this reaction. In another set of ^{19}F NMR experiments, several representative solvents were chosen and used in a reaction with *cis*-4-tert-butyl-1-(pentafluorophenyl)cyclohexanol (**93**) in equimolar concentrations. A total of seven solvents were examined, which included deuterated benzene (C_6D_6), dimethylformamide (DMF), acetonitrile (CH_3CN), tetrahydrofuran (THF), dichloromethane (CH_2Cl_2), and *tert*-butyl alcohol (*t*-BuOH). For all non-deuterated solvents, an addition of 10% volume ratio of C_6D_6 was used for NMR sample lock. An experiment using DMSO-d_6 was repeated as a standard reaction, and also used as a basis for comparison. Once treated with sodium methoxide (2 equiv.), each reaction

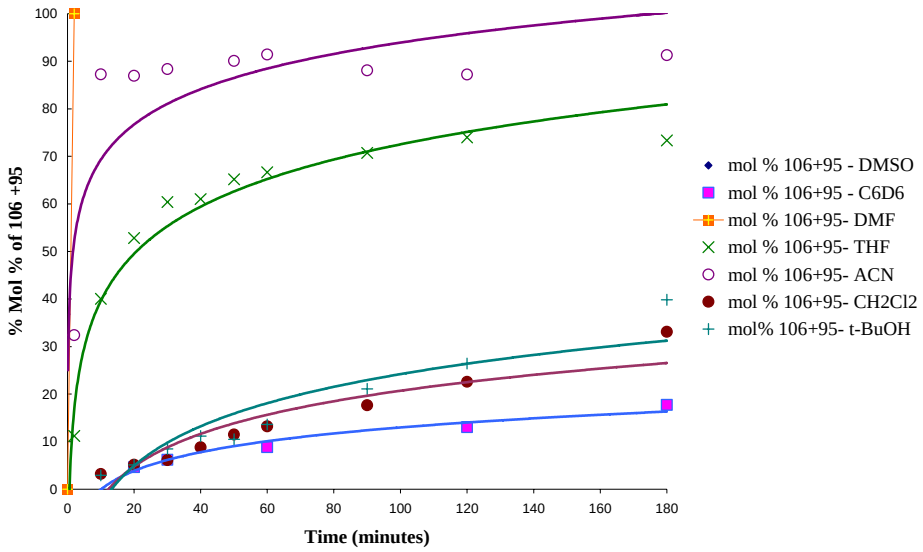

Figure 2.23. Solvent Effect Study on Fragmention: A graph comparing relative formation of **106** and **95** versus time in minutes.

was monitored over a 3 hour time period at 2, 5, 10 minute, and 30 minute intervals between scans. Surprisingly, fragmentation was observed in every solvent, including *t*-BuOH, and the data collected from these trials were used to compare relative rates of

reactivity. In Figure 2.23, a graph correlated from integrations of ^{19}F resonances has been compiled to show rates of formation of pentafluorobenzene (**106**) and tetrafluoroanisole (**95**) versus time in minutes. From the graph given on the previous page, we can show that the rate of fragmentation is influenced by

$$DMSO \sim DMF > CH_3CN > THF > t\text{-}BuOH > CH_2Cl_2 > C_6D_6.$$

Although fragmentation was the primary reaction observed in all of solvent in the following relationship:the solvents studied, THF did promote a small amount of direct substitution product (**100**), as well as rapid formation of dimethoxy species (**96**, **97**) within 10 minutes of reactivity. As mentioned previously, *tert*-butanol showed an uncanny ability to promote fragmentation of *cis*-alcohol (**93**) slightly faster than CH_2Cl_2 or C_6D_6. It was predicted before experimentation that this solvent would be the slowest, and direct *tert*-butoxy substitution (by deprotonation of tert-butanol by base) was also a possibility. Deuterated benzene, however, had the slowest reaction rate of all of the solvents, and upon initiation of reaction the contents within the NMR tube had "greasy" immobilized look after addition of sodium methoxide. It is this immiscibility that may have slowed reactivity within this solvent system. From this study, we have learned that fragmentation occurs in a representative number of solvent systems, and this may be advantageous should an appropriate application be developed.

Other Considerations

Sodium Methoxide vs. Magnesium Methoxide. As we have observed and previously mentioned, sodium methoxide has enhanced basicity in DMSO due to the solvation of the sodium cation in solution, leaving a "bare" methoxide ion. In an experiment using GC-MS analysis, we investigated the change in reactivity based on a

switch in counterion. In this case, we tested magnesium methoxide (0.76 M in CH_3OH) to see if reaction would be slower or faster, based on our assertion that increased solvation of the counterion will increase basicity and therefore further promote fragmentation of the pentafluorobenzylic alcohols. A reaction was prepared using the *cis*-C_6F_5 alcohol (**93**) treated with 3 equivalents of magnesium methoxide in DMSO. The reaction was sampled after 15 minutes and analyzed by GC-MS (Figure 2.24). Based on the GC analysis, about 40% (GC Area %) of the starting alcohol remained after fifteen minutes of reaction time. This is much slower in comparison with reactions using at least 2 equivalents of sodium methoxide, where reaction time is less than 2 minutes for complete fragmentation. The formation of pentafluorobenzene (**106**) was also observed in this reaction, which is rare with typical reactions utilizing DMSO as the solvent.

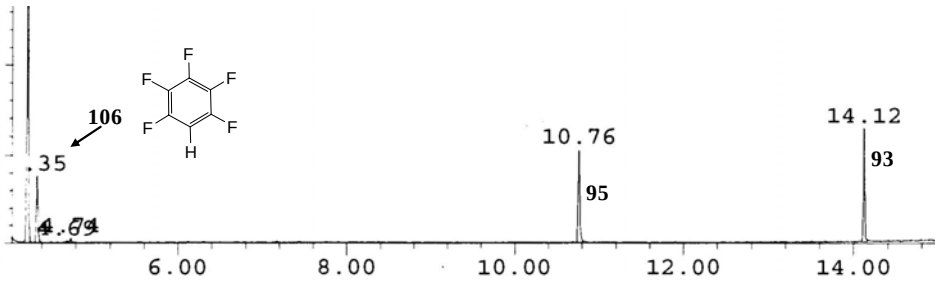

Figure 2.24. GC-MS of *cis*-C_6F_5 alcohol (**93**) reaction using $Mg(OCH_3)_2$ in DMSO-d_6.

Isomerization Studies. In most fragmentation reactions discussed so far, *cis*- and *trans*-4-*tert*-butyl-1-(pentafluorophenyl)cyclohexanol (**88**, **93**) have been primarily used, and interconversion between the two species has not been observed. The *trans*-isomer with its sterically hindered aryl ring would appear to have a higher propensity to switch stereochemistry. To see if isomerization could occur under the proper conditions, we designed an experiment to induce a change in configuration. Under inert atmosphere, the *trans*-C_6F_5 alcohol (**93**) was treated with 2.7 equivalents of n-butyllithium (2.5 M in

hexanes), and was allowed to react for several hours before being analyzed. Scheme 2.10 depicts the reaction mechanistically, where deprotonation of *trans*-alcohol **88** leads to fragmentation forming the ketone (**94**) and the C_6F_5 anion which is stabilized through lithiation.

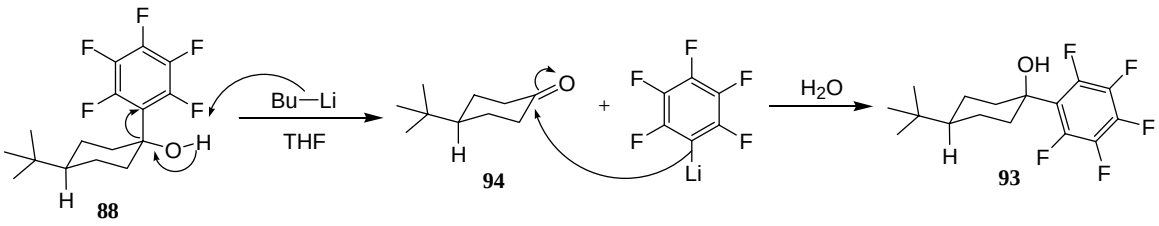

Scheme 2.10. *Trans* to *cis*-C_6F_5 alcohol isomerization using n-butyllithium.

It has been predicted that this lithiated pentafluorobenzene can re-attack the ketone to reform the less sterically hindered *cis*-alcohol (**93**). In Figure 2.25, small amounts of *cis*-alcohol have formed from isomerization of the *trans*-alcohol as observed from the GC-MS analysis. A small amount of 4-*tert*-butylcyclohexanone (**94**) also formed, which confirms the suggested mechanism given in Scheme 2.10.

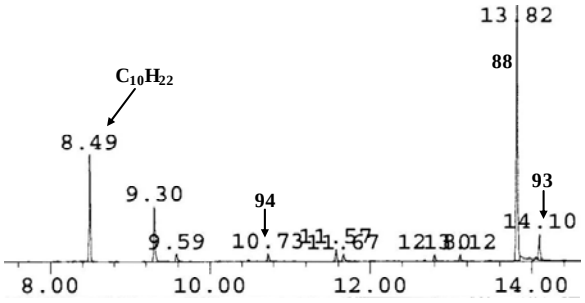

Figure 2.25. GC-MS analysis of *trans*-C_6F_5 alcohol (**88**) isomerization to *cis*-C_6F_5 alcohol (**93**).

Relative Rates of Reactivity

In one final experiment, we wanted to tackle one last question: Which pentafluorobenzylic alcohol fragments faster? Therefore, in another set of reactions, all

six pentafluorobenzylic alcohols (**88**, **93**, **102-105**) were prepared in equal concentrations in separate NMR tubes. A stock solution of 45:55 (v/v) % DMSO-d_6:CH_3OH was prepared to ensure that each of the samples would have precisely the same ratio of solvents. Two microliters of fluorobenzene (1F, -113.26 ppm relative to $CFCl_3$, 0 ppm) was added to each NMR tube as a calibration reference. By automation, each of the samples, once treated with 5 equivalents of sodium methoxide were scanned at 5 minute intervals for the first hour and every 10 minutes every hour after for a total of 8 hours. With the NMR data, we plotted the depletion of starting alcohol over time (Figure 2.26).

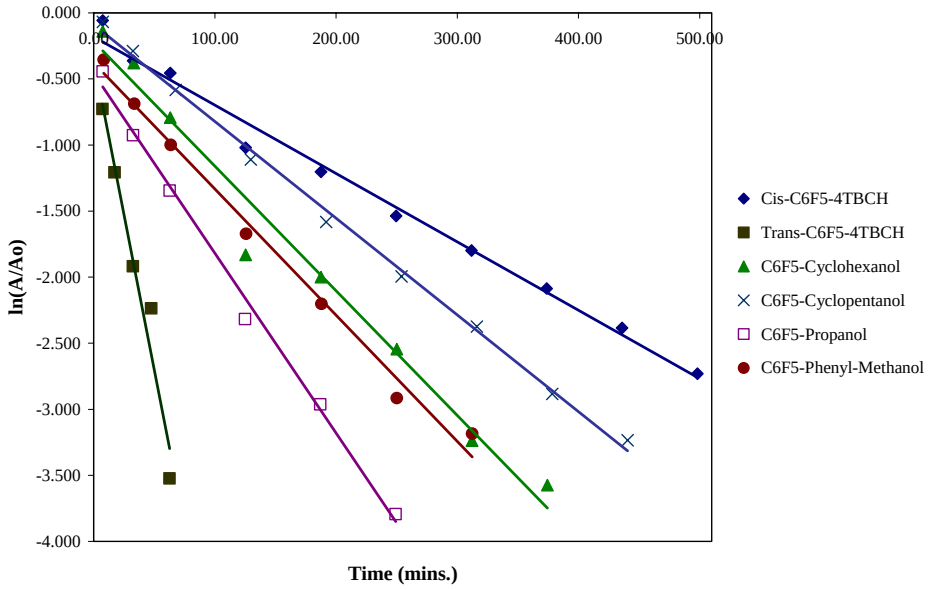

Figure 2.26. The depletion of pentafluorobenzylic alcohols over time reacted with 5 equiv. of $NaOCH_3$ in 45:55 (v/v) % DMSO-d_6:CH_3OH.

Depletion of alcohols in all of the experiments conducted was caused by both fragmentation and aromatic substitution since a mixed solvent system was used. The relative rates of depletion, nonetheless, may be directly correlated to fragmentation as it occurs simultaneously with substitution. Based on the linear plot of $\ln([A]/[A]_0)$ versus

time (min.) above, we can relate the reactivity of each pentafluorobenzylic in these particular reactions by the following order:

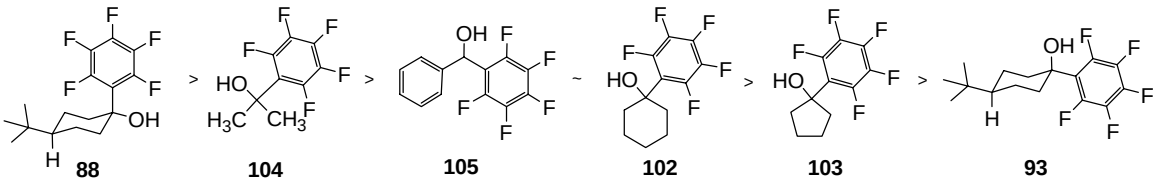

Based on this relationship, it is interesting to note the drastic difference in reactivities between the *cis*- and *trans*-C_6F_5 alcohols (**88**, **93**), where the *cis*-alcohol was still prevalent after an 8 hour period and the *trans* was depleted after 1 hour, as observed with the NMR resonances over time. Also interesting to note is the reactivities of the other alcohols, where the C_6F_5-propanol (**104**) has a higher rate of depletion due its lack of steric hindrance, with depletion of alcohol complete after four hours. Depletion of alcohols **105** to **102** finished an hour apart at 5, 6, and 7 hours, respectively. The linearity of the plots in Figure 2.26, show that the depletion of alcohols studied in this experiment follow pseudo-first order kinetics. The rate order of this reaction can also be attributed to the excess of sodium methoxide used (5 equiv.), forcing first order conditions. A compilation of rate constant values, k_1 and R^2, for each of the alcohols are presented in Table 2.1.

Table 2.1. Rate Constant, k_1, and R^2 Values for Depletion of Pentafluorobenzylic Alcohols **88**, **93**, and **102-105**.

Alcohol	k_1 (sec^{-1})	R^2
93	8.60×10^{-6}	0.9895
88	7.80×10^{-4}	0.9613
102	1.57×10^{-4}	0.9769
103	1.20×10^{-4}	0.9971
104	2.30×10^{-4}	0.9945
105	1.58×10^{-4}	0.9899

Conclusions

As presented in this chapter, the base-catalyzed fragmentation of pentafluorobenzylic alcohols is a malleable reaction that appears to work in many different reaction conditions. We have demonstrated that fragmentation, under base conditions, may work for a large range of structurally variant pentafluorobenzylic alcohols and occurs at differents rates in a representative group of solvents. We have managed to slow the fragmentation reaction using mixed DMSO-CH_3OH system, where a competing substitution reaction occurs, and resulting products fragment themselves. Through the mixed solvent experiments, an exact mechanism of fragmentation was not only determined but observed using ^{19}F NMR as a primary analytical tool. Most importantly, though, we have presented a novel C-C bond cleaving reaction that has not been reported anywhere else in the literature.

Based on all of these findings, we can only speculate the multitude of applications that are possible. So far, we have generally envisioned the fragmentation of pentafluorobenzylic alcohols as a process that can be translated into protecting group chemistry of ketones. Our concept is depicted in Scheme 2.11, where "protection" of a ketone can occur readily using a Grignard reaction. It is predicted, that as long as the reaction is not heated, modifications can be made to the alkyl (R, R') functionalities under moderately acidic conditions. Deprotection of the ketone can then occur under base

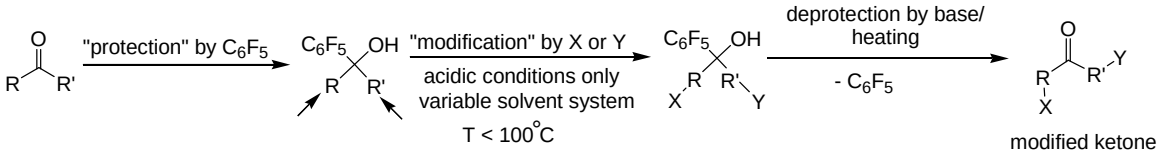

Scheme 2.11. Application of pentafluorobenzylic fragmentation: Ketone protecting groups.

conditions or after significant heating resulting in the desired modification of the ketone. At the moment, this specific application has not been attempted, and this is a future direction of this project.

CHAPTER THREE

Rapid Screening of Potential Metal Catalysts using Modified GC Injection Port Liners

Results and Discussion

General Methods

The analysis of metal catalytic activity on a variety of organic compounds of interest may be accomplished rapidly using our GC injection port method. The efficiency and convenience of this analytical tool is summarized in Figure 3.1. Depending on the

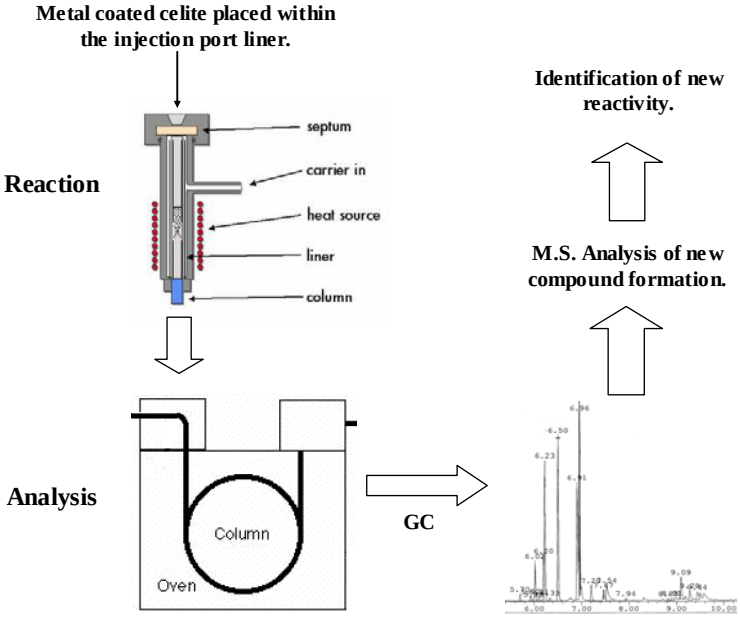

Figure 3.1. Summary of Rapid Screening Method of Catalytic Activity of Metals using GC-MS.

temperature program (start T, end T and ramp rate), reaction and subsequent analysis can be completed in less than 15 minutes/sample, from time of injection to the end of a run. With a mass spectral matching database program, we identified many new peak

formations, and used the percent quality match as a confirmation. For our specific studies, we chose a representative group of thirteen organic molecules, all with differing functionalities such as esters, epoxides, amides, and amines (Figure 3.2). This set of

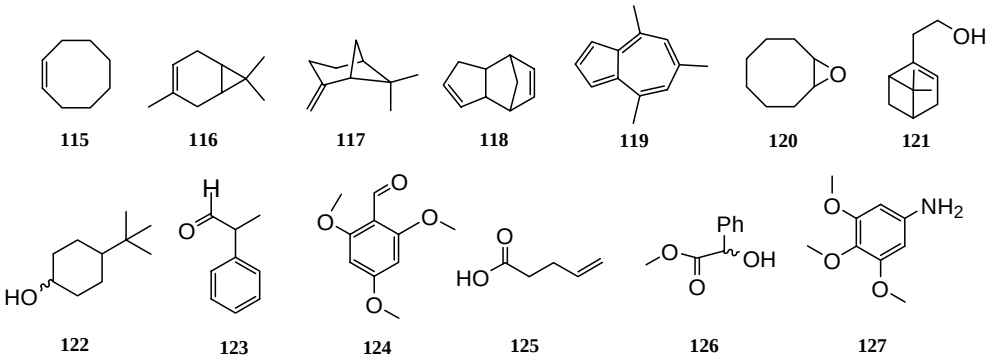

Figure 3.2. Thirteen compounds of varying functionalities chosen to be studied by the rapid screening technique.

compounds, varying also in ring size and aromaticity, were all screened against nine different metal salt "contaminated" liners. Detailed preparation of these liners is discussed in Chapter Four of this thesis. The metal halogen salts chosen for this study had oxidation states of (I), (II), (III), or (IV), which included zinc chloride ($ZnCl_2$), copper chloride ($CuCl_2$), silver perchlorate ($AgClO_4$), zirconium chloride ($ZrCl_4$), rhodium chloride ($RhCl_3$), and ruthenium chloride ($RuCl_3$). Other unusual metal liners that we prepared included hydrogen hexachloroplatinate (H_2PtCl_6), bromopentacarbonylmanganese ($Br(CO)_5Mn$), and cyclopentadienyl tungsten tricarbonyl chloride ($CpW(CO)_3Cl$). Another property we looked for before preparing an injection port liner was solubility of the metal in a solvent such as methanol or ethanol. It was especially important that we get all of our metals into solution so that we could coat it onto our solid support, which in this project was acid-washed Celite™. Once coated onto the Celite™ and evaporated, the material was placed into a new injection port liner and

conditioned before use. In particular, all liners were conditioned at 300° C for several hours in a "retired" Hewlett Packard 5890 GC to make sure that no harmful volatiles, specifically from the metal we used, ruined our analytical column. With the preparation of our GC samples of pre-selected organic compounds, our goal was to observe, liner by liner, what new reactions could be discovered by this technique. The bulk of this chapter will highlight some of the most representative and interesting reactions observed.

Trends Involving Catalytic Reactivity

Strained Bicyclic Organic Molecules. At the beginning of this project, trends and similar reactivities were immediately observed amongst the bicyclic and strained organic compounds such as β-pinene (**117**), nopol (**121**), and 3-carene (**116**). These molecules, in particular, were prone to ring cleaving reactions when passed through most metal liners. It should be noted that these compounds are stable when passed through clean liners at 250° C. β-Pinene (**117**), for example, was observed to be extremely reactive towards $CuCl_2$ and $ZrCl_4$. In both experiments, similar products were produced all related to cleavage of its strained ring system. Scheme 3.1 shows the major products based on observations from the GC-MS analysis of both liners.

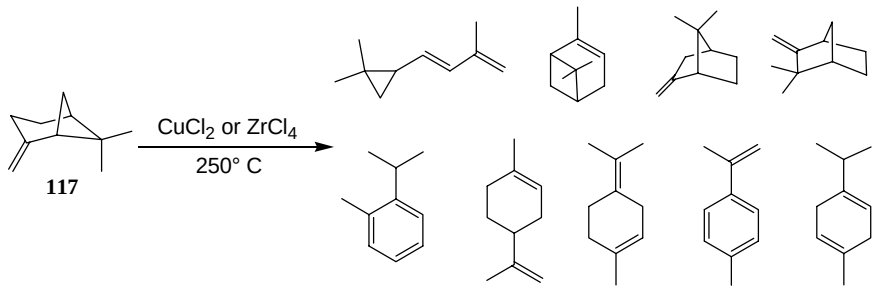

Scheme 3.1. Common cleavage products of β-Pinene as passed through either liners prepared with $CuCl_2$ or $ZrCl_4$.

Nopol (**121**) formed several of the same products as β-pinene (**117**), since structurally they share the same bicyclic structure. This compound, however, also showed unique reactivity towards several different liners. Though small percentages of ring cleavage products such as limonene or α-pinene were formed in 1-2 area %, loss of the ethanol chain also occurred in a retro-ene reaction to form β-pinene (**117**). Several liners such as $CuCl_2$, $ZnCl_2$, $Br(CO)_5Mn$, $ZrCl_4$, and $AgClO_4$ also promoted this reaction. The GC-MS analysis in Figure 3.3 shows that nopol (**121**) largely remains unreacted after passing through the $AgClO_4$-treated liner; however the formation of β-pinene was the most abundant reaction product with this liner.

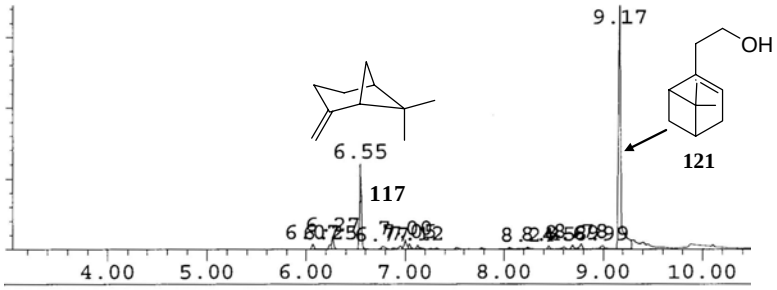

Figure 3.3. Silver facilitated retro-Ene reaction of Nopol (**121**) forming β-Pinene (**117**). This reaction readily occurred with other metal liners.

3-Carene (**116**), surprisingly, showed great resilience towards all of the metal liners analyzed. Most rearrangement and ring-cleaving reactions barely occurred, with 3-carene staying mostly intact through all of the runs. Of all of the metal liners analyzed, though, $RhCl_3$ showed the greatest reactivity towards 3-carene. The GC-MS analysis (Figure 3.4) shows that two main products have formed from ring cleavage, which have gained aromaticity to form *ortho*- and *para*-cymene (**128**, **129**) giving peaks of 16% and 17%, respectively, relative to 3-carene (**116**).

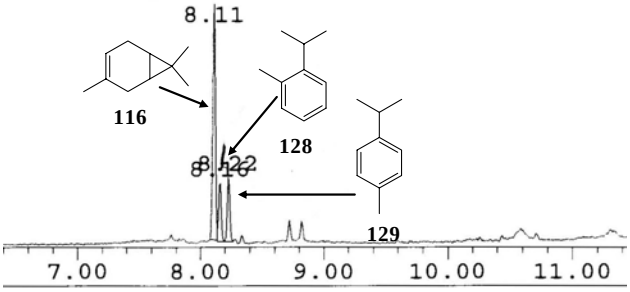

Figure 3.4. Significant ring cleavage products of 3-carene (**116**) after passage through a $RhCl_3$ liner.

*Hydrolysis and Oxidation Reactions of 4-tert-Butylcyclohexanol (**122**).*

Predictable yet interesting reactions occurred with 4-*tert*-butylcyclohexanol (**122**). When passed through $ZnCl_2$, $CuCl_2$, and $AgClO_4$, the alcohol formed dehydration products (**130**). Formation of the cyclohexenes (**130**) was observed with GC-MS analysis of 4-*tert*-butylcyclohexanol (**122**) passed through a $ZnCl_2$ liner (Figure 3.5). Another reaction

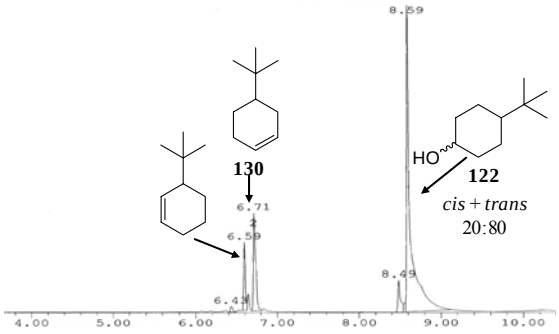

Figure 3.5. GC-MS analysis of 4-*tert*-butylcyclohexanol (**122**) after passage through a $ZnCl_2$ liner.

was also observed with 4-*tert*-butylcyclohexanol (**122**) passed through liners prepared with $ZrCl_4$ and $RuCl_3$. In addition to dehydration, oxidation was also observed by GC-MS analysis (Figure 3.6). The new product formation at 10.1 minutes was identified as 4-*tert*-butylcyclohexanone (**131**) as a result of ruthenium catalysis. For the $ZrCl_4$ liner, the starting alcohol was completely consumed to form dehydration and oxidation products.

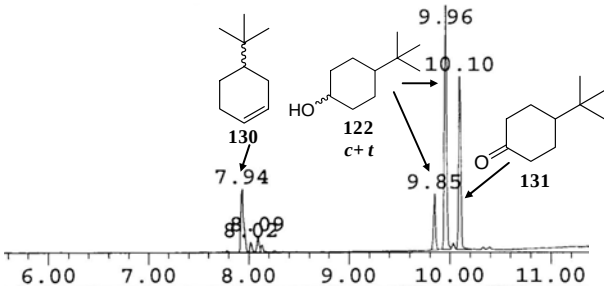

Figure 3.6. GC-MS analysis of 4-*tert*-butylcyclohexanol (**122**) after passage through a $RuCl_3$ liner.

Cyclization of 4-Pentenoic acid. During the study of 4-pentenoic acid (**125**) through a $ZnCl_2$ liner, a cyclization product was identified. By GC-MS analysis, we observed that not only did changes in the retention time occur, but that the MS data also showed different fragmentation patterns in comparison with the carboxylic acid (Figure 3.7). The spectral matching program used in this project identified the new compound as 5-methyl-dihydrofuran-2-one (**132**), which had an acceptable quality match of 91%.

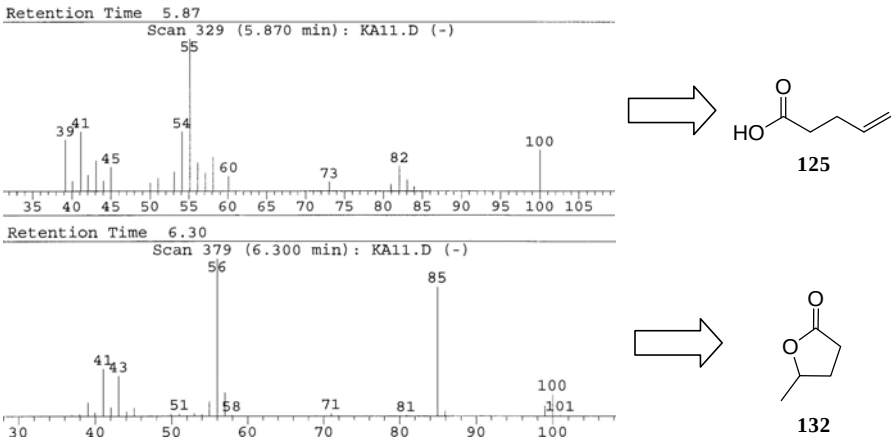

Figure 3.7. Mass Spectral matching analysis identified a cyclization product of 4-pentenoic acid (**125**) after passage through a $ZnCl_2$ liner.

Cycloaddition of Dicyclopentadiene. One of the most interesting reactions that was observed by our rapid screening method was the cycloaddition of dicyclopentadiene (**118**). In exposing this particular molecule to several different metals such as $ZrCl_4$, $Br(CO)_5Mn$, $AgClO_4$, $CuCl_2$, and $CpW(CO)_3Cl$, we noticed a significant product with

four minutes longer retention time than the starting material and 66 mass units heavier (Figure 3.8). Initially this reaction was confusing but upon further analysis it was apparent that the new product was a result of a [2+2] cycloaddition of cyclopentadiene to dicyclopentadiene. In Scheme 3.2, a mechanism for this reaction has been rationalized, where under high temperatures dicyclopentadiene appears to also undergo a retro-Diels Alder to form cyclopentadiene that then does a 4 + 2 cycloaddition to dicyclopentadiene.

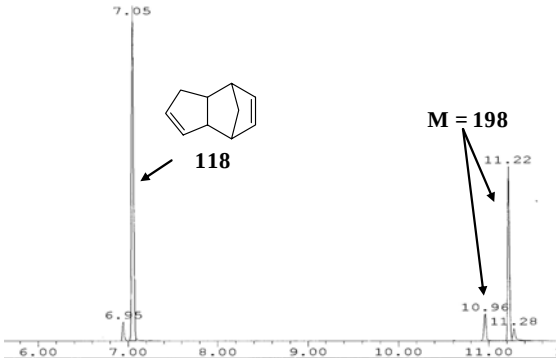

Figure 3.8. GC-MS analysis of dicyclopentadiene (**118**) after passage through $AgClO_4$.

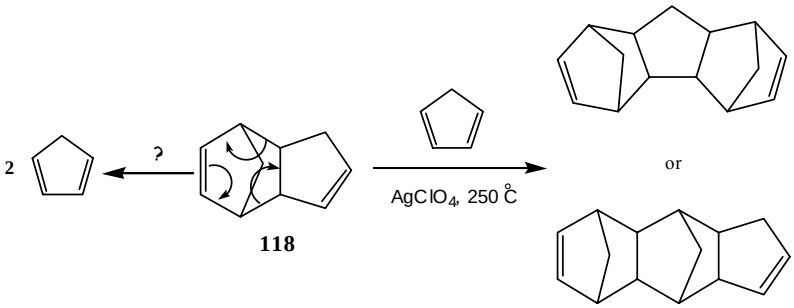

Scheme 3.2. Suggested Mechanism for cycloaddition of dicyclopentadiene (**118**).

Curiously, these results could not be replicated when these experiments were repeated. When dicyclopentadiene was screened for reactivity using a new $AgClO_4$ liner, no product formation occurred. At this point, some five months later, the dicyclopentadiene was replaced with a new bottle and the GC was fitted with a new column. The fact that we have observed the dicyclopentadiene reaction with other metal liners would seem to

suggest that this is not the only factor involved with the cycloaddition. We can only hypothesize that the occurrence of reactivity lies with the dicyclopentadiene itself, where with an older supply of reagent the source of cyclopentadiene is greater. This availability of free cyclopentadiene was the main driving factor for the cycloaddition of dicyclopentadiene.

Carbon-Carbon Bond Insertion Reaction of Cyclooctene. In rapid screening studies using cyclooctene, an interesting carbon-carbon bond inserting reaction was observed. Using a $RuCl_3$–treated liner, a new molecule was identified by GC-MS (Figure 3.9) and formed in nearly a 100% yield. At this point, this was the cleanest reaction observed from any organic molecule screened against a metal liner. From this exciting

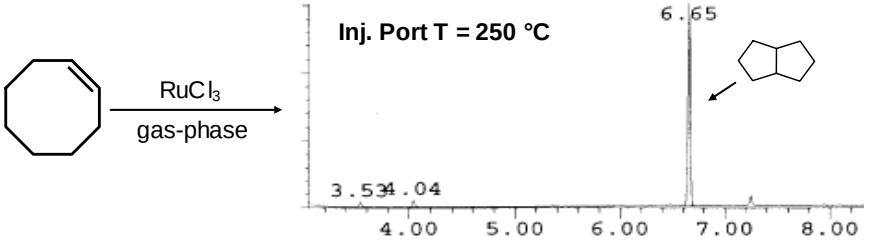

Figure 3.9. Cyclooctene (**115**) after passage through a $RuCl_3$ liner formed octahydropentalene (**133**).

result, an experiment was conducted to see if we could translate this reactivity from gas-phase (GC) conditions to solution at lower reaction temperatures. In a pressure tube reaction, cyclooctene (1 mL) and $RuCl_3$ (5 wt. %) were combined and heated in the oven for 1 week at 150° C. Although not as clean as the gas-phase reaction, the ruthenium catalyzed carbon-carbon bond insertion still occurred (Figure 3.10).

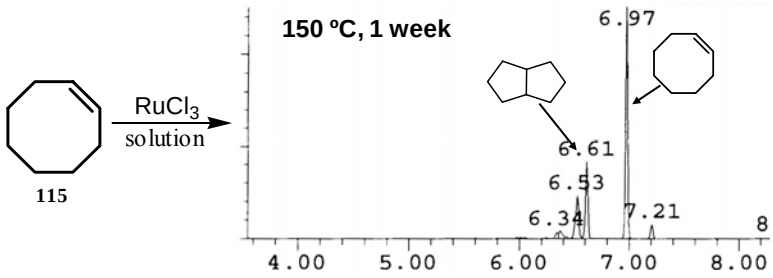

Figure 3.10. GC-MS analysis of cyclooctene reacted with $RuCl_3$ for 1 week.

Fragmentation Analysis of Pentafluorobenzylic Alcohols using a $NaOCH_3$ Liner

In a final experiment, we wanted to demonstrate the versatility of our rapid screening technique by studying the nature of base catalysis on molecules of interest. Naturally, the first experiment prepared involved testing the fragmentation of pentafluorobenzylic alcohols as passed through a base-coated liner. In this case, a liner was prepared with 5% by weight sodium methoxide coated onto Celite™. This liner was conditioned for 1 hour at 300° C before use. *Cis*-4-*tert*-butyl-1-(pentaflurophenyl)-cyclohexanol (**93**), the compound used in many of the fragmentation experiments discussed in Chapter Two, was first passed through a clean liner and analyzed by GC-MS for reference (Figure 3.11). The *cis*-alcohol (**93**) was then passed through the sodium

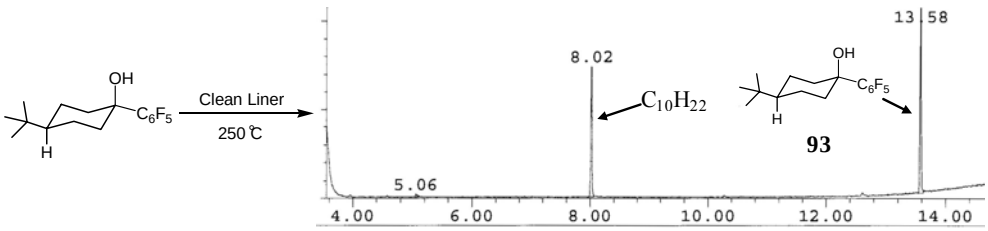

Figure 3.11. GC-MS of *cis*-C_6F_5 Alcohol (**93**) after passage through a clean liner. Note: $C_{10}H_{22}$ was used as an internal standard.

methoxide prepared liner and analyzed for reactivity. GC-MS analysis of this run showed that complete fragmentation of the *cis*-alcohol occurred (Figure 3.12). Based on this observation, it is clear that gas-phase conditions also promote the fragmentation of pentafluorobenzylic alcohols.

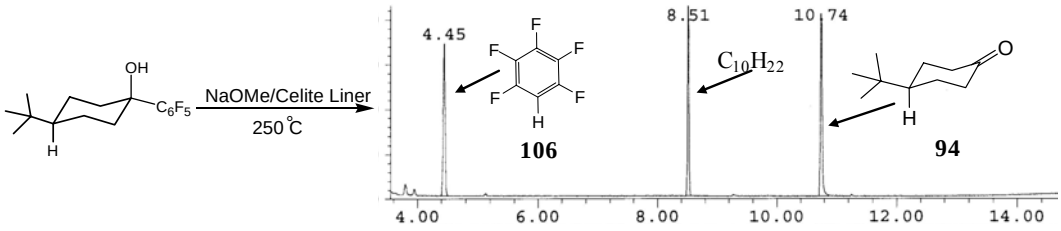

Figure 3.12. GC-MS of *cis*-C_6F_5 Alcohol (**93**) after passage through the sodium methoxide liner. Note:$C_{10}H_{22}$ was used as an internal standard

Conclusion

The use of modified injection port liners in the screening of potential metal catalysts has been presented in this chapter. We have demonstrated that a large range of compounds can be analyzed rapidly and efficiently through our technique. For the select group of organic molecules we studied in this project, we have shown that both predicable and unique reactivities towards any given metal catalyst can occur. It is also our hope, as demonstrated with the fragmentation example, that this rapid screening technique can be used to the study of other types of reactivities beyond metals, such as base or acid catalysis of organic molecules.

CHAPTER FOUR

Experimental

General Methods

All reactions involving air- or moisture-sensitive reagents were carried out under inert atmosphere of argon or nitrogen. The argon was the purified grade (≤ 3 ppm 0_2, H_2O). A vacuum/inert atmosphere double manifold was used to remove air and introduce argon or nitrogen to a reaction system. The manifold was maintained under static pressure using inert gas, with an oil-filled bubbler isolating the system from the atmosphere.

All glassware was oven-dried as necessary. Anhydrous solvents and liquid reagents were transferred by syringe or cannula through a septum. Syringe and needles were stored in an oven prior to use. Anhydrous solvents, such as diethyl ether, were purchased from either the Aldrich Chemical Company or ACROS Chemical. Solvents such as ethyl acetate, hexanes, and dichloromethane used for chromatography and workups were obtained from VWR International and distilled prior to use. Most chemicals needed for synthesis were commercially available from Aldrich, ACROS, or VWR International. The pentafluorophenyl magnesium bromide used in the Grignard reactions for this study was purchased from Aldrich as a 0.5 M solution in diethyl ether. Deionized (DI) water was used to prepare aqueous solutions. Methanol purchased from EMD was used as the main solvent for coating metal chloride salts onto Celite™. The Celite™ was purchased from Aldrich and acid-washed before use.

Chromatography

Thin layer chromatography plates (silica, 0.25 mm layer) were purchased from Silicycle or Whatman and visualized using UV irradiation, PMA or vanillin staining. Flash chromatography was performed with 230-400 mesh silica gel obtained from EM Science. Concentration of isolated samples was accomplished *in vacuo* using rotary evaporation with a water aspirator. Additional evaporation to constant weight of a sample was done using mechanical pump vacuum at 0.1 Torr of pressure. Capillary gas chromatography (GC) was performed using a Hewlett Packard 5890 Series II equipped with an SE-54 column (30 m x 0.25 mm) with helium or hydrogen carrier and FID detection. Gas chromatography-mass spectroscopy (GC-MS) was performed with a Hewlett Packard G1800A GCD system with electron impact ionization. In some instances, a HP 6890 Series autoinjector with automatic sample loader was used for multiple samples, and to minimize slight change in retention time that is caused by manual injection error.

Instrumentation

^{1}H , ^{13}C, and ^{19}F NMR were obtained using a Bruker DPX-300 spectrometer operating at 300 MHz for proton, 75 MHz for carbon, and 282 MHz for fluorine. A Bruker AMX-360 spectrometer was also used operating at 360 MHz for proton and 90 MHz for carbon. Unless otherwise stated, DMSO-d_6 was used as the solvent reference (2.48 ppm for ^{1}H). Fluorobenzene (singlet (s), -113.26 ppm, relative to CCl_3F (s) at 0 ppm) was used as a fluorine reference for all ^{19}F NMR experiments. Chemical shifts were expressed in ppm (δ) and peaks reported as singlets (s), doublets (d), double-doublets (dd), triplets (t), triplet of doublets (td), or multiplets (m) with all coupling constants (J) expressed in Hertz (Hz).

The X-ray structure of *trans*-4-tert-butyl-(2,3,5,6-tetrafluoro-4-methoxy-phenyl)-cyclohexanol (**101**) was determined by Dr. Kevin K. Klausmeyer. The crystals were placed in Paratone oil, affixed to a cryo-loop and immediately placed in the nitrogen cold stream. Diffracted intensities were collected on a Bruker-Nonius X8 APEX diffractometer using graphite-monochromated MoKα- X-radiation. The data was corrected for Lorentz, polarization and X-ray absorption effects, the latter using the program SADABS. The structure was solved by direct methods which gave positions of all non-hydrogen atoms using SHELXTL ver. 6.12. Refinements were made by full-matrix least squares on all F^2 data using SHELXL. Anisotropic thermal parameters were included for all non-hydrogen atoms.

Experimental Procedures

Cis- and trans-4-tert-Butyl-1-(pentafluorophenyl)cyclohexanol **(93, 88)**: Pentafluorophenylmagnesium bromide (25 mL, 12.5 mmol) was added under inert atmosphere to a 50 mL round bottom flask containing a stir bar. The flask was cooled by a dry ice and acetone bath to -78 ºC. A solution of 4-*tert*-butylcyclohexanone (1.556 g, 10.1 mmol) in 2 mL of anhydrous ether was added dropwise to the stirring Grignard reagent. The reaction mixture was allowed to stir for 15 minutes, then warmed slowly to room temperature. The solution was then treated cautiously with 20 mL of saturated NH_4Cl aqueous solution. A light brown precipitate immediately formed upon addition of NH_4Cl, and this mixture transferred to a separatory funnel with additional ether. The organic layer was separated and washed once with a saturated NaCl solution, then dried using $MgSO_4$. The organic layer was rotary evaporated down till a brown gel formed on the bottom of the recovery flask, and further solidification occurred under pump vacuum.

The isomers were purified with column chromatography using 100% dichloromethane as eluent. The *cis* and *trans* isomers are easily separated, with the *trans* isomer eluting after the *cis* isomer. *Cis*- isomer: ^{1}H NMR (360 MHz, $CDCl_3$) δ 2.31 (t, 3 Hz, 1H), 2.15 (d, 14 Hz, 2H), 2.02 (t, 14 Hz, 2H), 1.67 (m, 2H), 1.57 (m, 2H), 1.11 (tt, 4, 8 Hz, 1H), 0.89 (s, 9H); ^{13}C NMR (90 MHz, $CDCl_3$) δ 146.6, 143.8, 141.2, 139.2, 138.4, 136.7, 121.6, 74.9, 47.1, 37.7, 32.5, 27.5, 22.3; ^{19}F NMR (282 MHz, DMSO-d_6): δ -139.15 (dd, J = 23, 6 Hz, 2F), -158.09 (t, J = 23 Hz, 1F), -163.55 (td, J = 23, 6 Hz, 2F). GC-MS: 322, 57 (base).

Trans- isomer: ^{1}H NMR (360 MHz, $CDCl_3$) δ 2.76 (d, 13 Hz, 2H), 1.81 (d, 13 Hz, 2H), 1.64 (t, 14 Hz, 2H), 1.16 (q, 12 Hz, 1H), 1.05 (m, 2H), 0.82 (s, 9H); ^{13}C NMR (90 MHz, $CDCl_3$) δ 147.6, 144.8, 141.6, 139.4, 136.7, 118.15, 76.0, 47.2, 40.0, 33.4, 32.2, 27.5, 25.1, 20.9; ^{19}F NMR (282 MHz, DMSO-d_6):δ -138.20 (dd, J = 23, 6 Hz, 2F), -157.16 (t, J = 23 Hz, 1F), -163.41 (td, J = 23, 6 Hz, 1F). GC-MS: 322, 57 (base).

1-(Pentafluorophenyl)cyclohexanol **(102)**: Pentafluorophenylmagnesium bromide (20 mL, 10.0 mmol) was added under inert atmosphere to a 50 mL round bottom flask containing a stir bar, and cooled to -78 ºC using a dry ice/acetone bath. Cyclohexanone (1.040 mL, 10.0 mmol) was added dropwise to the stirring Grignard reagent. The mixture stirred briefly and was allowed to warm to room temperature. The reaction was treated with 20 mL of saturated NH_4Cl solution, and a solid precipitated out of solution. The crude product was extracted using an additional 20 mL of ether using a separatory funnel. The organic layer was washed once with saturated NaCl solution and dried with $MgSO_4$. The crude solution was concentrated down to a brown solid. The final product was purified with column chromatography using 100% dichloromethane as eluent. Concentration yielded a fine yellow powder. ^{1}H NMR (360 MHz, $CDCl_3$) δ 2.34 (s, 1H), 2.06 (m, 4H), 1.76 (m, 3H), 1.61 (m, 2H), 1.25 (ddt, J=9.0, 6.0, 3.0 Hz, 1H); ^{13}C NMR

(90 MHz, $CDCl_3$) δ 146.5, 143.8, 141.2, 139.3, 138.4, 136.5, 121.6, 75.3, 37.3, 25.2, 21.5; ^{19}F NMR: δ -139.33 (dd, J = 23, 6 Hz, 2F), -158.11 (t, J = 23 Hz, 1F), -163.54 (td, J = 23, 6 Hz, 2F). GC-MS: 266, 210 (base).

1-(Pentafluorophenyl)cyclopentanol **(103)**: Pentafluorophenylmagnesium bromide (20 mL, 10.0 mmol) was added under inert atmosphere into a 50 mL round bottom flask containing a stir bar, and cooled to -78 ºC using a dry ice/acetone bath. Cyclopentanone (0.88 mL, 9.95 mmol) was added dropwise to the stirring Grignard reagent. After 15 minutes, the mixture was allowed to warm to room temperature. Saturated NH_4Cl (20 mL) was added slowly to the mixture, causing a precipitate to form out of solution. The crude product was extracted using 20 mL of ether, and the organic phase was washed once with saturated NaCl solution. The organic phase was dried with $MgSO_4$, filtered, and concentrated. Purification was done by column chromatography using 100% dichloromethane and separated any unreacted starting ketone from the product. The final product was concentrated in vacuo, where a yellow crystalline solid formed. ^1H NMR (360 MHz, $CDCl_3$) δ 2.36 (m, 2H), 2.09 (m, 2H), 1.93 (m, 2H), 1.80 (m, 2H); ^{13}C NMR (90 MHz, $CDCl_3$) δ 146.6, 143.9, 141.5, 139.0, 119.2, 81.2, 40.4, 22.4; ^{19}F NMR:δ -138.08 (dd, J = 23, 6 Hz, 2F), -157.82 (t, J = 23 Hz, 1F), -163.68 (td, J = 23, 6 Hz, 2F). GC-MS: 252, 223 (base).

2-Pentafluorophenyl-2-propanol **(104)**: In a 100 mL pear-shaped flask with stir vane, pentafluorophenylmagnesium bromide (25 mL, 12.5 mmol) was added under inert atmosphere and cooled to -78 ºC using a dry ice/acetone bath. Distilled acetone (0.924 mL, 12.5 mmol) was added dropwise into the Grignard reagent with good stirring. The reaction was allowed to stir for 15 minutes, then to warm up to room temperature. Saturated NH_4Cl solution (20 mL) was added slowly to the mixture, followed by an more

ether (20 mL). The organic phase was separated, washed once with saturated NaCl solution and dried with $MgSO_4$. This product was purified using column chromatography using 100% dichloromethane as eluent. The fractions of isolated, purified product were concentrated in vacuo to yield a dark brown oil. ^{1}H NMR (300 MHz, $CDCl_3$) δ 1.73 (t, 2 Hz, 6H); ^{13}C NMR (90 MHz, $CDCl_3$) δ 146.2, 143.4, 141.3, 139.3, 138.5, 136.5, 121.1, 73.3, 30.3; ^{19}F NMR:δ -139.61 (dd, J = 23, 6 Hz, 2F), -158.21 (t, J = 23 Hz, 1F), -163.71 (td, J = 23, 6Hz, 2F). GC-MS: 226, 211 (base).

1-Pentafluorophenyl-1-phenyl-methanol **(105)**: Pentafluorophenylmagnesium bromide (25 mL, 12.5 mmol) was added under inert atmosphere to a 100 mL pear-shaped flask with stir vane and cooled to -78 ºC using a dry ice/acetone bath. Benzaldehyde (1 mL, 9.85 mmol) was added dropwise to the Grignard reagent. The reaction was allowed to stir for 15 minutes and warm to room temperature before workup. Saturated NH_4Cl (20 mL) was added to the mixture, followed by ether (20 mL). The organic phase was separated, washed once with saturated NaCl solution and dried with $MgSO_4$. The crude product was purified with column chromatography using 100% dichloromethane as eluent. The product was brought to constant weight under vacuum to yield a dark brown oil. ^{1}H NMR (300 MHz, $CDCl_3$) δ 7.35 (m, 6H), 6.22 (s, 1H); ^{13}C NMR (75 MHz, $CDCl_3$) δ 192.7, 146.3, 143.0, 142.4, 139.3, 135.9, 117.0, 67.5; ^{19}F NMR:δ -143.26 (dd, J = 23, 8.5 Hz, 2F), -153.33 (t, J = 23 Hz), -162.85 (td, J = 23, 8.5 Hz, 2F). GC-MS: 274, 79 (base).

Diphenyl-(2,4,6-trifluorophenyl)methanol (**110**): 2,4,6-Trifluorobenzonitrile (2.0 d, 12.7 mmol) and copper(I) chloride (57 mg, 0.424 mmol) were weighed out in a round bottom flask with stir bar and placed under inert atmosphere. Both reagents were dissolved in 20 mL of anhydrous THF, and at good stir, 10 mL of 3.0 M

phenylmagnesium bromide (30 mmol) was added. This reaction was allowed to reflux for 2 hours. Once cooled to ambient temperature, 40 mL of aqueous H_2SO_4 (15% in water) was added, and the reaction was allowed to stir for 2 hours. The crude product was extracted with excess ether (3 x 15 mL), dried with magnesium sulfate, and concentrated. This product was subsequently purified by column chromatography 15 to 75% CH_2Cl/Hexanes with 0.332 g of isolated diphenyl-(2,4,6-trifluorophenyl)methanone (**112**). The isolated ketone was then treated with 2 mL of phenylmagnesium bromide (6 mmol) and allowed to react overnight. The resulting alcohol (**110**) was treated treated with acid, extracted with excess ether, and purified by column chromatography using 10-20% EtOAc/Hex. ^{19}F NMR:δ -99.24 (d, J = 7.68 Hz, 2F), -109.99 (t, J = 7.47 Hz, 1F). GC-MS: 314, 159 (base).

Fragmentation reaction of pentafluorobenzylic alcohols: Purified alcohols (20 mg) were weighed into 25 mL round bottom flasks with small stir bar and rubber septa for GC-monitored reactions or weighed directly into oven-dry NMR tubes for ^{19}F NMR-monitored experiments. Deuterated dimethylsulfoxide (0.6 mL) were used in both types of experiments, as was the sodium methoxide (4.37 M in methanol, 2 equivalents). GC-monitored reactions were sampled at regular time intervals, and worked up with distilled water and volatile solvent such as distilled dichloromethane, hexanes, or 2-methylbutane. The organic layer was dried with $MgSO_4$, filtered, and analyzed by GC-MS.

Preparation of samples for use in gas-phase GC injection port microreactions: Selected organic compounds with varying functionalities were prepared similarly for GC-MS analysis. For liquid compounds, between 10 to 20 μL of compound was placed in a 2 mL glass GC vial with septum cap. Distilled dichloromethane was filled to the 1.5 mL

mark on all samples. For solid compounds, about 2-5 milligrams of compound was weighed directly into the vial and dissolved with dichloromethane up to the 1.5 mL mark.

Preparation of metal-coated Celite™ for use in gas-phase GC injection port microreactions: Acid-washed Celite™ (1 g) was weighed out in a 25 mL round bottom flask. Metal chloride salts (50 mg, 5% weight relative to Celite™) were weighed into glass 4-dram vials and dissolved with 2 mL of methanol. The dissolved metal salt solution was added to the acid-washed Celite™ with an addition of 3-5 mL of methanol to wash out the vial and coat all of the Celite™. The suspension was rotary evaporated using a fritted 14/20 size glass adapter attachment to ensure that the Celite™ remained in the flask. The Celite™ was dried in an oven at 80 ºC for several hours before use. The metal-coated Celite™ was packed carefully at a depth of 12 mm in new glass injection port liners (4 mm-diameter, 79 mm-length) manufactured by SGE (Part no. 092219). All metallated injection port liners were conditioned under N_2 for a period of 24 hours in a separate Hewlett-Packard 5890 GC at 250 ºC before experimentation commenced to minimize possible damage to the capillary column from harmful volatiles.

APPENDICES

APPENDIX A

LIST OF FIGURES

LIST OF TABLES

Table A.1. A reference of fluorine-19 NMR chemical shifts of the major compounds studied.

	^{19}F Chemical Shifts (PPM)	**No. of Equivalent F's/ Splitting Pattern**	**Assignment (relative to H or alkyl group)**
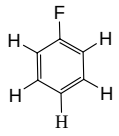 Mol. Wt.: 96.1 g/mol	-113.26* (calibrated using CCl_3F at 0.00)	1F, s	Para
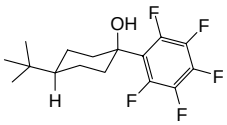 Mol. Wt.: 322 g/mol	-139.07 -158.52 -163.81	2F, ddd 1F, t 2F, td	Ortho Para Meta
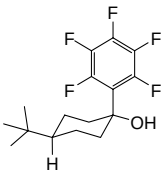 Mol. Wt.: 322 g/mol	-137.95 -156.93 -163.19	2F, ddd 1F, t 2F, td	Ortho Para Meta
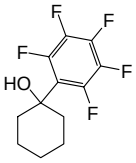 Mol. Wt.: 266 g/mol	-139.32 -158.02 -163.53	2F, ddd 1F, t 2F, td	Ortho Para Meta
 Mol. Wt. 252 g/mol	-138.07 -157.81 -163.68	2F, ddd 1F, t 2F, td	Ortho Para Meta
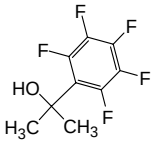 Mol. Wt.: 226 g/mol	-139.59 -158.18 -163.72	2F, ddd 1F, t 2F, td	Ortho Para Meta
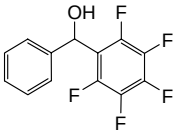 Mol. Wt.: 273 g/mol	-143.31 -156.29 -162.84	2F, ddd 1F, t 2F, td	Ortho Para Meta

* All fluorine-19 chemical shifts in this project were calibrated using fluorobenzene (-113.26

Table A.2. A reference of fluorine-19 NMR chemical shifts of the major intermediate and products formed during fragmentation and substitution reactions of pentafluorobenzylic alcohols.

	^{19}F Chemical Shifts (PPM)	**No. of Equivalent F's/ Splitting Pattern**	**Assignment (relative to H or alkyl group)**
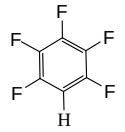 Mol. Wt.: 168 g/mol	-139.14 -155.00 -162.80	2F, dd 1F, t 2F, td	Ortho Para Meta
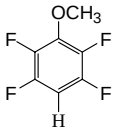 Mol. Wt.: 180 g/mol	-140.50 -158.15	2F, dd 2F, dd	Ortho Meta
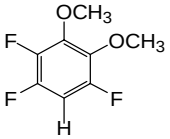 Mol. Wt.: 192 g/mol	-142.40 -156.33 -164.26	1F, dd 1F, d 1F, d	Ortho (L) Ortho (R) Meta
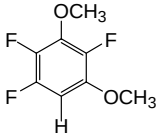 Mol. Wt.: 192 g/mol	-133.68 -141.98 -159.00	1F, d 1F, d 1F, dd	Meta (R) Ortho Meta (L)
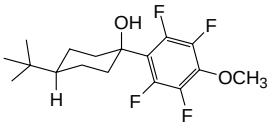 Mol. Wt.: 334 g/mol	-140.60 -159.10	2F, dd 2F, dd	Meta Ortho
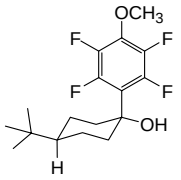 Mol. Wt.: 334 g/mol	-139.14 -158.71	2F, dd 2F, dd	Meta Ortho

* All fluorine-19 chemical shifts in this project were calibrated using fluorobenzene (-113.26 PPM).

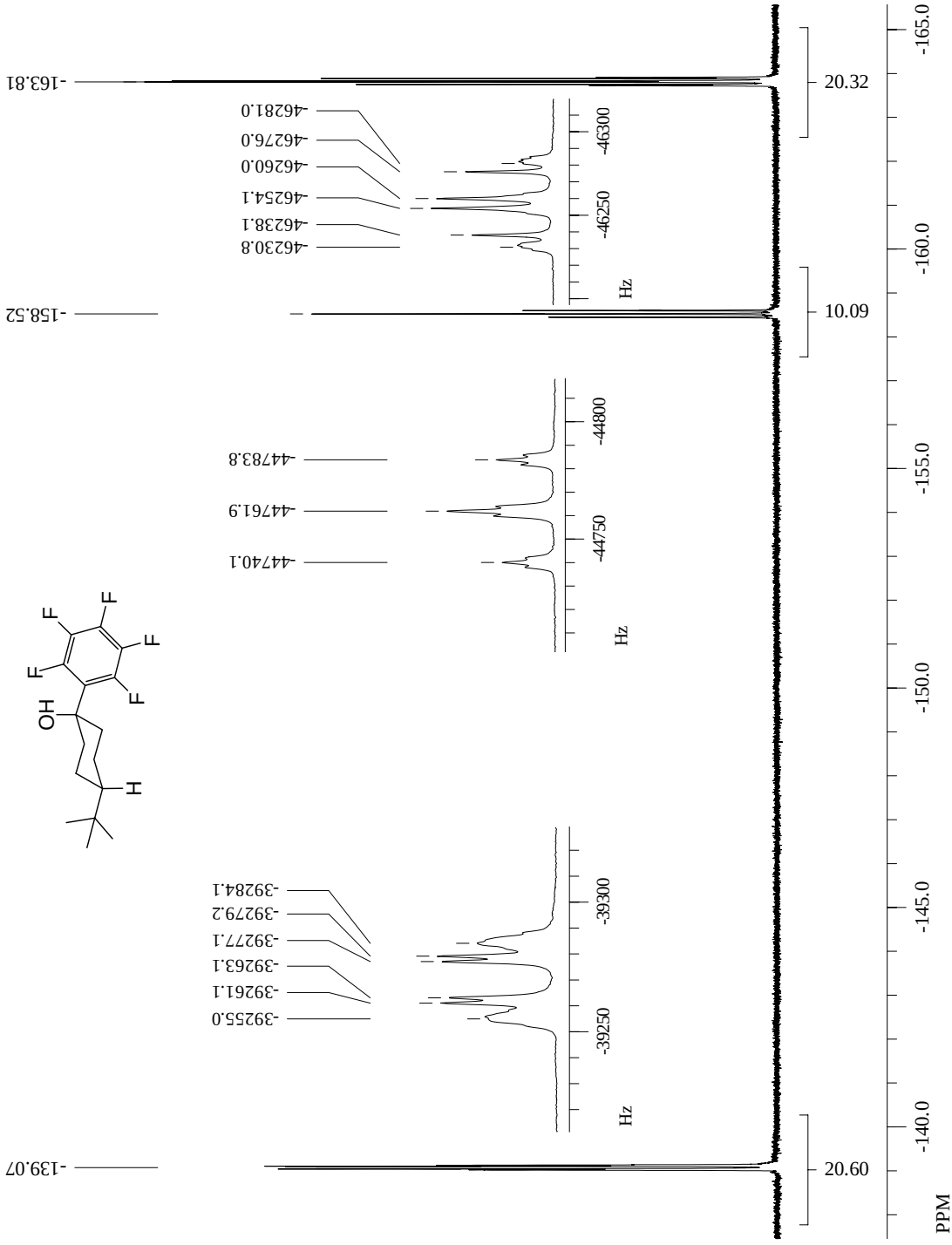

Figure A.1. ^{19}F NMR (282 MHz, DMSO-d_6) of *cis*-4-*tert*-Butyl-1-(pentafluorophenyl)cyclohexanol (**93**).

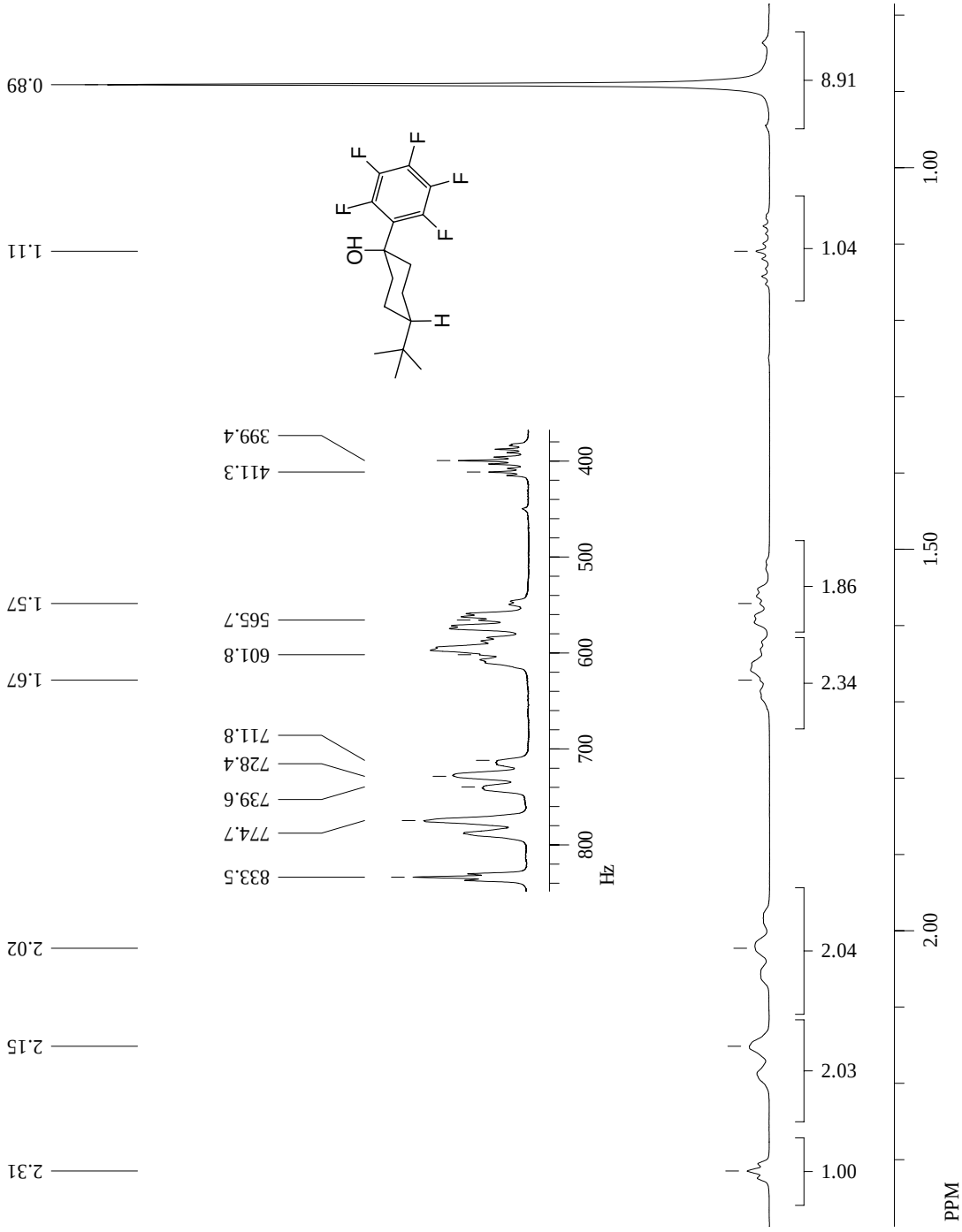

Figure A.2. ^{1}H NMR (360 MHz, $CDCl_3$) of *cis*-4-*tert*-Butyl-1-(pentafluorophenyl)cyclohexanol (**93**).

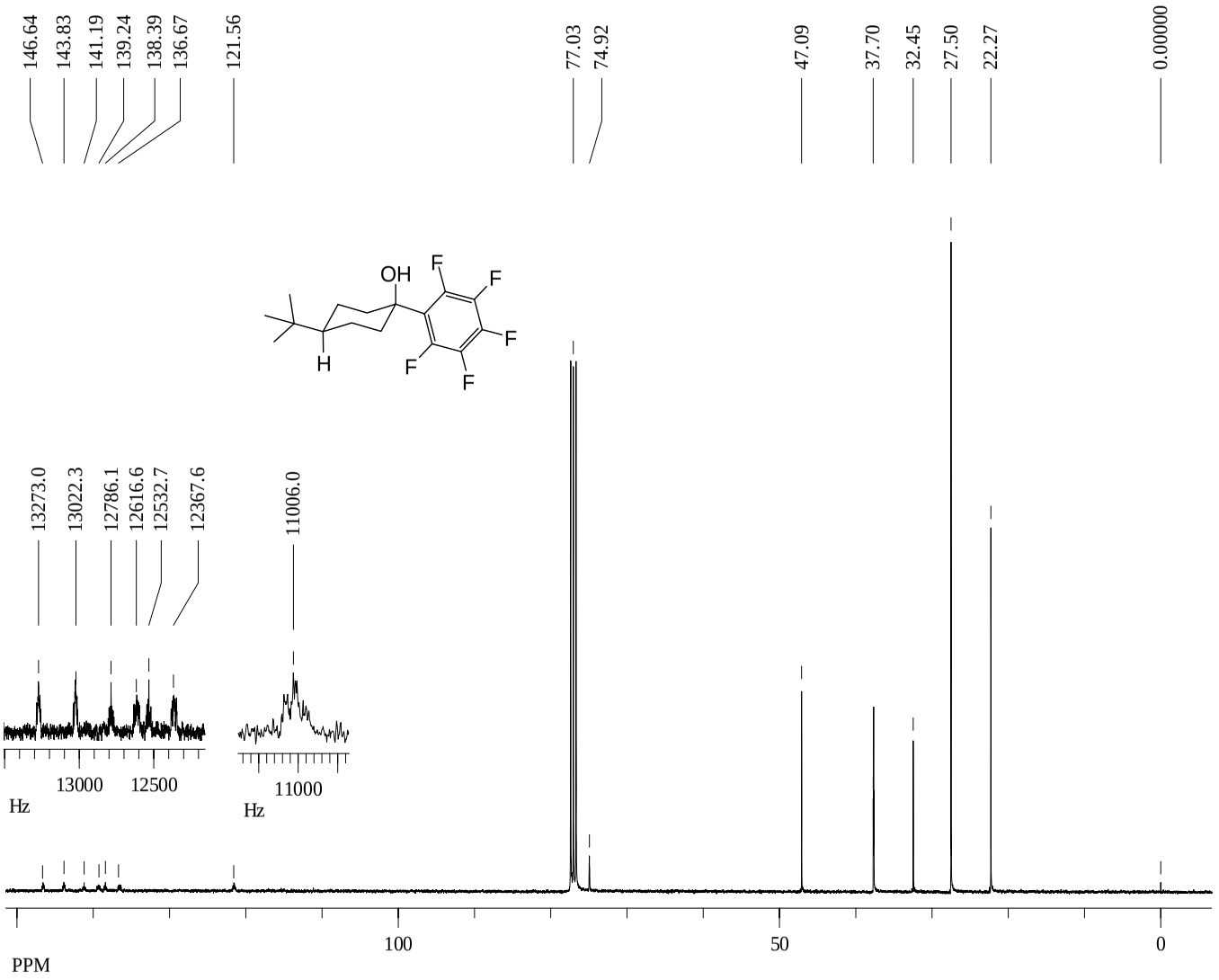

Figure A.3. ^{13}C NMR (90 MHz, $CDCl_3$) of *cis*-4-*tert*-Butyl-1-(pentafluorophenyl)cyclohexanol (**93**).

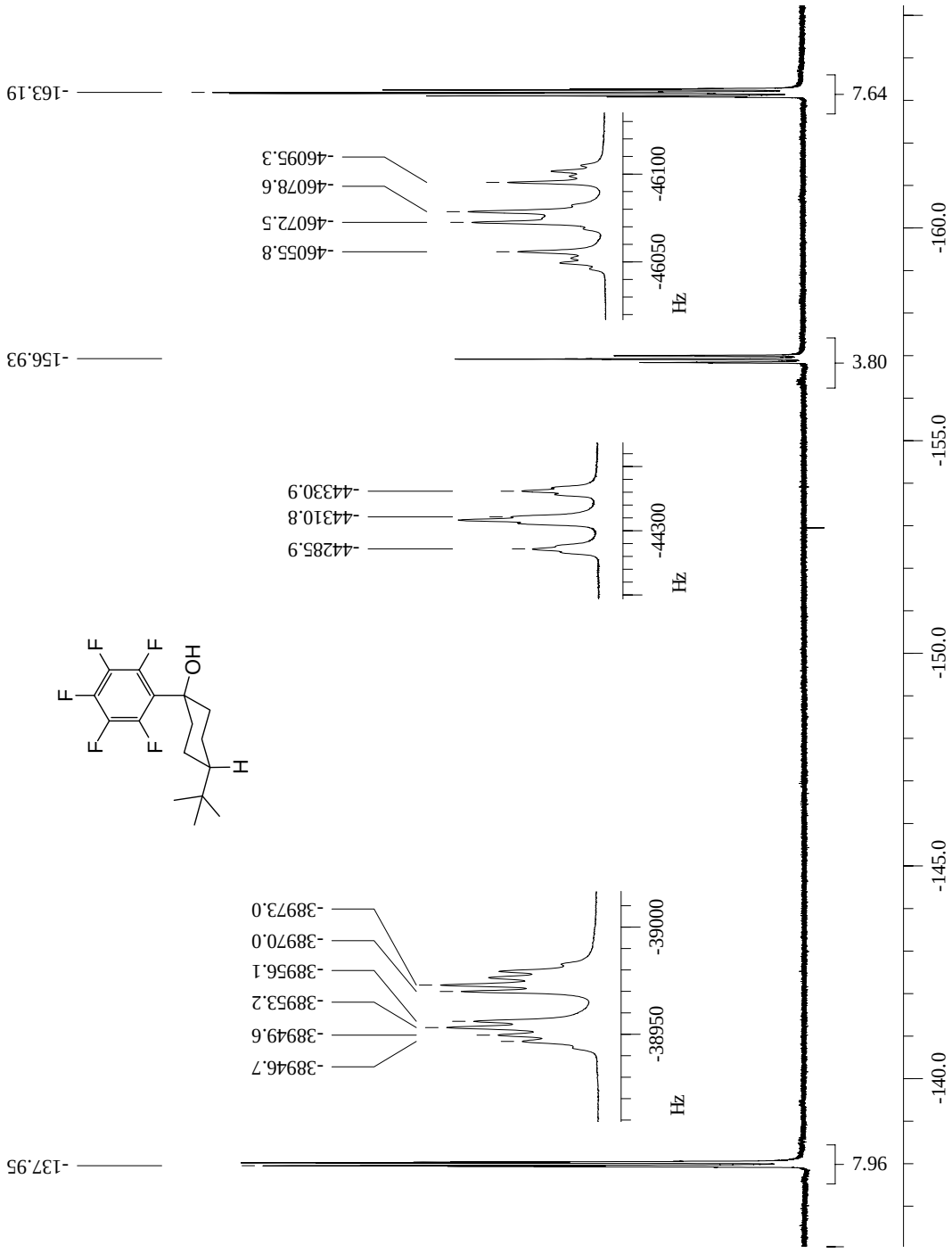

Figure A.4. ^{19}F NMR (282 MHz, DMSO-d_6) of *trans*-4-*tert*-Butyl-1-(pentafluorophenyl)cyclohexanol (**88**).

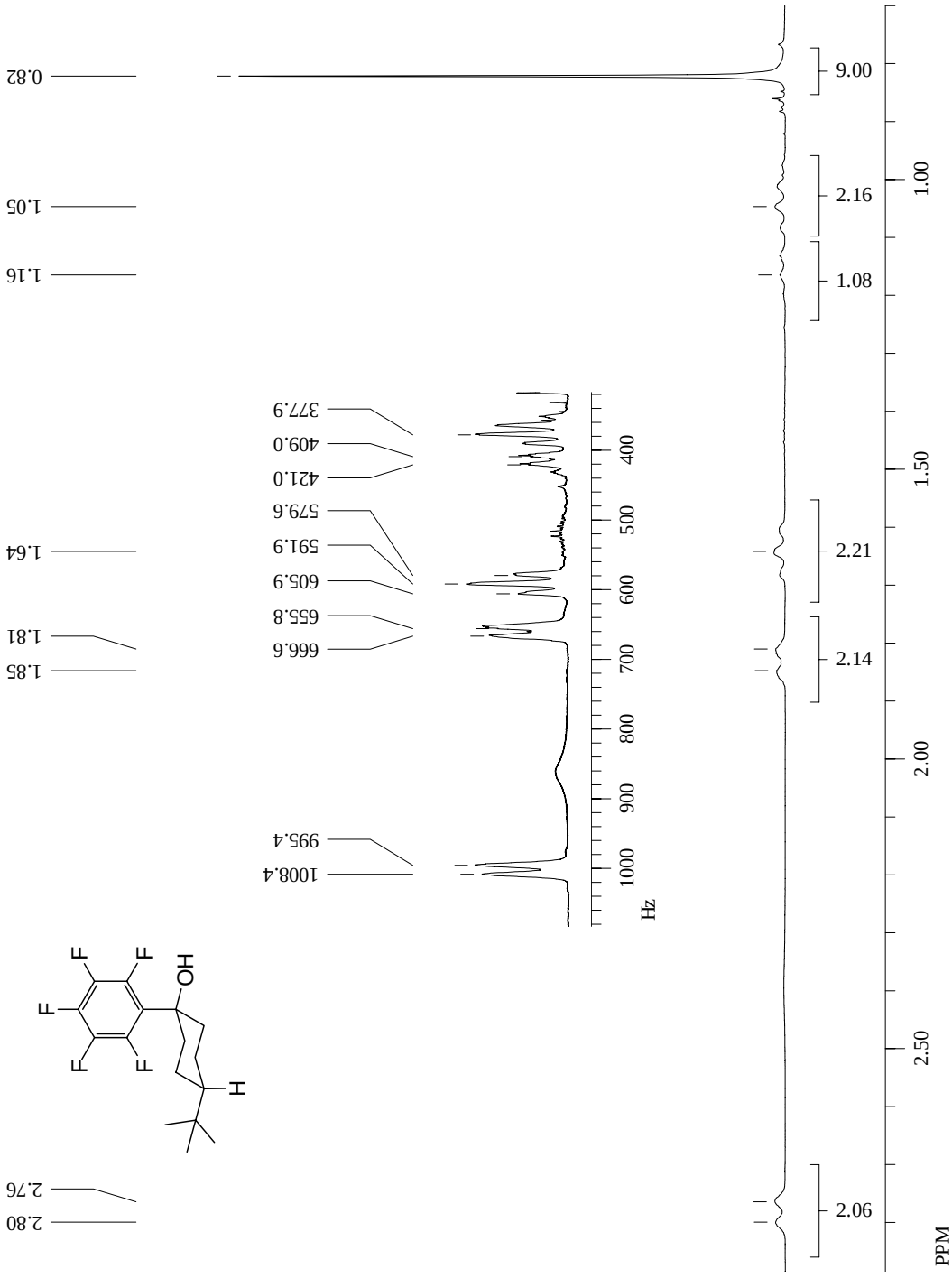

Figure A.5. ^{1}H NMR (360 MHz, $CDCl_3$) of *trans*-4-*tert*-Butyl-1-(pentafluorophenyl)cyclohexanol (**88**).

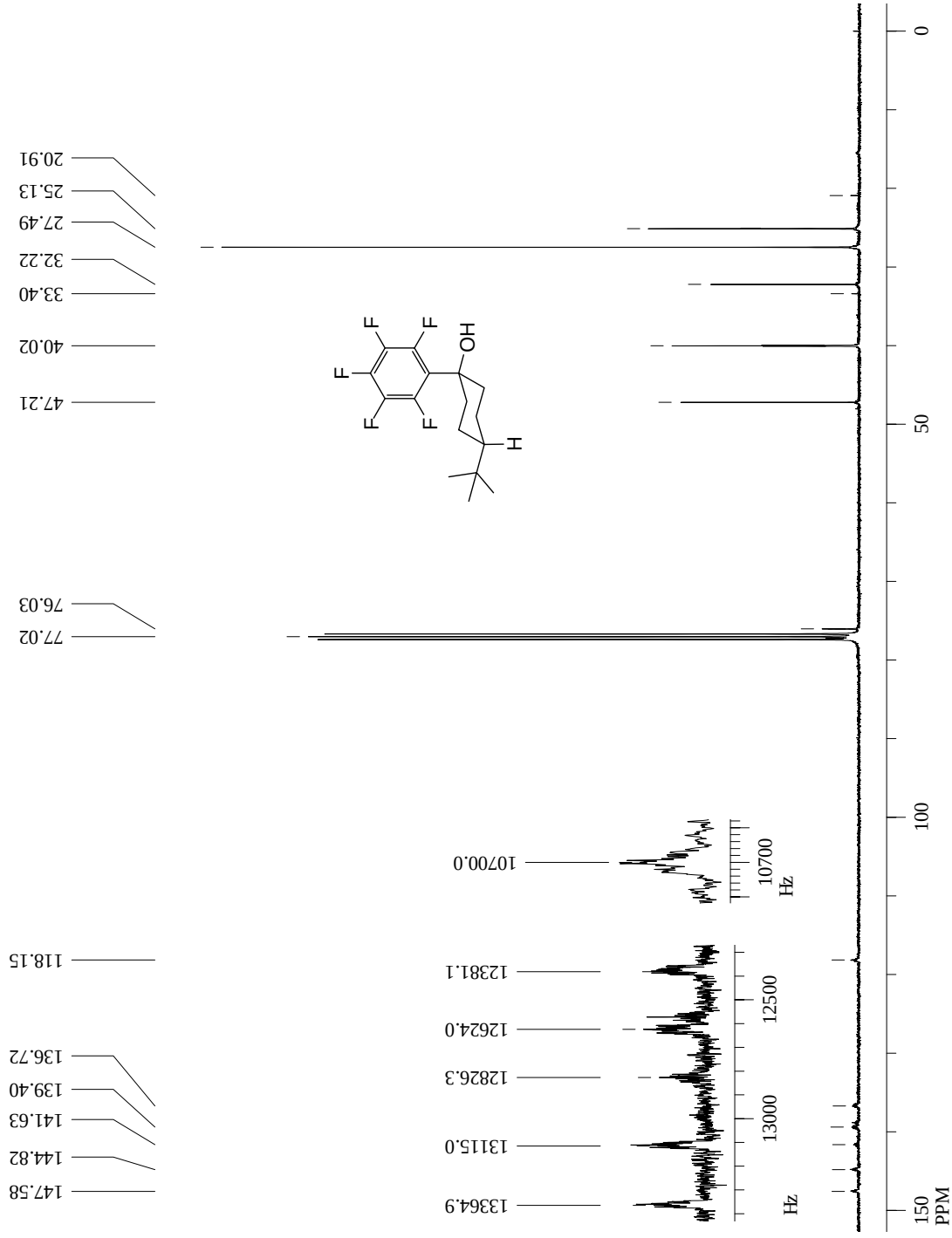

Figure A.6. ^{13}C NMR (90 MHz, $CDCl_3$) of *trans*-4-*tert*-Butyl-1-(pentafluorophenyl)cyclohexanol (**88**).

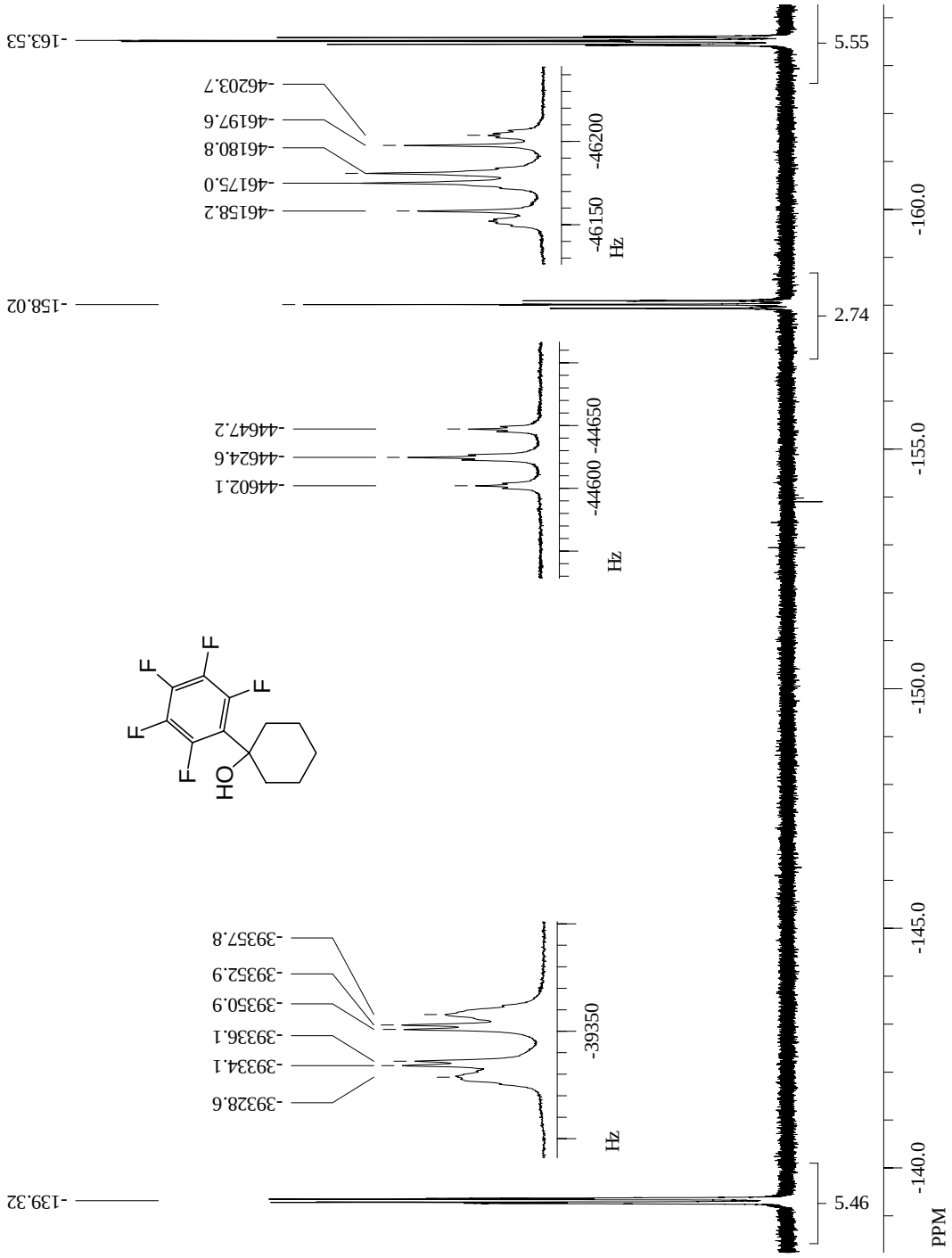

Figure A.7. ^{19}F NMR (282 MHz, DMSO-d_6) of 1-(Pentafluorophenyl)cyclohexanol (**102**).

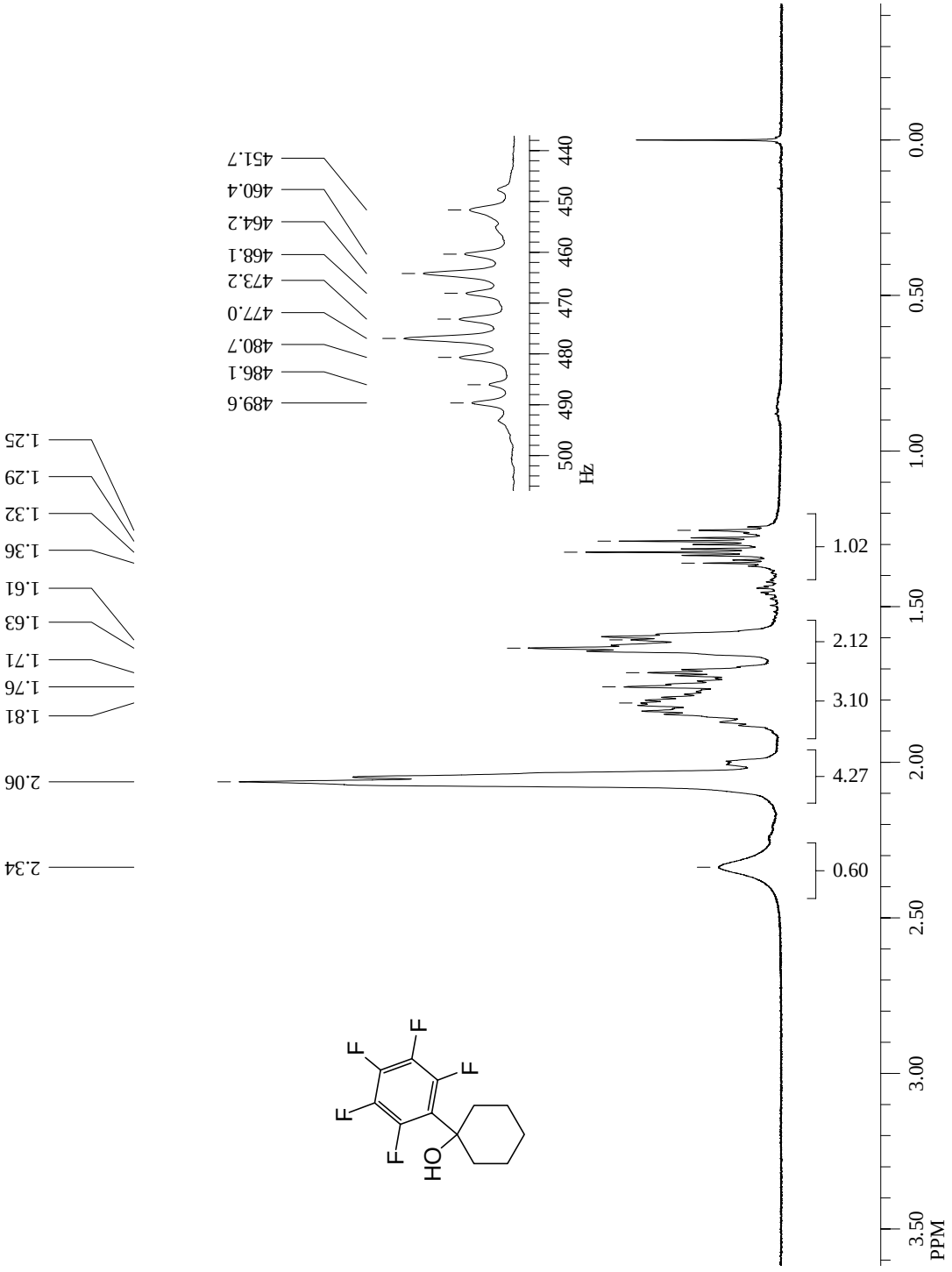

Figure A.8. ^{1}H NMR (360 MHz, $CDCl_3$) of 1-(Pentafluorophenyl)cyclohexanol (**102**).

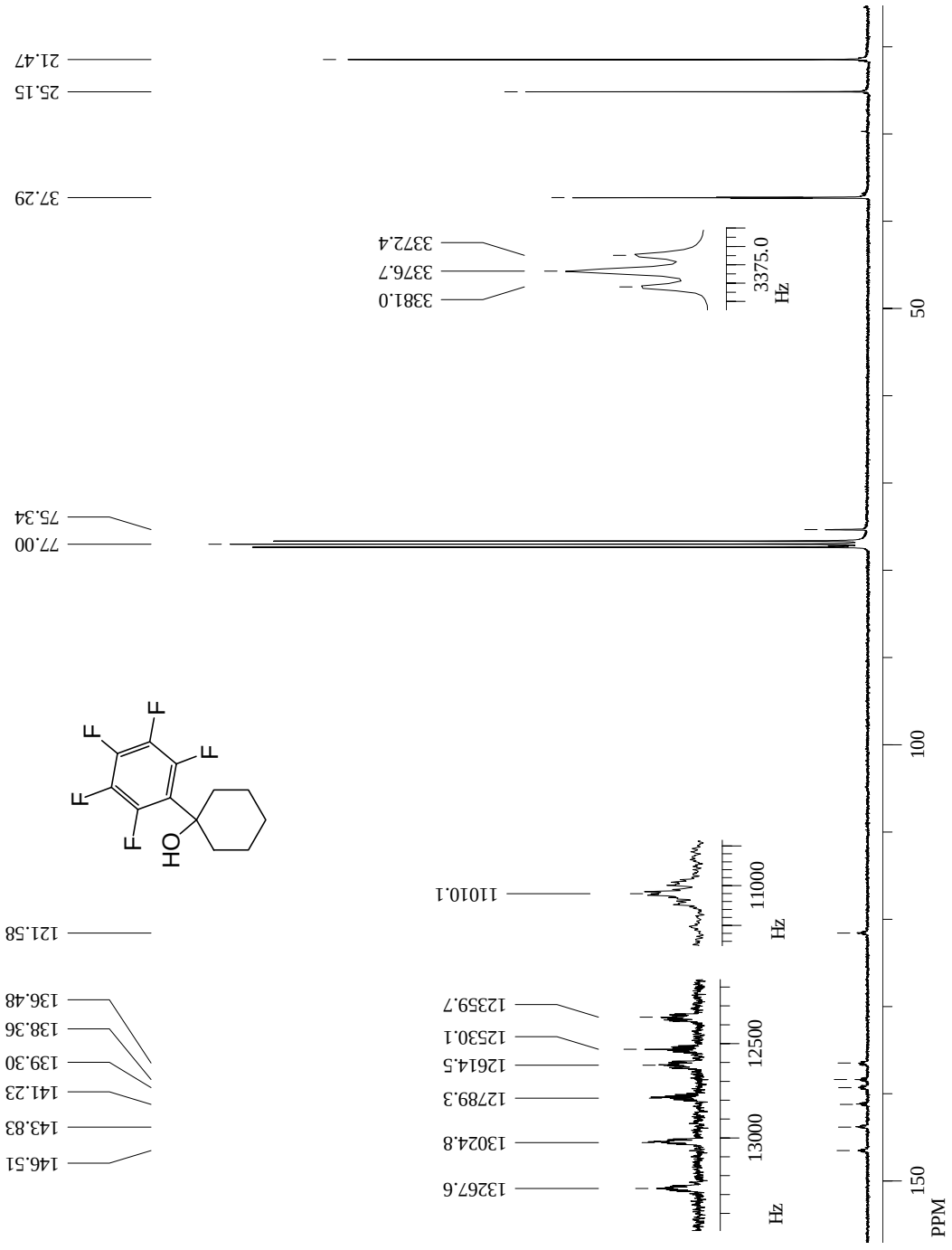

Figure A.9. ^{13}C NMR (90 MHz, $CDCl_3$) of 1-(Pentafluorophenyl)cyclohexanol (**102**).

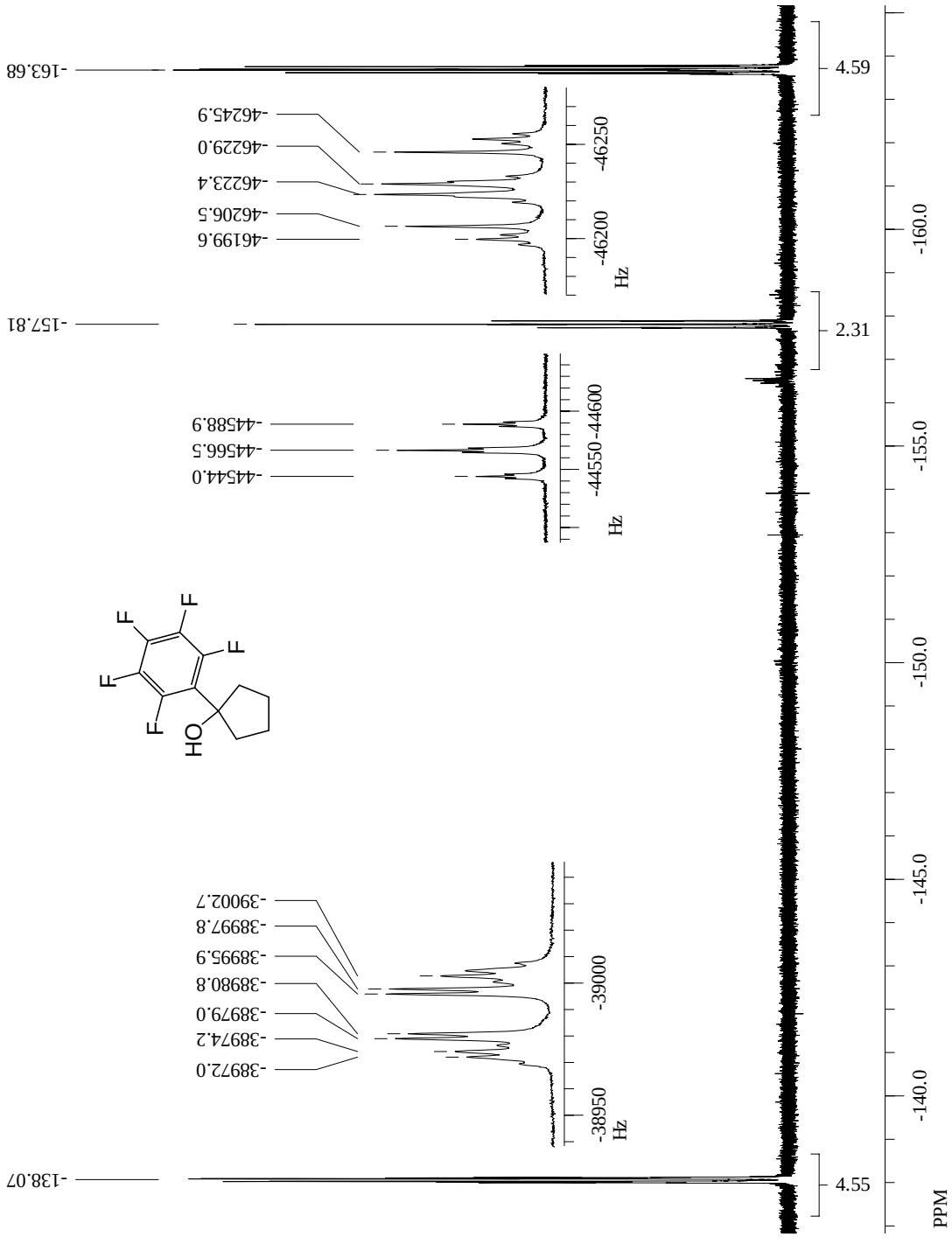

Figure A.10. ^{19}F NMR (282 MHz, DMSO-d_6) of 1-(Pentafluorophenyl)cyclopentanol (**103**).

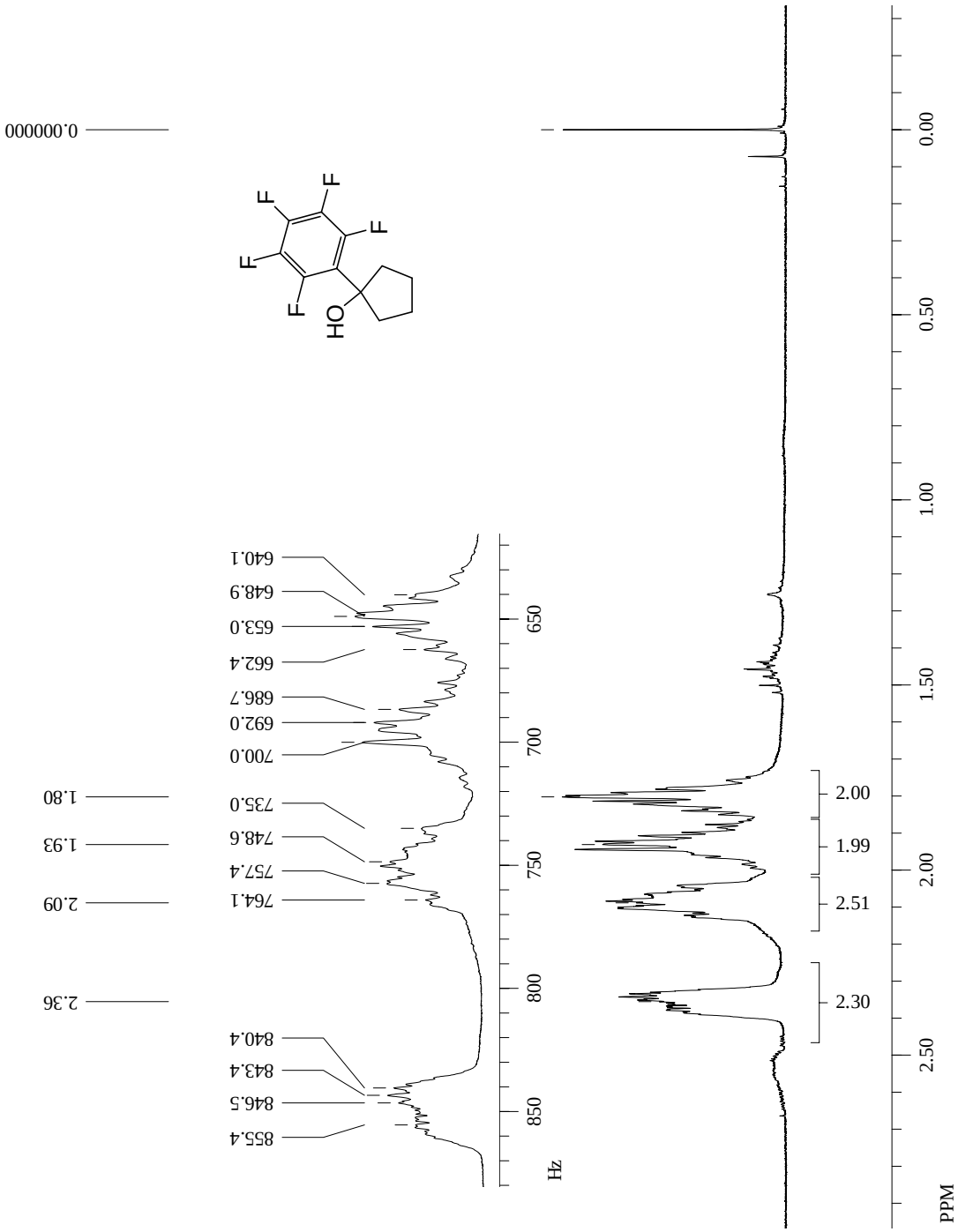

Figure A.11. ^{1}H NMR (360 MHz, $CDCl_3$) of 1-(Pentafluorophenyl)cyclopentanol (**103**).

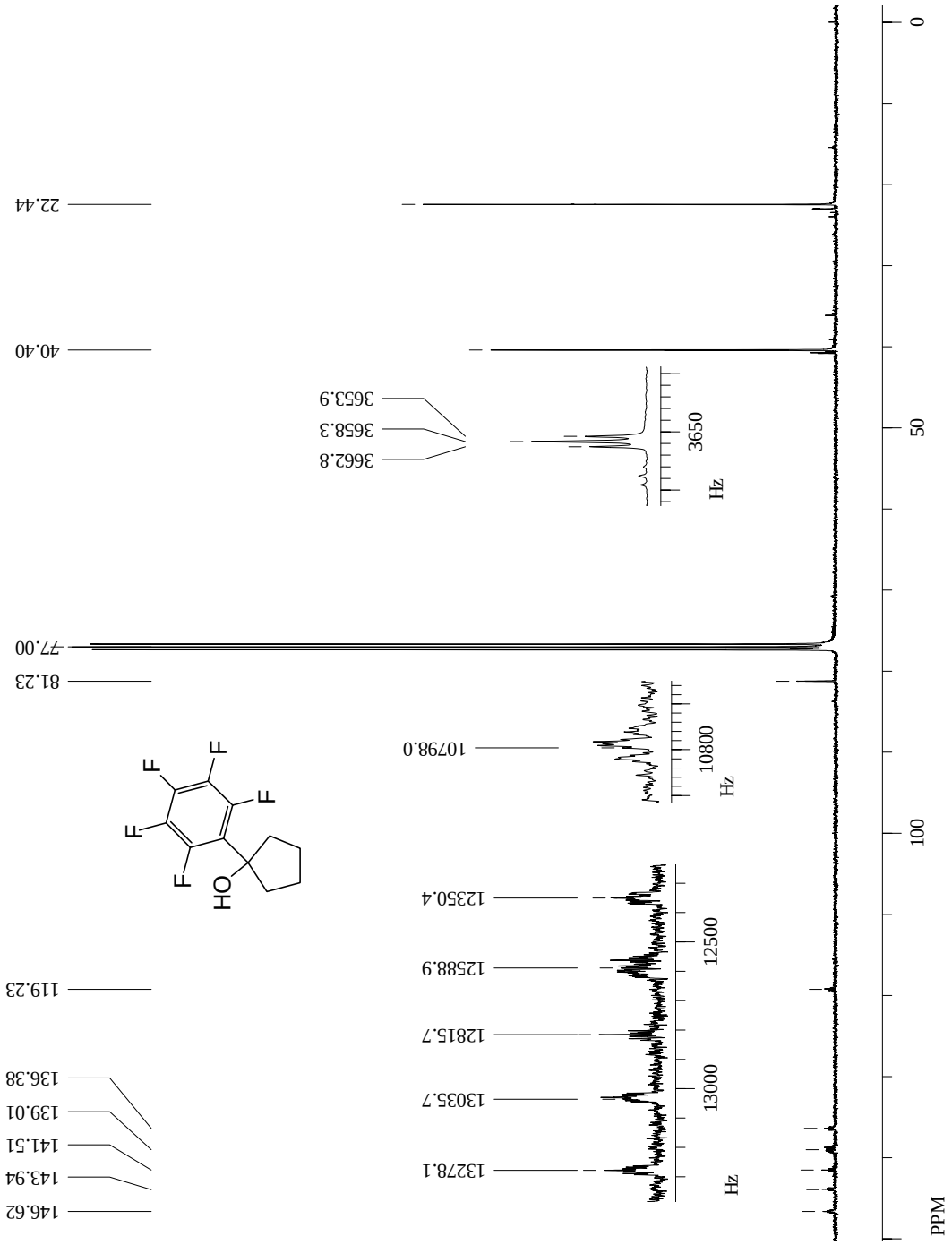

Figure A.12. ^{13}C NMR (90 MHz, $CDCl_3$) of 1-(Pentafluorophenyl)cyclopentanol (**103**).

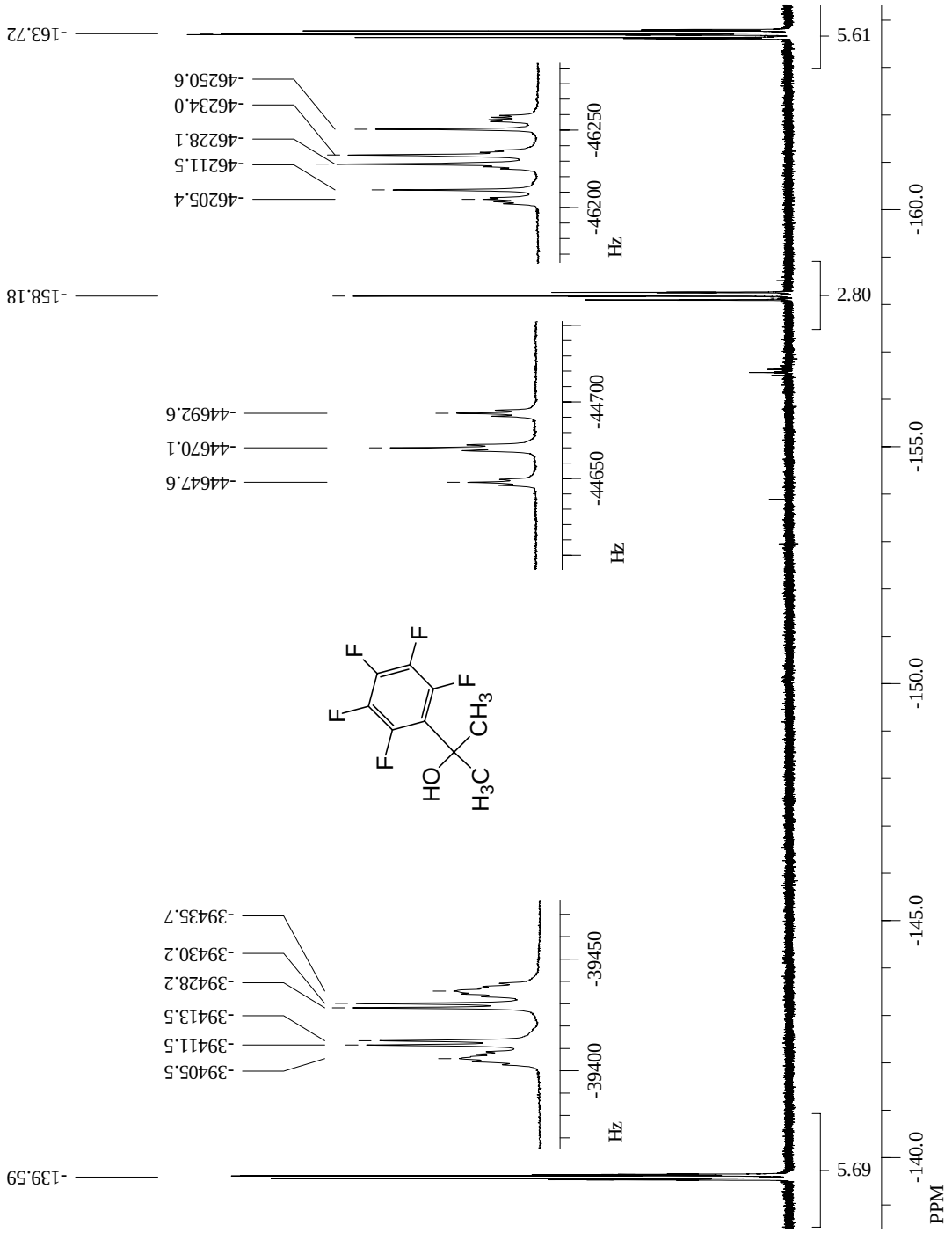

Figure A.14. ^{19}F NMR (282 MHz, DMSO-d_6) of 2-(Pentafluorophenyl)-2-propanol (**104**).

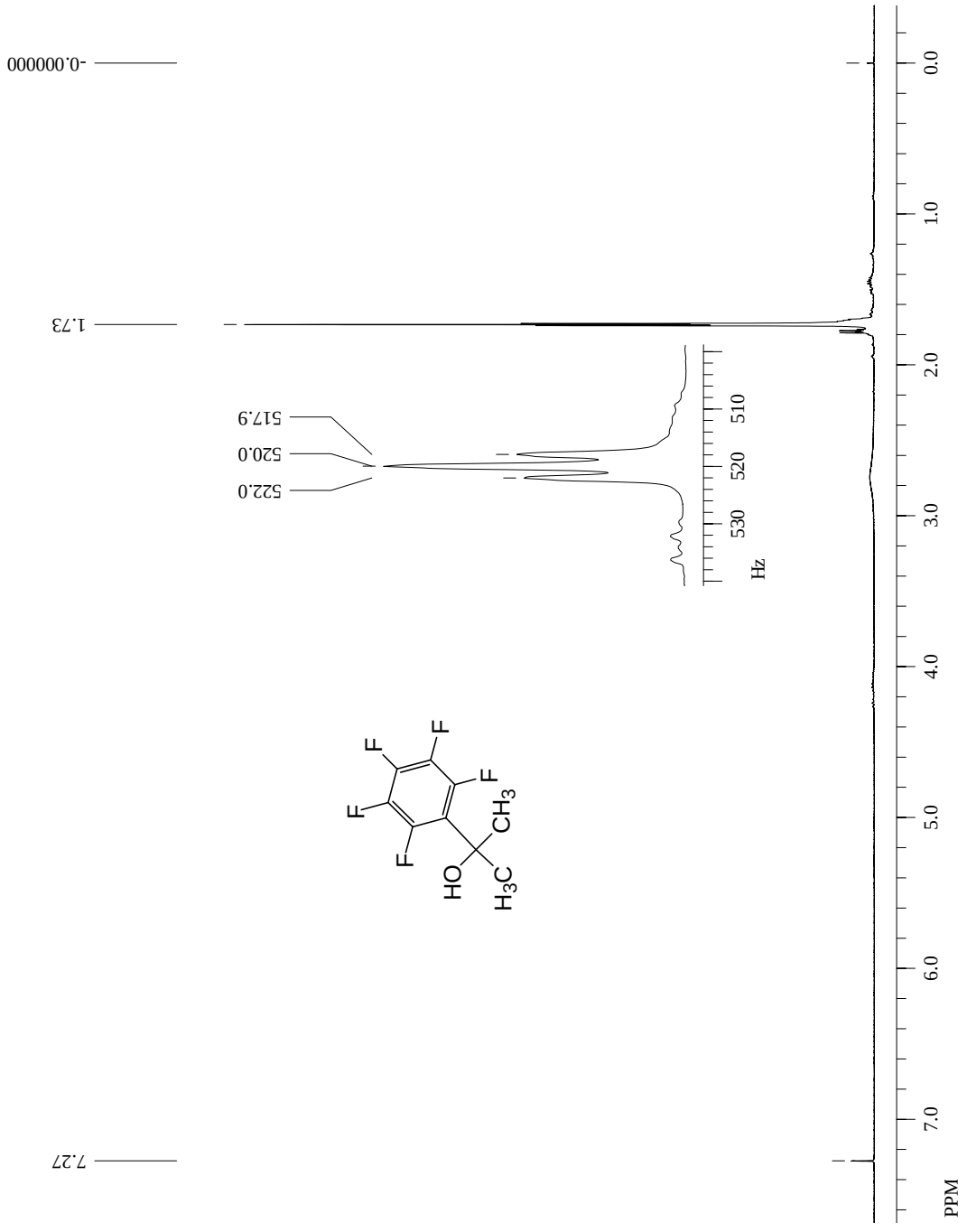

Figure A.14. ^{1}H NMR (300 MHz, $CDCl_3$) of 2-(Pentafluorophenyl)-2-propanol (**104**).

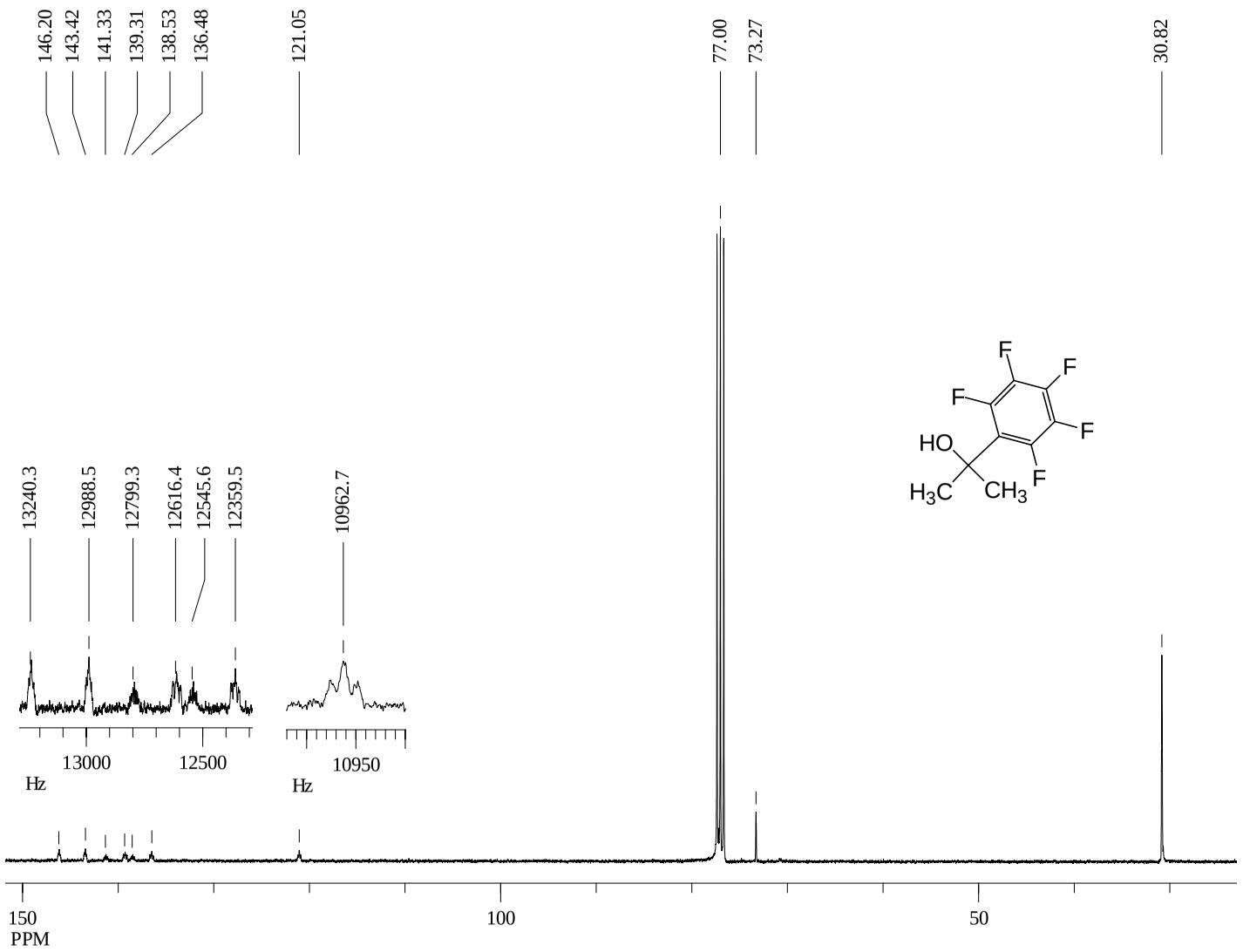

Figure A.15. ^{13}C NMR (90 MHz, $CDCl_3$) of 2-(Pentafluorophenyl)-2-propanol (**104**).

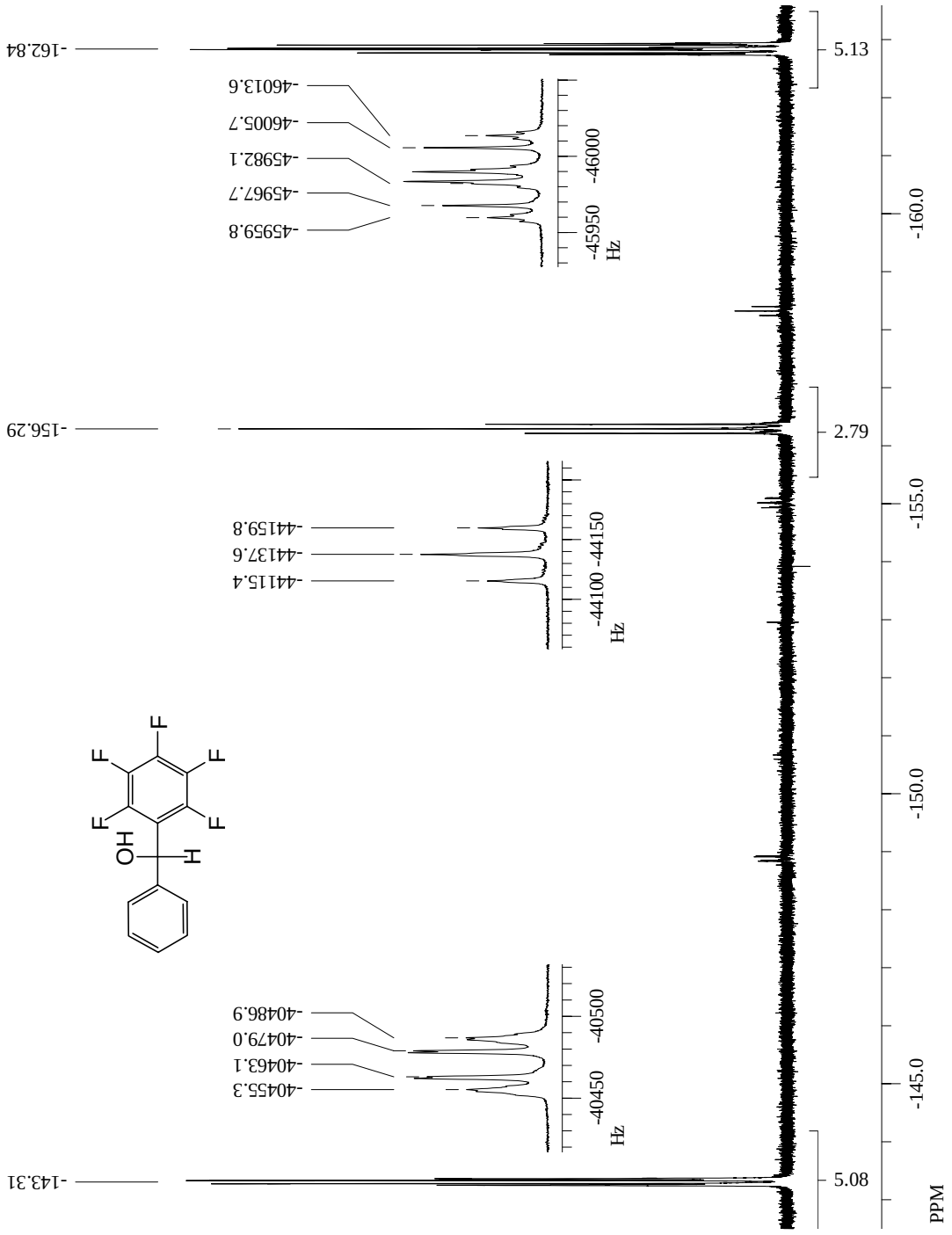

Figure A.16. ^{19}F NMR (282 MHz, DMSO-d_6) of Pentafluorophenyl-phenylmethanol (**105**).

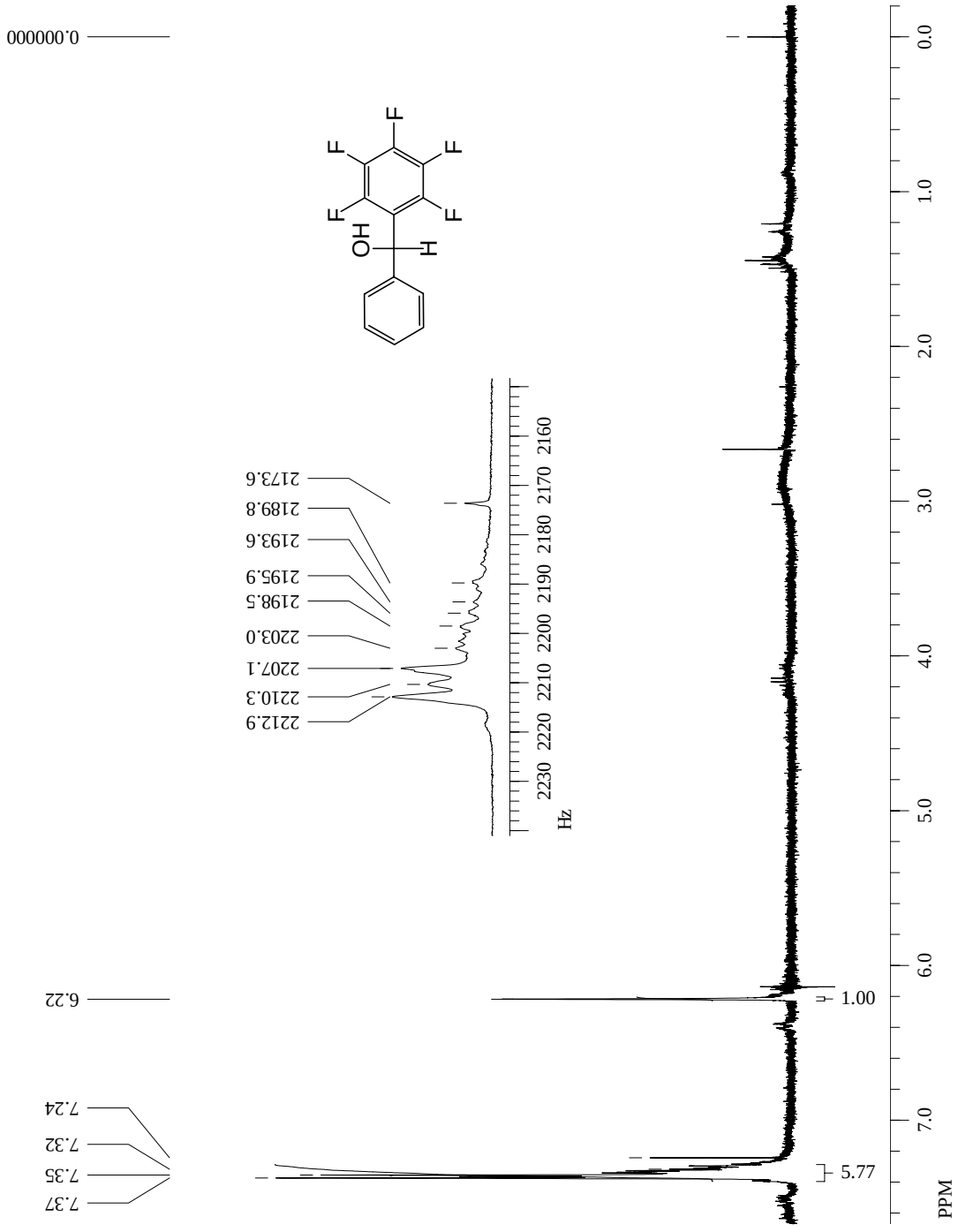

Figure A.17. ^{1}H NMR (300 MHz, $CDCl_3$) of Pentafluorophenyl-phenylmethanol (**105**).

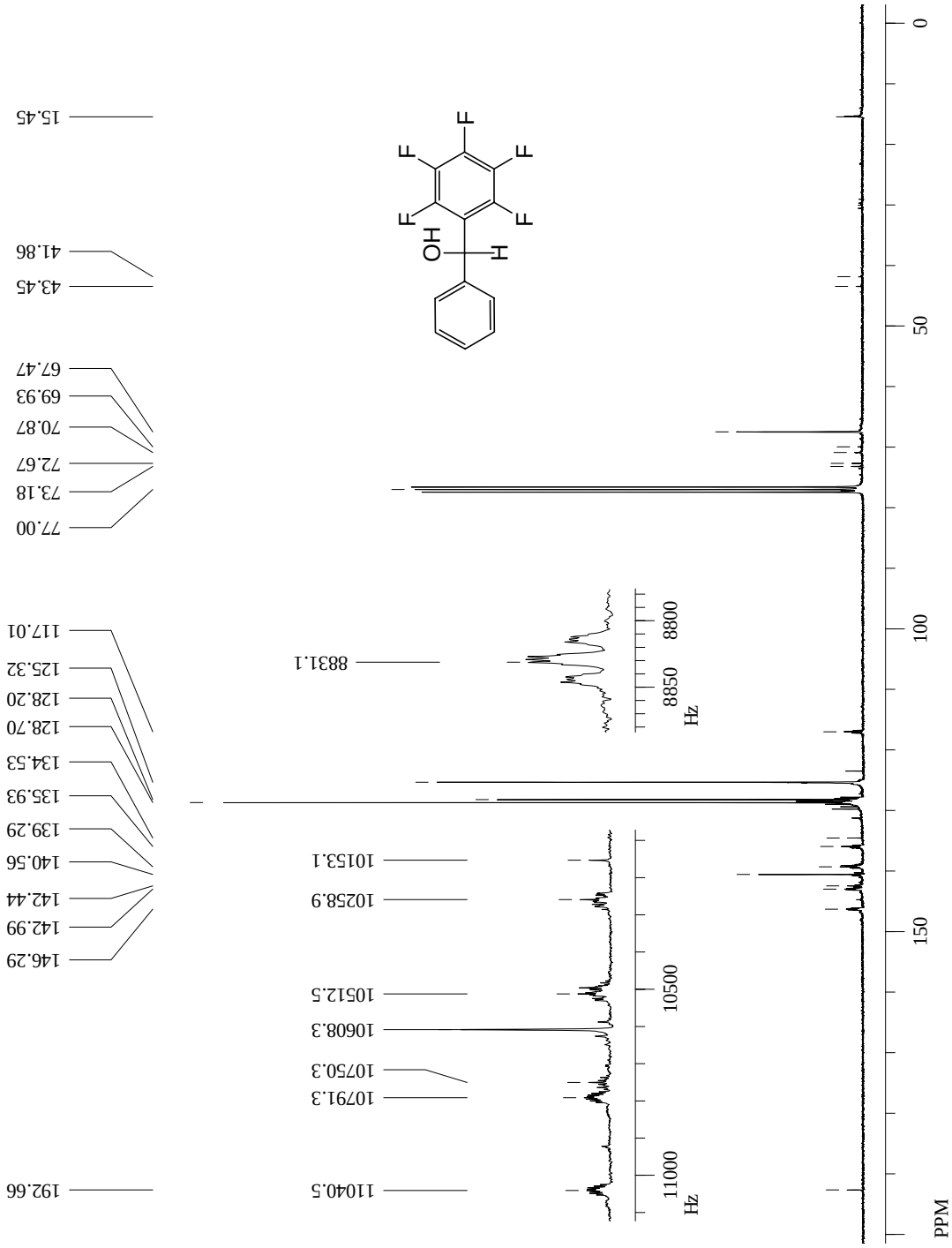

Figure A.18. ^{13}C NMR (75 MHz, $CDCl_3$) of Pentafluorophenyl-phenylmethanol (**105**).

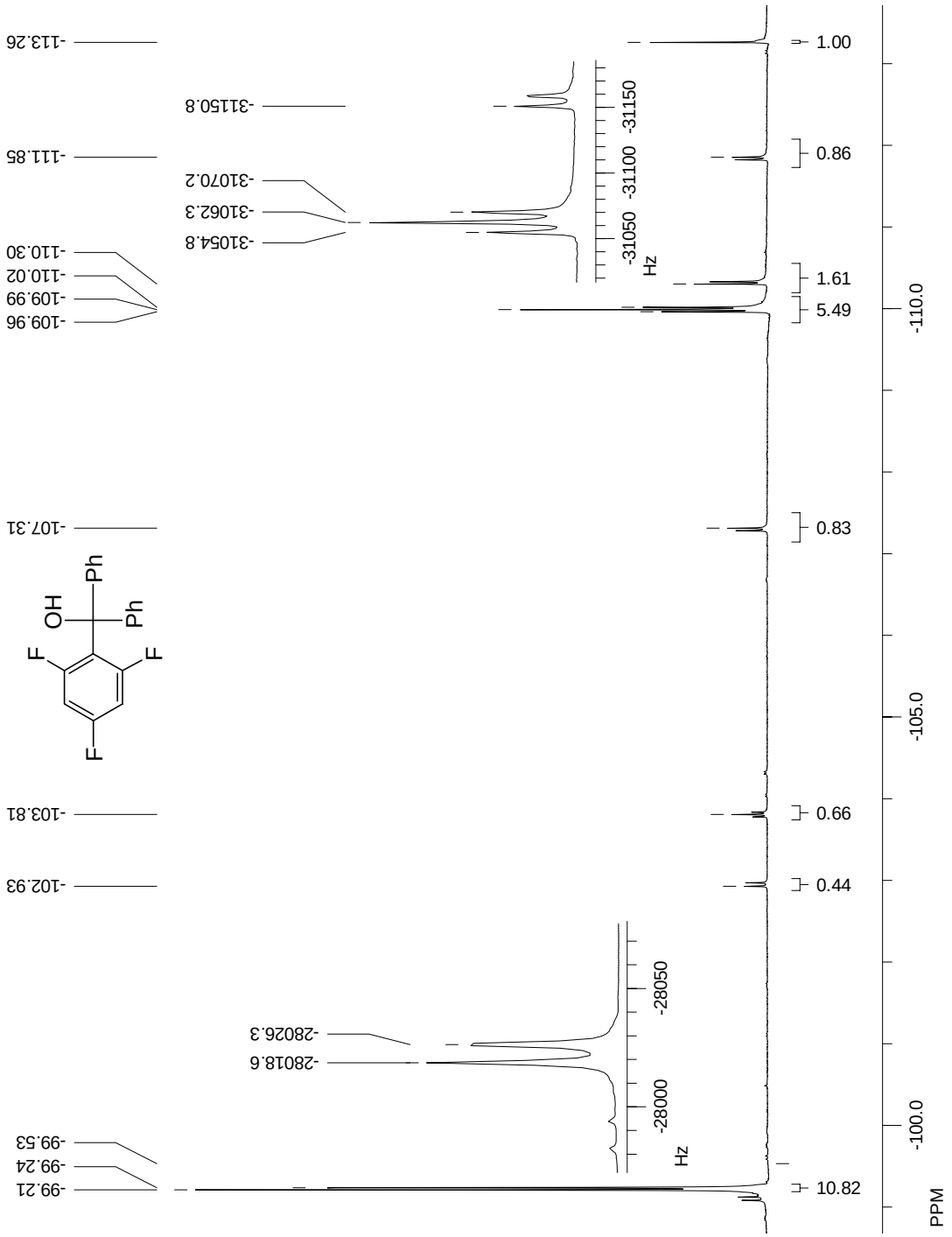

Figure A.19. ^{19}F NMR (282 MHz, DMSO-d_6) of Diphenyl-(2,4,6-trifluorophenyl)methanol. (**110**).

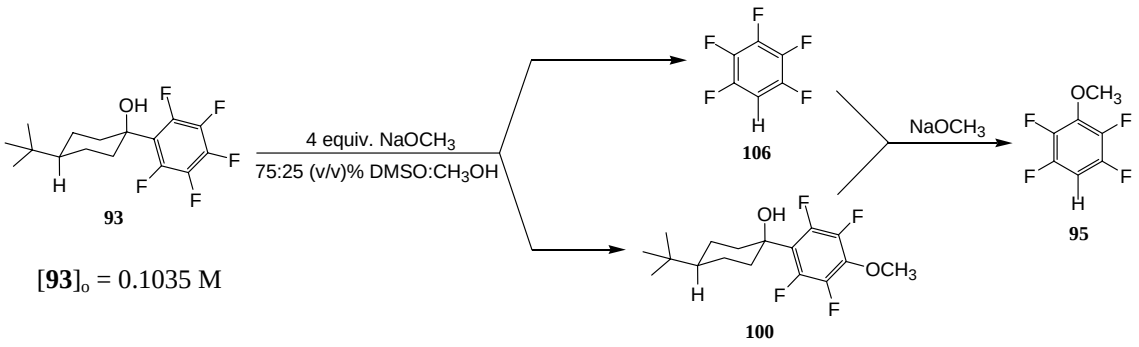

$[\mathbf{93}]_o$ = 0.1035 M

Table A.3. ^{19}F NMR Kinetic Data for *cis*-C_6F_5 Alcohol (**93**) Reaction in 75:25 (v/v) % of DMSO-d6:MeOH treated with 4 equivalents of Sodium Methoxide.

Scan No.	Time, min.	% **93** Remaining (avg. integrals)	% Formation of **106**	% Formation of **100**	% Formation of **95**
1	0	100 (10.086)	0	0	0
2	1.75	80.5(11.009)	7.26 (0.993)	9.14 (1.249)	3.08 (0.421)
3	3.75	53.1 (7.375)	8.58 (1.192)	26.2 (3.641)	12.1 (1.677)
4	5.75	33.8 (4.883)	7.97 (1.152)	38.3 (5.533)	20.0 (2.886)
5	7.75	22.1 (3.179)	9.96 (1.432)	42.2 (6.069)	25.7 (3.692)
6	9.75	16.3 (2.424)	4.13 (0.615)	48.5 (7.229)	31.1 (4.641)
7	11.75	14.6 (2.332)	2.46 (0.391)	50.6 (8.042)	32.3 (5.140)
8	13.75	8.21 (1.114)	-	56.2 (7.616)	35.6 (4.823)
9	15.75	6.54 (0.934)	-	57.0 (8.132)	36.5 (5.213)
10	17.75	4.35 (0.635)	-	56.9 (8.288)	38.8 (5.654)
11	19.75	3.29 (0.522)	-	58.3 (9.262)	38.4 (6.102)
12	21.75	-	-	59.8 (9.926)	40.2 (6.681)
13	23.75	-	-	60.2 (9.323)	39.8 (6.161)
14	25.75	-	-	59.8 (8.864)	40.2 (5.960)
15	27.75	-	-	59.0 (8.741)	41.0 (6.076)
16	29.75	-	-	58.1 (8.476)	42.0 (6.116)

Note 1: There a +/- 1% error on all percentages reported in this table.
Note 2: Addition of fluorobenzene (2 µL) was used as a chemical shift reference (-113.26 ppm) and as an internal standard to calibrate peak integrations.

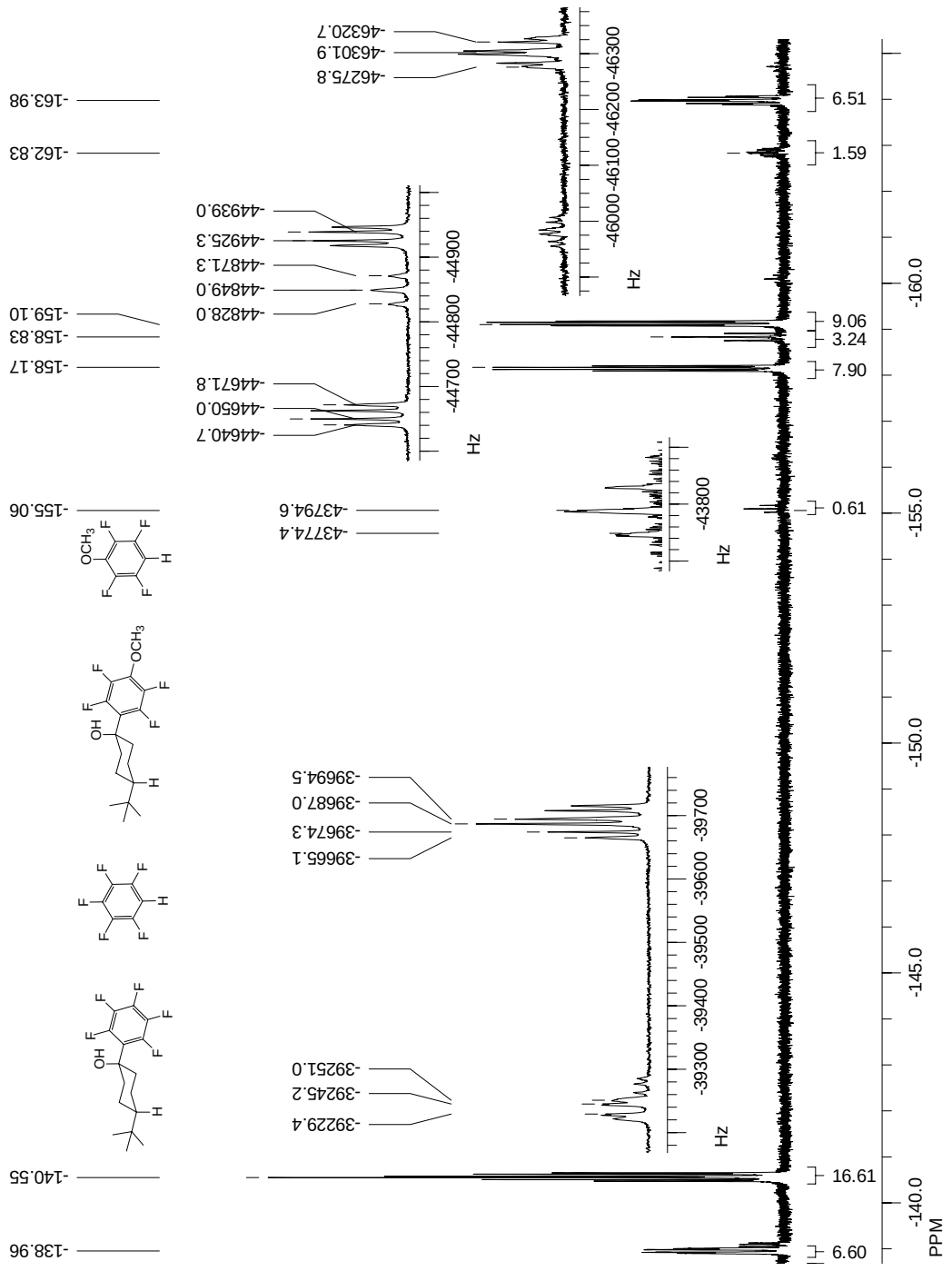

Figure A.20. Representative ^{19}F NMR Spectra of *cis*-C_6F_5 Alcohol (**93**) Reaction at t = 5.75 min. (See Table A.1/A.2 for specific chemical shift assignments and Table A.3 for reaction conditions).

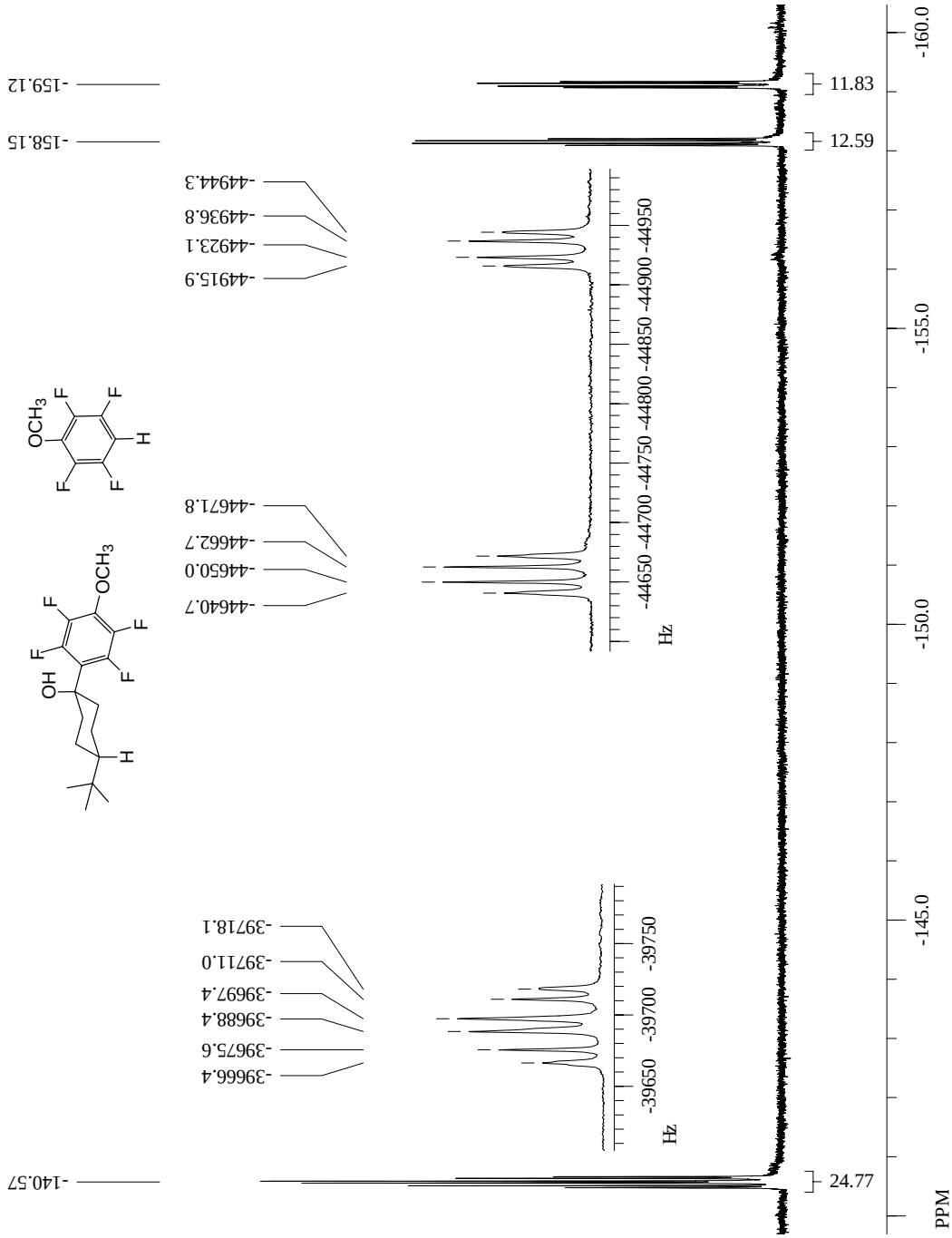

Figure A.21. Representative ^{19}F NMR Spectra of *cis*-C_6F_5 Alcohol (**93**) Reaction at t = 29.75 min. (See Table A.1/A.2 for specific chemical shift assignments and Table A.3 for reaction conditions).

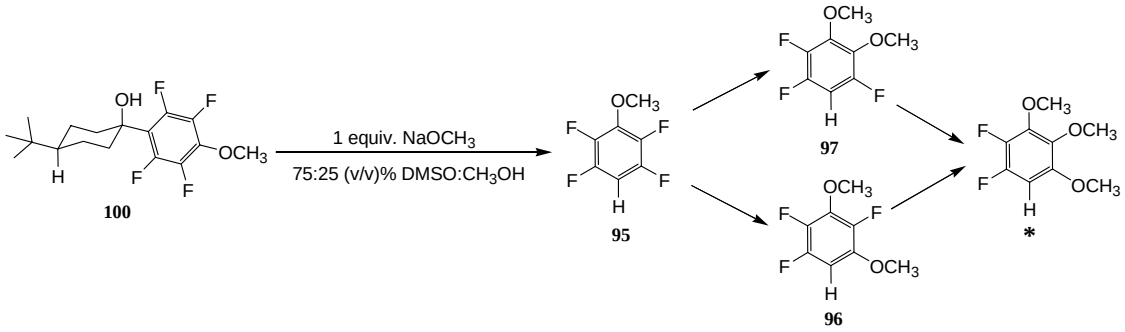

Table A.4. ^{19}F NMR Kinetic Data for methoxy-substituted *cis*-C_6F_5 Alcohol (**100**) Reaction in 75:25 (v/v) % of DMSO-d6:MeOH treated with 1 equivalent of Sodium Methoxide.

Scan No.	Time, min.	% **100** Remaining (avg. integrals)	% Formation of **95**	% Formation of **96**	**%** Formation of **97**
1	0	100 (46.221)	0	0	0
2	2.00	100 (35.168)	-	-	-
3	4.42	99.5 (32.027)	0.53 (0.172)	-	-
4	9.42	98.0 (37.326)	2.03 (0.773)	-	-
5	14.42	96.3 (47.711)	3.66 (1.812)	-	-
6	19.42	95.7 (36.604)	4.34 (1.659)	-	-
7	24.42	94.5 (31.927)	5.47 (1.847)	-	-
8	29.42	94.5 (39.334)	5.51 (2.293)	-	-
9	34.42	92.8 (42.381)	7.21 (3.293)	-	-
10	39.42	91.8 (39.168)	8.20 (3.497)	-	-
11	44.42	90.7 (33.921)	10.23 (3.473)	-	-
12	~ 1.5 days*	7.05 (2.073)	64.4 (18.929)	2.73 (0.804)	5.85 (1.720)

* Though not confirmed by any other analytical technique, the formation 1,2-difluoro-3,4,5-trimethoxybenzene appears to form in this reaction. It is the only compound that can specifically form from both *ortho*– and *meta*-trifluorodimethoxybenzene. Percent formation of this compound was 20.0% (5.888) at t ~ 1.5 days.

Note 1: There a +/- 1% error on all percentages reported in this table.
Note 2: Addition of fluorobenzene (2 µL) was used as a chemical shift reference (-113.26 ppm) and as an internal standard to calibrate peak integrations.

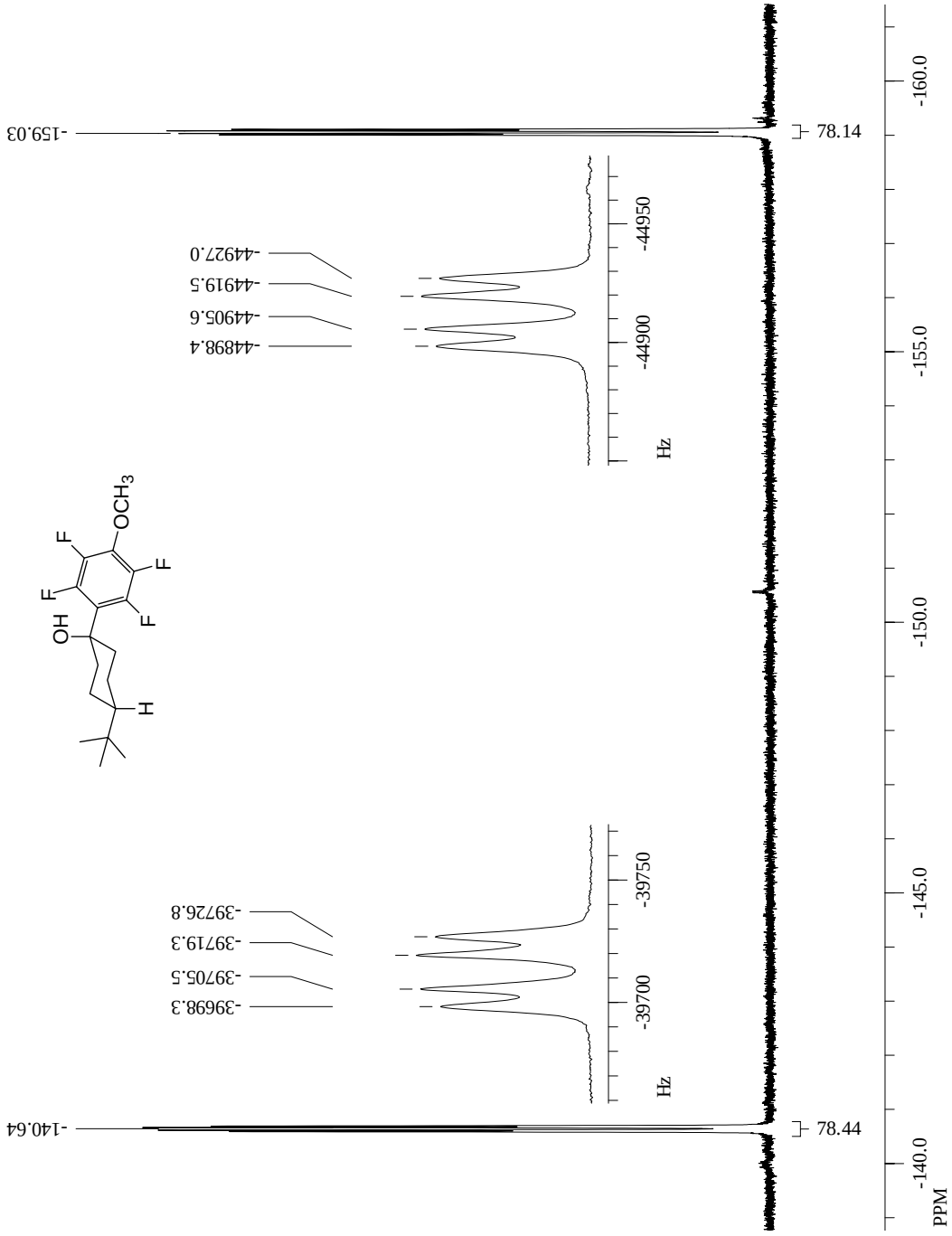

Figure A.22. ^{19}F NMR Spectra of methoxy-substituted *cis*-C_6F_5 Alcohol (**100**).
(See Table A.1/A.2 for specific chemical shift assignments).

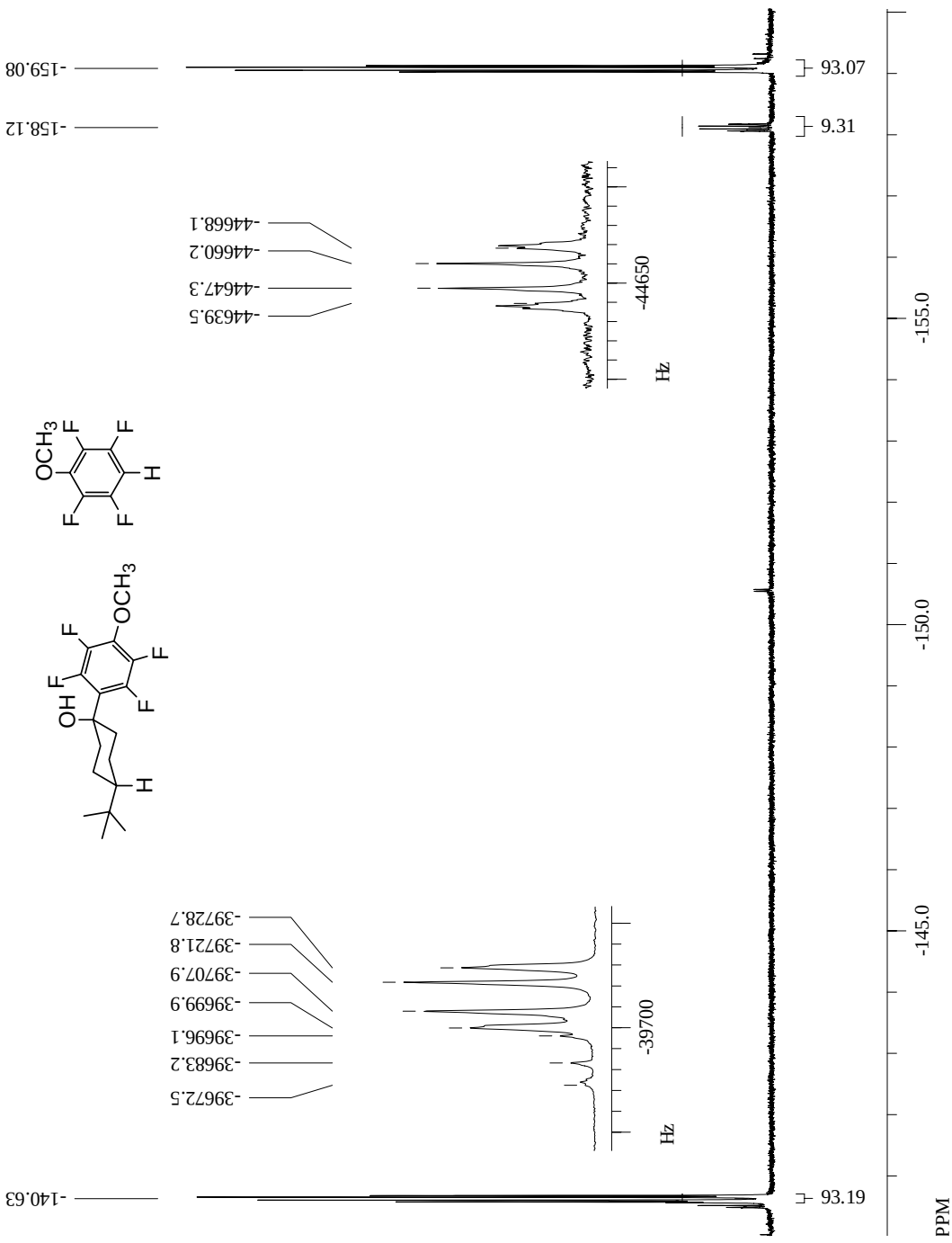

Figure A.23. Representative ^{19}F NMR Spectra of methoxy-substituted *cis*-C_6F_5 Alcohol (**100**) Reaction at t = 45 min. (See Table A.1/A.2 for specific chemical shift assignments and Table A.4 for reaction conditions).

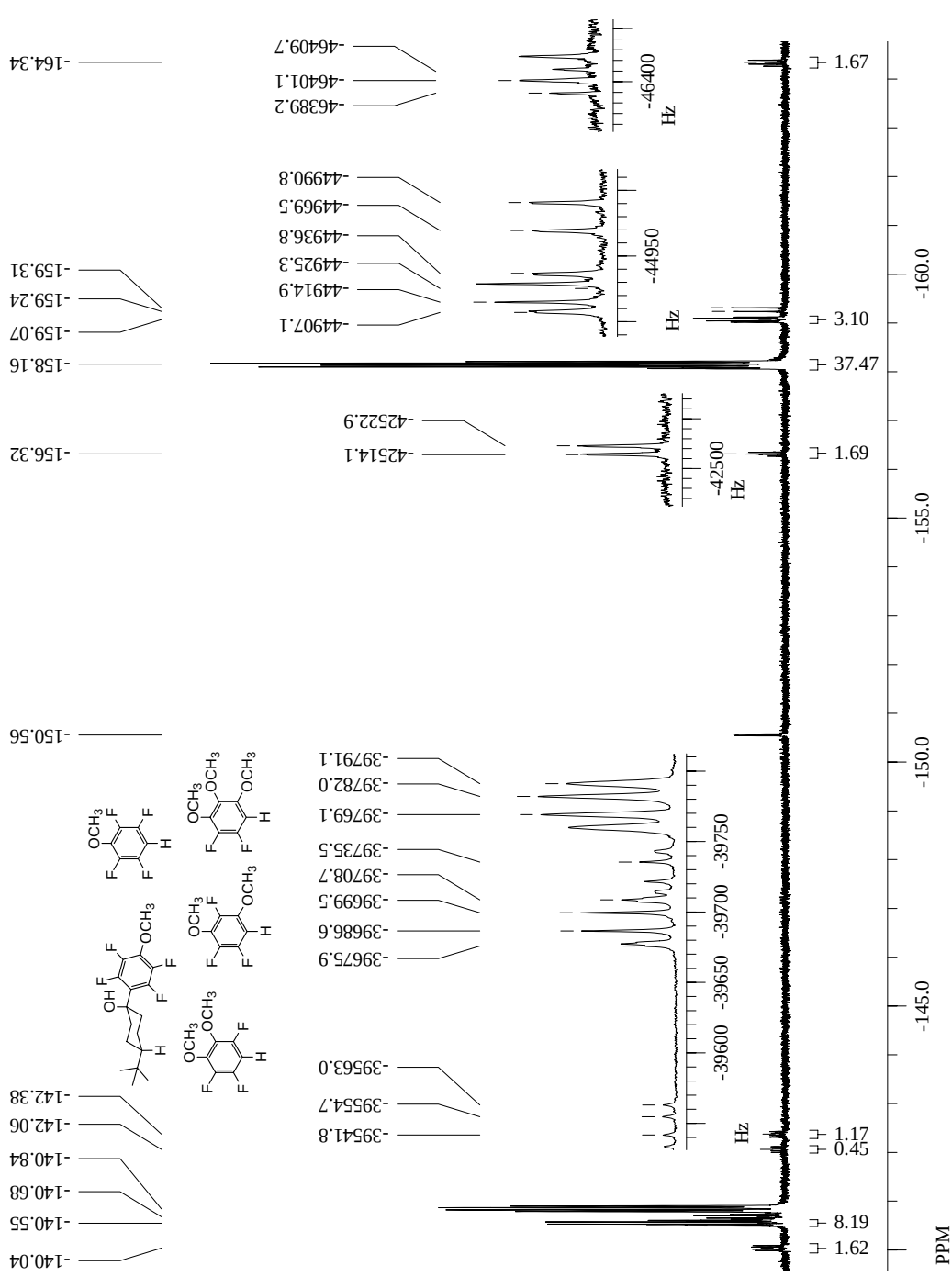

Figure A.24. Representative ^{19}F NMR Spectra of methoxy-substituted *cis*-C_6F_5 Alcohol (**100**) Reaction at t = 1.5 days. (See Table A.1/A.2 for specific chemical shift assignments and Table A.4 for reaction conditions).

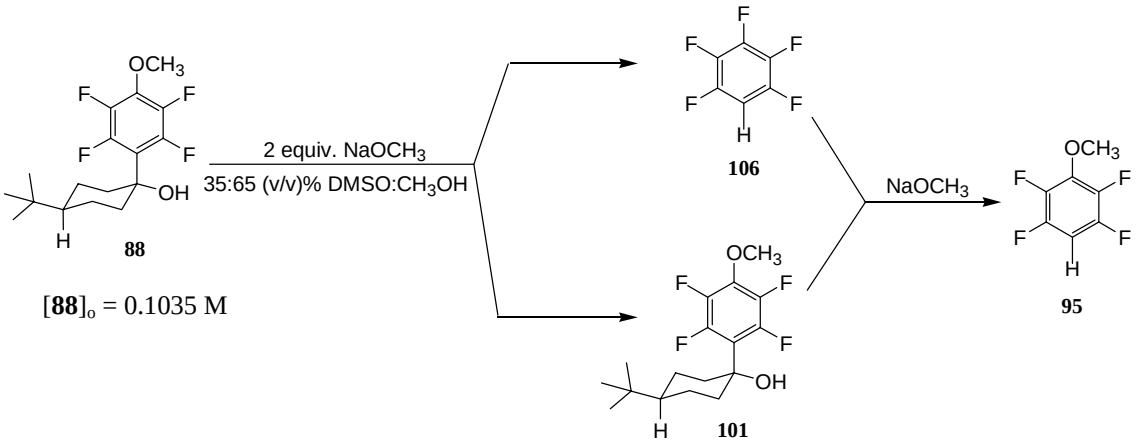

Table A.5. ^{19}F NMR Kinetic Data for *trans*-C_6F_5 Alcohol (**88**) Reaction in 35:65 (v/v) % of DMSO-d6:MeOH treated with 2 equivalents of Sodium Methoxide.

Scan No.	Time, min. (appx. hr)	% **88** Remaining (avg. integrals)	% Formation of **106**	% Formation of **101**	% Formation of **95**
1	0	100 (11.546)	0	0	0
7	31.02 (0.5)	78.2 (8.586)	5.28 (0.580)	16.5 (1.817)	-
13	61.02 (1.0)	66.1 (6.756)	7.81 (0.798)	26.1 (2.669)	-
16	91.02 (1.5)	48.5 (4.889)	10.8 (1.085)	39.8 (4.017)	1.0 (0.096)
19	121.02 (2.0)	41.0 (4.408)	11.6 (1.241)	45.4 (4.874)	2.0 (0.217)
22	151.02 (2.5)	42.0 (5.126)	10.9 (1.330)	44.2 (5.396)	2.9 (0.356)
25	181.02 (3.0)	37.1 (4.434)	11.8 (1.413)	47.9 (5.720)	3.1 (0.374)
28	241.02 (4.0)	29.6 (3.175)	11.6 (1.242)	54.6 (5.861)	4.2 (0.455)
31	301.02 (5.0)	24.0 (2.683)	12.3 (1.370)	57.8 (6.456)	5.8 (0.652)
32	331.02 (5.5)	21.6 (2.241)	11.5 (1.194)	60.4 (6.273)	6.5 (0.674)
33	361.02 (6.0)	20.4 (2.573)	12.1 (1.516)	60.6 (7.625)	6.9 (0.866)
34	391.02 (6.5)	18.5 (2.141)	12.1 (1.402)	62.5 (7.240)	7.0 (0.809)
35	421.02 (7.0)	16.2 (1.883)	11.9 (1.384)	63.5 (7.375)	8.4 (0.978)
36	451.02 (7.5)	16.1 (1.801)	12.4 (1.385)	64.0 (7.138)	7.4 (0.824)
37	481.02 (8.0)	15.0 (1.892)	12.0 (1.520)	65.4 (8.268)	7.6 (0.956)
38	541.02 (9.0)	12.8 (1.481)	12.2 (1.412)	66.4 (7.707)	8.7 (1.015)
39	601.02 (10.0)	9.6 (1.197)	10.0 (1.256)	69.2 (8.661)	11.1 (1.393)
41	661.02 (11.0)	9.0 (1.010)	10.3 (1.155)	69.4 (7.792)	11.3 (1.265)

Note 1: There a +/- 1% error on all percentages reported in this table.
Note 2: Addition of fluorobenzene (2 µL) was used as a chemical shift reference (-113.26 ppm) and as an internal standard to calibrate peak integrations.

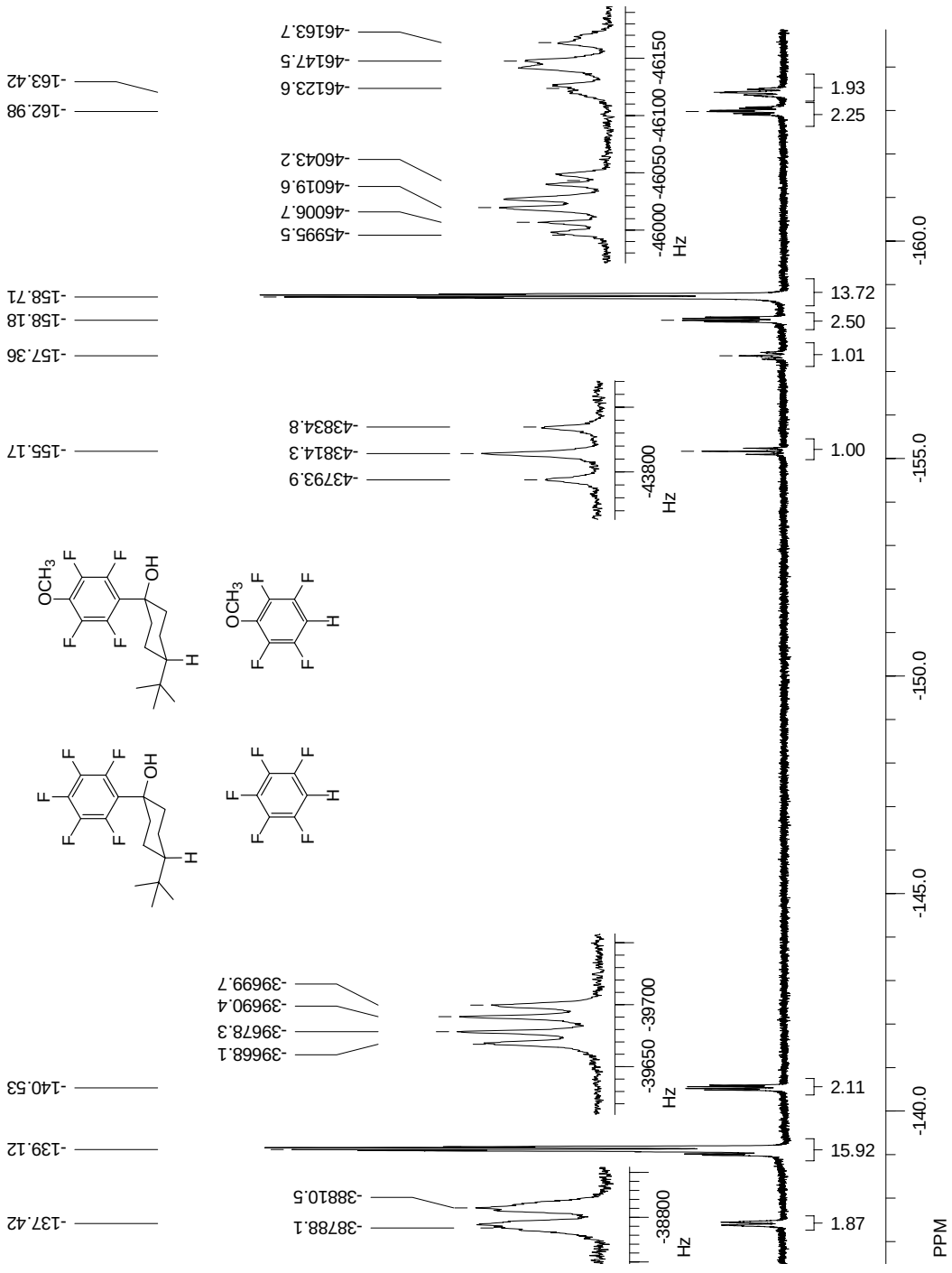

Figure A.25. Representative ^{19}F NMR Spectra of *trans*-C_6F_5 Alcohol (**88**) Reaction at t = 11 hours. (See Table A.1/A.2 for specific chemical shift assignments and Table A.5 for reaction conditions).

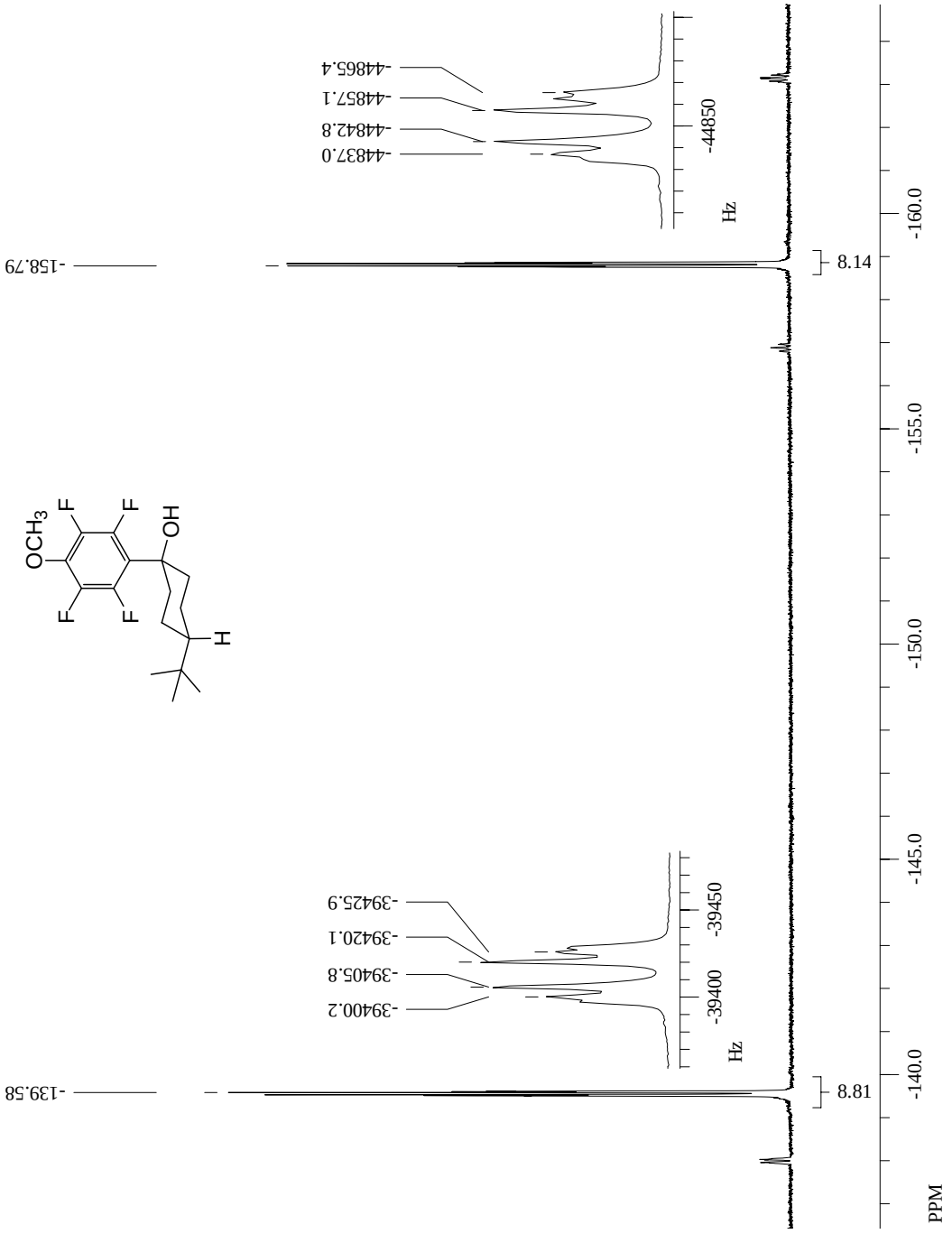

Figure A.26. ^{19}F NMR Spectra of methoxy-substituted *trans*-C_6F_5 Alcohol (**101**).
(See Table A.1/A.2 for specific chemical shift assignments.)

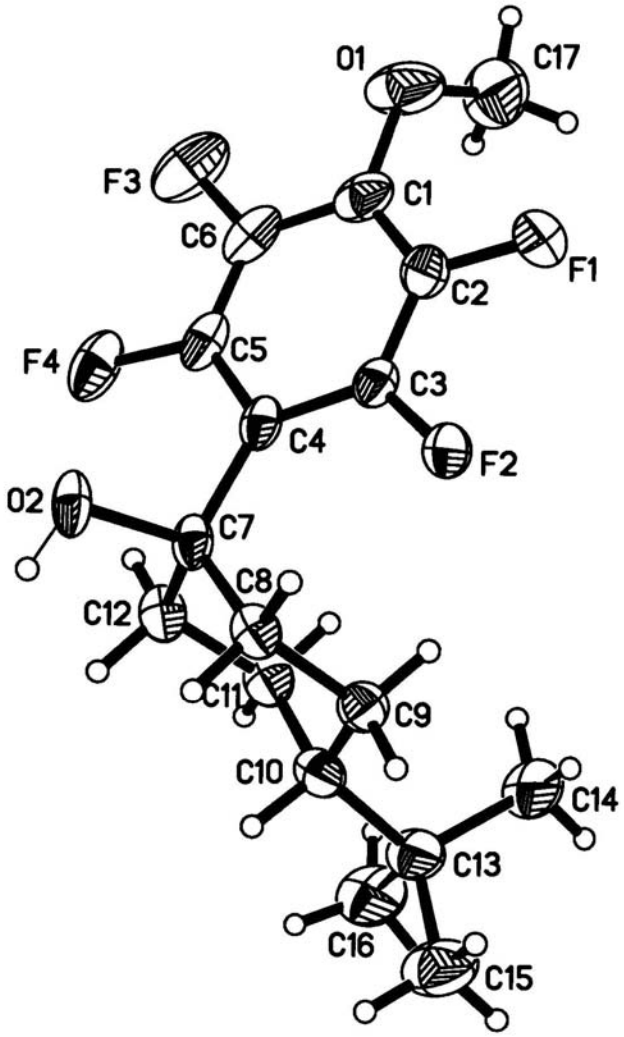

Figure A.27. X-ray structure of *trans*-4-tert-butyl-(2,3,5,6-tetrafluoro-4-methoxy-phenyl)-cyclohexanol (**101**).

Table A.6.a. Geometric Parameters for *trans*-4-*tert*-Butyl-1-(4-methoxyphenyl)-cyclohexanol (**101**) in (Å) and (°).

F(1)-C(2)	1.346(3)	F(2)-C(3)	1.342(3)
F(3)-C(6)	1.343(3)	F(4)-C(5)	1.343(3)
F(5)-C(19)	1.346(3)	F(6)-C(20)	1.341(3)
F(7)-C(23)	1.340(3)	F(8)-C(22)	1.346(3)
F(9)-C(36)	1.353(3)	F(10)-C(37)	1.346(3)
F(11)-C(40)	1.357(3)	F(12)-C(39)	1.346(3)
O(1)-C(1)	1.360(3)	O(1)-C(17)	1.386(4)
O(2)-C(7)	1.447(3)	O(3)-C(18)	1.368(3)
O(3)-C(34)	1.432(4)	O(4)-C(24)	1.441(3)
O(5)-C(35)	1.355(3)	O(5)-C(51)	1.415(4)
O(6)-C(41)	1.444(3)	C(1)-C(2)	1.371(4)
C(1)-C(6)	1.384(4)	C(2)-C(3)	1.389(3)
C(3)-C(4)	1.390(3)	C(4)-C(5)	1.394(3)
C(4)-C(7)	1.539(3)	C(5)-C(6)	1.367(4)
C(7)-C(8)	1.518(3)	C(7)-C(12)	1.534(3)
C(8)-C(9)	1.533(3)	C(9)-C(10)	1.521(4)
C(10)-C(11)	1.518(4)	C(10)-C(13)	1.561(4)
C(11)-C(12)	1.529(3)	C(13)-C(16)	1.528(4)
C(13)-C(15)	1.528(4)	C(13)-C(14)	1.530(4)
C(18)-C(19)	1.367(4)	C(18)-C(23)	1.378(4)
C(19)-C(20)	1.379(4)	C(20)-C(21)	1.396(3)
C(21)-C(22)	1.383(3)	C(21)-C(24)	1.542(3)
C(22)-C(23)	1.380(3)	C(24)-C(29)	1.528(3)
C(24)-C(25)	1.537(3)	C(25)-C(26)	1.529(3)
C(26)-C(27)	1.519(4)	C(27)-C(28)	1.533(3)
C(27)-C(30)	1.556(4)	C(28)-C(29)	1.522(3)
C(30)-C(31)	1.524(4)	C(30)-C(33)	1.531(4)
C(30)-C(32)	1.533(4)	C(35)-C(40)	1.377(4)
C(35)-C(36)	1.379(4)	C(36)-C(37)	1.363(3)
C(37)-C(38)	1.398(3)	C(38)-C(39)	1.380(3)
C(38)-C(41)	1.552(3)	C(39)-C(40)	1.388(4)
C(41)-C(46)	1.526(3)	C(41)-C(42)	1.527(3)
C(42)-C(43)	1.523(3)	C(43)-C(44)	1.527(3)
C(44)-C(45)	1.531(3)	C(44)-C(47)	1.549(4)
C(45)-C(46)	1.525(4)	C(47)-C(50)	1.530(4)
C(47)-C(48)	1.537(4)	C(47)-C(49)	1.537(4)

Table A.6.b. Geometric Parameters for *trans*-4-*tert*-Butyl-1-(4-methoxyphenyl)-cyclohexanol (**101**) in (Å) and (°).

C(1)-O(1)-C(17)	116.8(2)	C(18)-O(3)-C(34)	112.8(2)
C(35)-O(5)-C(51)	120.1(3)	O(1)-C(1)-C(2)	123.4(3)
O(1)-C(1)-C(6)	120.3(3)	C(2)-C(1)-C(6)	116.2(2)
F(1)-C(2)-C(1)	119.8(2)	F(1)-C(2)-C(3)	118.3(2)
C(1)-C(2)-C(3)	121.8(2)	F(2)-C(3)-C(2)	115.1(2)
F(2)-C(3)-C(4)	121.9(2)	C(2)-C(3)-C(4)	123.0(2)
C(3)-C(4)-C(5)	113.6(2)	C(3)-C(4)-C(7)	127.3(2)
C(5)-C(4)-C(7)	119.0(2)	F(4)-C(5)-C(6)	115.9(2)
F(4)-C(5)-C(4)	120.1(2)	C(6)-C(5)-C(4)	123.9(2)
F(3)-C(6)-C(5)	119.2(3)	F(3)-C(6)-C(1)	119.3(3)
C(5)-C(6)-C(1)	121.5(2)	O(2)-C(7)-C(8)	107.55(19)
O(2)-C(7)-C(12)	105.98(17)	C(8)-C(7)-C(12)	108.4(2)
O(2)-C(7)-C(4)	105.80(18)	C(8)-C(7)-C(4)	116.73(19)
C(12)-C(7)-C(4)	111.8(2)	C(7)-C(8)-C(9)	115.0(2)
C(10)-C(9)-C(8)	111.7(2)	C(11)-C(10)-C(9)	107.5(2)
C(11)-C(10)-C(13)	115.3(2)	C(9)-C(10)-C(13)	113.5(2)
C(10)-C(11)-C(12)	111.2(2)	C(11)-C(12)-C(7)	112.6(2)
C(16)-C(13)-C(15)	108.4(3)	C(16)-C(13)-C(14)	109.1(2)
C(15)-C(13)-C(14)	108.6(3)	C(16)-C(13)-C(10)	110.0(2)
C(15)-C(13)-C(10)	109.0(2)	C(14)-C(13)-C(10)	111.6(2)
C(19)-C(18)-O(3)	122.9(2)	C(19)-C(18)-C(23)	116.7(2)
O(3)-C(18)-C(23)	120.4(3)	F(5)-C(19)-C(18)	120.1(2)
F(5)-C(19)-C(20)	118.9(3)	C(18)-C(19)-C(20)	121.0(2)
F(6)-C(20)-C(19)	116.3(2)	F(6)-C(20)-C(21)	119.6(2)
C(19)-C(20)-C(21)	124.1(2)	C(22)-C(21)-C(20)	113.1(2)
C(22)-C(21)-C(24)	127.6(2)	C(20)-C(21)-C(24)	119.0(2)
F(8)-C(22)-C(23)	114.7(2)	F(8)-C(22)-C(21)	121.7(2)
C(23)-C(22)-C(21)	123.6(2)	F(7)-C(23)-C(18)	119.1(2)
F(7)-C(23)-C(22)	119.4(2)	C(18)-C(23)-C(22)	121.5(2)

Table A.6.c. Geometric Parameters for *trans*-4-*tert*-Butyl-1-(4-methoxyphenyl)-cyclohexanol (**101**) in (Å) and (°).

O(4)-C(24)-C(29)	108.14(18)	O(4)-C(24)-C(25)	106.29(18)
C(29)-C(24)-C(25)	107.36(19)	O(4)-C(24)-C(21)	106.33(18)
C(29)-C(24)-C(21)	115.92(19)	C(25)-C(24)-C(21)	112.32(19)
C(26)-C(25)-C(24)	112.09(19)	C(27)-C(26)-C(25)	112.0(2)
C(26)-C(27)-C(28)	107.69(19)	C(26)-C(27)-C(30)	114.4(2)
C(28)-C(27)-C(30)	113.9(2)	C(29)-C(28)-C(27)	112.4(2)
C(28)-C(29)-C(24)	115.18(19)	C(31)-C(30)-C(33)	107.8(3)
C(31)-C(30)-C(32)	108.7(2)	C(33)-C(30)-C(32)	108.6(3)
C(31)-C(30)-C(27)	112.6(2)	C(33)-C(30)-C(27)	110.1(2)
C(32)-C(30)-C(27)	109.0(2)	O(5)-C(35)-C(40)	128.5(3)
O(5)-C(35)-C(36)	116.6(3)	C(40)-C(35)-C(36)	114.9(2)
F(9)-C(36)-C(37)	119.3(2)	F(9)-C(36)-C(35)	118.4(2)
C(37)-C(36)-C(35)	122.3(3)	F(10)-C(37)-C(36)	115.2(2)
F(10)-C(37)-C(38)	120.3(2)	C(36)-C(37)-C(38)	124.5(2)
C(39)-C(38)-C(37)	112.2(2)	C(39)-C(38)-C(41)	127.0(2)
C(37)-C(38)-C(41)	120.5(2)	F(12)-C(39)-C(38)	121.7(2)
F(12)-C(39)-C(40)	114.3(2)	C(38)-C(39)-C(40)	124.0(2)
F(11)-C(40)-C(35)	121.0(2)	F(11)-C(40)-C(39)	116.9(3)
C(35)-C(40)-C(39)	122.1(2)	O(6)-C(41)-C(46)	109.06(18)
O(6)-C(41)-C(42)	105.54(18)	C(46)-C(41)-C(42)	107.95(19)
O(6)-C(41)-C(38)	106.13(18)	C(46)-C(41)-C(38)	115.89(19)
C(42)-C(41)-C(38)	111.75(18)	C(43)-C(42)-C(41)	113.17(19)
C(42)-C(43)-C(44)	111.96(19)	C(43)-C(44)-C(45)	107.28(19)
C(43)-C(44)-C(47)	113.95(19)	C(45)-C(44)-C(47)	115.3(2)
C(46)-C(45)-C(44)	111.9(2)	C(45)-C(46)-C(41)	115.7(2)
C(50)-C(47)-C(48)	109.0(2)	C(50)-C(47)-C(49)	107.7(2)
C(48)-C(47)-C(49)	108.4(2)	C(50)-C(47)-C(44)	109.5(2)
C(48)-C(47)-C(44)	111.6(2)	C(49)-C(47)-C(44)	110.5(2)

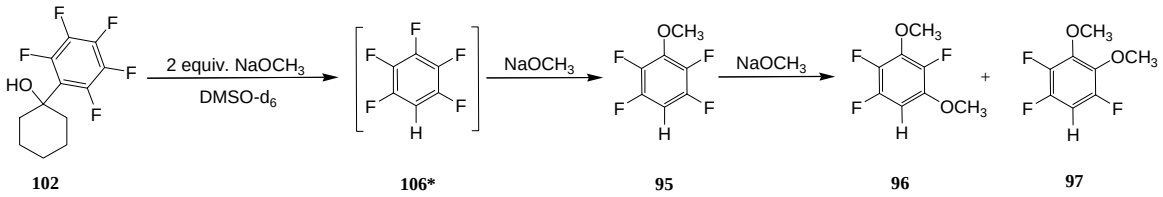

$[\mathbf{102}]_o$ = 0.1035 M

Table A.7. ^{19}F NMR Kinetic Data for C_6F_5-Cyclohexanol (**102**) Reaction in DMSO-d_6 treated with 2 equivalents of Sodium Methoxide.

Scan No.	Time, min.	% **102** Remaining (avg. integrals)	% Formation of **95**	% Formation of **96**	**%** Formation of **97**
1	0	100 (2.694)	0	0	0
2	4.03	-	87.8 (2.212)	2.70 (0.068)	9.45 (0.238)
3	6.23	-	82.2 (2.194)	3.90 (0.104)	13.9 (0.370)
4	8.43	-	77.3 (2.050)	5.69 (0.151)	17.0 (0.452)
5	10.6	-	74.6 (1.976)	4.95 (0.131)	20.5 (0.542)
6	12.8	-	70.3 (1.813)	6.20 (0.160)	23.5 (0.606)
7	18.0	-	65.4 (1.745)	6.25 (0.167)	28.4 (0.758)
8	23.2	-	60.4 (1.573)	7.06 (0.184)	32.6 (0.849)
9	28.4	-	56.8 (1.499)	7.34 (0.194)	35.9 (0.947)
10	33.6	-	54.7 (1.493)	7.22 (0.197)	38.1 (1.038)
11	43.8	-	49.0 (1.342)	8.58 (0.235)	42.4 (1.161)
12	54.0	-	45.2 (1.234)	9.62 (0.263)	45.2 (1.235)
13	64.2	-	42.5 (1.118)	10.1 (0.266)	47.4 (1.245)

* Pentafluorobenzene is not visualized in this reaction, however it is an important part of the mechanism.
Note 1: There a +/- 1% error on all percentages reported in this table.
Note 2: Addition of fluorobenzene (2 µL) was used as a chemical shift reference (-113.26 ppm) and as an internal standard to calibrate peak integrations.

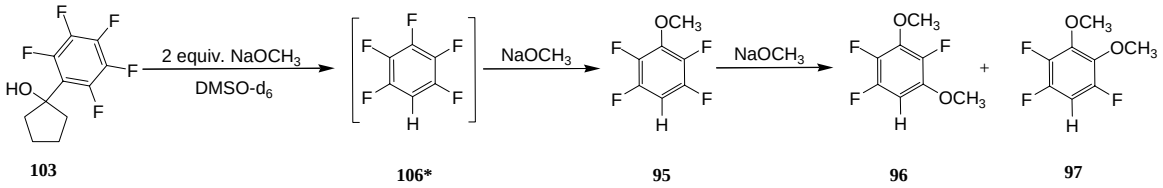

$[\mathbf{103}]_o$ = 0.1035 M

Table A.8. ^{19}F NMR Kinetic Data for C_6F_5-Cyclopentanol (**103**) Reaction in DMSO-d_6 treated with 2 equivalents of Sodium Methoxide.

Scan No.	Time, min.	% **103** Remaining (avg. integrals)	% Formation of **95**	% Formation of **96**	**%** Formation of **97**
1	0	100 (2.311)	0	0	0
2	3.00	-	91.6 (1.889)	-	8.43 (0.174)
3	5.20	-	82.6 (1.733)	3.90 (0.081)	13.6 (0.285)
4	7.40	-	78.0 (1.655)	5.51 (0.117)	16.5 (0.351)
5	9.60	-	74.2 (1.622)	5.26 (0.115)	20.5 (0.449)
6	11.8	-	71.8 (1.538)	5.28 (0.113)	22.9 (0.490)
7	17.0	-	66.2 (1.442)	6.15 (0.134)	28.6 (0.623)
8	22.2	-	60.7 (1.315)	7.34 (0.159)	31.9 (0.692)
9	27.4	-	57.4 (1.302)	8.02 (0.182)	34.6 (0.785)
10	32.6	-	53.8 (1.200)	8.83 (0.197)	37.4 (0.834)
11	42.8	-	49.0 (1.124)	8.94 (0.205)	42.1 (0.965)
12	53.0	-	44.4 (1.001)	10.8 (0.244)	44.7 (1.007)
13	63.2	-	41.5 (0.925)	11.4 (0.255)	47.1 (1.049)

* Pentafluorobenzene is not visualized in this reaction, however it is an important part of the mechanism.
Note 1: There a +/- 1% error on all percentages reported in this table.
Note 2: Addition of fluorobenzene (2 µL) was used as a chemical shift reference (-113.26 ppm) and as an internal standard to calibrate peak integrations.

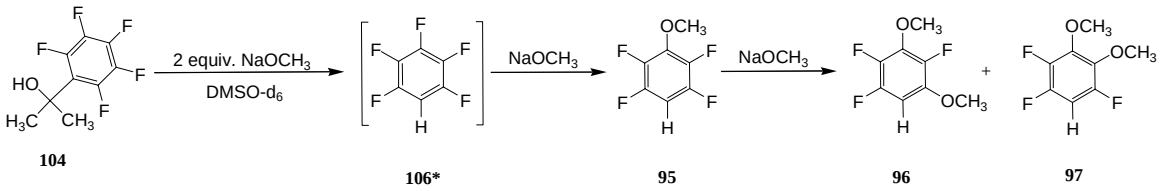

$[\mathbf{104}]_o$ = 0.1035 M

Table A.9. ^{19}F NMR Kinetic Data for 2-C_6F_5-2-Propanol (**104**) Reaction in DMSO-d_6 treated with 2 equivalents of Sodium Methoxide.

Scan No.	Time, min.	% **104** Remaining (avg. integrals)	% Formation of **95**	% Formation of **96**	**%** Formation of **97**
1	0	100 (2.773)	0	0	0
2	3.32	-	91.2 (2.251)	-	8.83 (0.218)
3	5.51	-	85.5 (2.173)	4.88 (0.124)	9.60 (0.244)
4	7.72	-	79.8 (2.063)	6.65 (0.172)	13.6 (0.351)
5	9.92	-	79.1 (2.063)	5.26 (0.137)	15.6 (0.407)
6	12.1	-	74.7 (1.926)	7.01 (0.181)	18.3 (0.473)
7	17.3	-	69.2 (1.943)	7.70 (0.216)	23.1 (0.648)
8	22.5	-	64.6 (1.652)	8.17 (0.209)	27.2 (0.696)
9	27.7	-	60.8 (1.605)	8.60 (0.227)	30.6 (0.808)
10	32.9	-	59.1 (1.568)	7.43 (0.197)	33.4 (0.886)
11	43.1	-	54.2 (1.419)	8.33 (0.218)	37.4 (0.979)
12	53.3	-	50.7 (1.313)	8.54 (0.221)	40.7 (1.054)
13	63.5	-	48.2 (1.243)	9.84 (0.254)	42.0 (1.083)

* Pentafluorobenzene is not visualized in this reaction, however it is an important part of the mechanism.
Note 1: There a +/- 1% error on all percentages reported in this table.
Note 2: Addition of fluorobenzene (2 µL) was used as a chemical shift reference (-113.26 ppm) and as an internal standard to calibrate peak integrations.

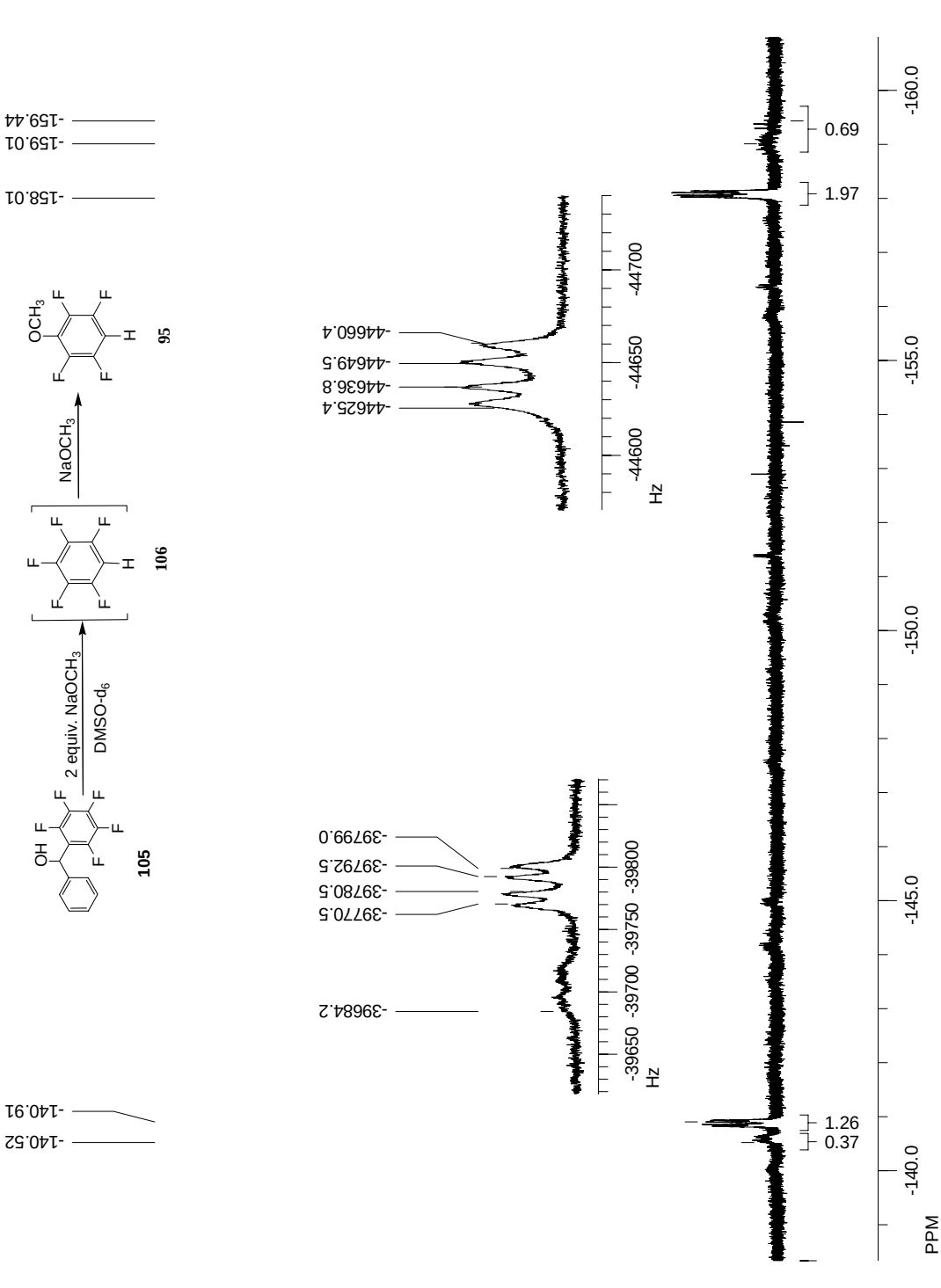

Figure A.28. ^{19}F NMR Spectra of (Pentafluorophenyl)-Phenylmethanol (**105**) Reaction in DMSO-d_6 at t_{rxn} ~ 1 hour.

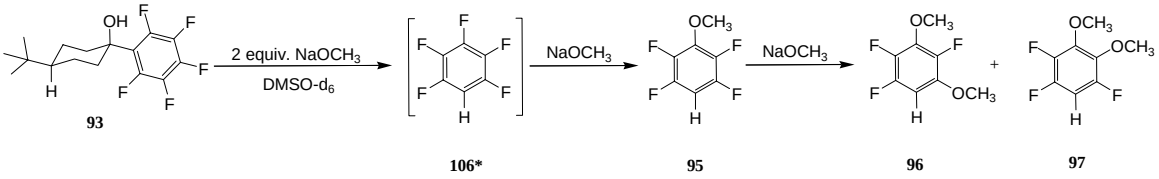

93 **106*** **95** **96** **97**

$[\mathbf{93}]_o$ = 0.1035 M

Table A.10. ^{19}F NMR Kinetic Data for Solvent Studies using **93** in DMSO-d_6 treated with 2 equivalents of Sodium Methoxide and monitored for 3 hours.

Scan No.	Time, min.	% **93** Remaining (avg. integrals)	% Formation of **95**	% Formation of **96**	**%** Formation of **97**
1	0	100 (5.538)	0	0	0
2	2.62	-	92.5 (4.348)	-	7.49 (0.352)
6	10.6	-	76.5 (2.140)	4.25 (0.119)	19.3 (0.540)
8	20.6	-	65.0 (2.772)	6.22 (0.265)	28.8 (1.226)
10	30.6	-	57.5 (2.759)	6.92 (0.332)	35.6 (1.706)
12	40.6	-	54.4 (2.405)	6.94 (0.307)	38.7 (1.712)
13	50.6	-	49.9 (2.435)	6.92 (0.338)	43.2 (2.110)
14	60.6	-	47.0 (2.289)	8.42 (0.409)	44.5 (2.162)
17	90.6	-	41.2 (2.063)	9.36 (0.469)	49.5 (2.481)
20	120.6	-	39.4 (1.836)	9.72 (0.453)	50.9 (2.373)
21	180.6	-	36.9 (1.827)	9.07 (0.449)	54.0 (2.676)

* Pentafluorobenzene is not visualized in this reaction, however it is an important part of the mechanism.
Note 1: There a +/- 1% error on all percentages reported in this table.
Note 2: Addition of fluorobenzene (2 µL) was used as a chemical shift reference (-113.26 ppm) and as an internal standard to calibrate peak integrations.

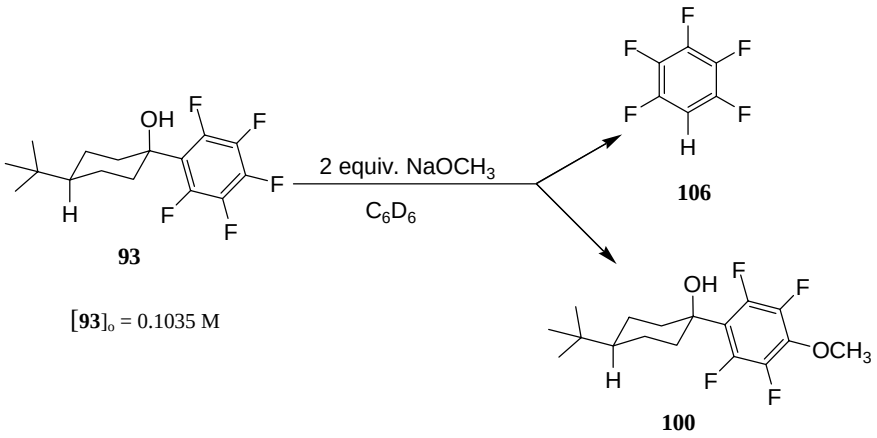

[**93**]$_o$ = 0.1035 M

Table A.11. ^{19}F NMR Kinetic Data for Solvent Studies using **93** in C_6D_6 treated with 2 equivalents of Sodium Methoxide and monitored for 3 hours.

Scan No.	Time, min.	% **93** Remaining (avg. integrals)	% Formation of **106**	% Formation of **100**
1	0	100 (2.994)	0	0
2	2.27	100 (2.916)	-	-
6	10.3	100 (3.158)	-	-
7	20.3	92.4 (2.760)	6.16 (0.184)	1.47 (0.044)
8	30.3*	95.0 (2.818)	3.20 (0.095)	1.79 (0.053)
9	60.3	91.0 (2.688)	5.11 (0.151)	3.86 (0.114)
10	120.3	85.0 (2.454)	8.35 (0.241)	6.65 (0.192)
11	180.3	79.7 (2.180)	11.0 (0.300)	9.32 (0.255)

* The discrepancy in this series of values are due to the integrations of the spectra.
Note 1: There a +/- 1% error on all percentages reported in this table.
Note 2: Addition of fluorobenzene (2 μL) was used as a chemical shift reference (-113.26 ppm) and as an internal standard to calibrate peak integrations.

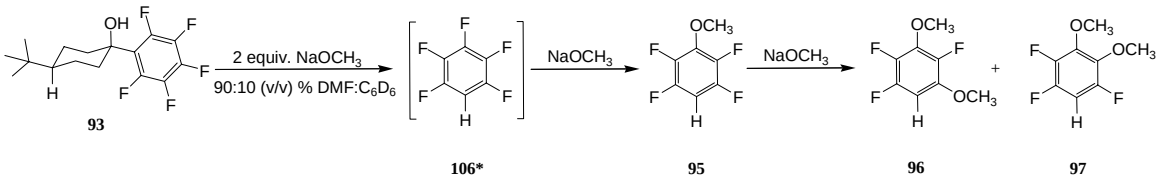

93 **106*** **95** **96** **97**

$[\mathbf{93}]_o$ = 0.1035 M

Table A.12. ^{19}F NMR Kinetic Data for Solvent Studies using **93** in 90:10 (v/v) % DMF:C_6D_6 treated with 2 equivalents of Sodium Methoxide and monitored for 2 hours.

Scan No.	Time, min.	% **93** Remaining (avg. integrals)	% Formation of **95**	% Formation of **96**	**%** Formation of **97**
1	0	100 (4.900)	0	0	0
2	2.25	-	100 (3.363)	-	-
5	13.8	-	89.6 (3.268)	2.55 (0.093)	7.87 (0.287)
6	20.3	-	86.2 (3.209)	3.98 (0.148)	9.81(0.365)
7	30.3	-	83.0 (2.835)	3.95 (0.135)	13.0 (0.445)
8	40.3	-	82.3 (3.060)	2.98 (0.111)	14.8 (0.549)
9	50.3	-	79.9 (2.709)	3.24 (0.110)	16.9 (0.572)
10	60.3	-	77.5 (2.973)	4.12 (0.158)	18.4 (0.706)
13	90.3	-	72.6 (2.644)	3.98 (0.145)	23.4 (0.853)
14	120.3	-	67.9 (2.527)	4.87 (0.181)	27.2 (1.011)

* Pentafluorobenzene is not visualized in this reaction, however it is an important part of the mechanism.
Note 1: There a +/- 1% error on all percentages reported in this table.
Note 2: Addition of fluorobenzene (2 µL) was used as a chemical shift reference (-113.26 ppm) and as an internal standard to calibrate peak integrations.

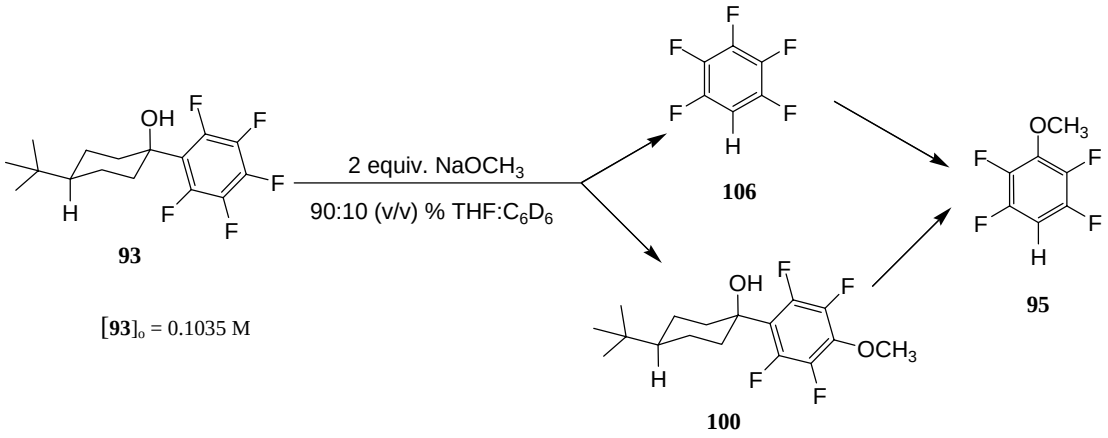

Table A.13. ^{19}F NMR Kinetic Data for Solvent Studies using **93** in 90:10 (v/v) % THF:C_6D_6 treated with 2 equivalents of Sodium Methoxide and monitored for 3 hours.

Scan No.	Time, min.	% **93** Remaining (avg. integrals)	% Formation of **106**	% Formation of **100**	% Formation of **95**
1	0	100 (3.963)	0	0	0
2	2.50	86.7 (3.103)	10.4 (0.374)	1.95 (0.070)	0.949 (0.034)
6	10.5	49.6 (1.675)	30.3 (1.023)	6.99 (0.236)	13.1 (0.441)
8	20.5	32.1 (1.153)	29.6 (1.063)	11.1 (0.398)	27.1 (0.974)
10	30.5	22.1 (0.718)	28.1 (0.915)	12.8 (0.418)	37.1 (1.203)
11	40.5	19.4 (0.638)	23.5 (0.773)	11.4 (0.376)	45.8 (1.508)
12	50.5	16.9 (0.489)	21.7 (0.626)	12.8 (0.370)	48.6 (1.404)
13	60.5	9.32 (0.262)	20.8 (0.585)	15.4 (0.434)	54.4 (1.531)
15	90.5	6.01 (0.171)	16.4 (0.466)	14.8 (0.422)	62.8 (1.786)
16	120.5	3.46 (0.106)	14.9 (0.455)	13.1 (0.402)	68.5 (2.097)
17	180.5	2.94 (0.092)	9.75 (0.305)	16.4 (0.512)	70.9 (2.219)

Note 1: There a +/- 1% error on all percentages reported in this table.
Note 2: Addition of fluorobenzene (2 µL) was used as a chemical shift reference (-113.26 ppm) and as an internal standard to calibrate peak integrations.

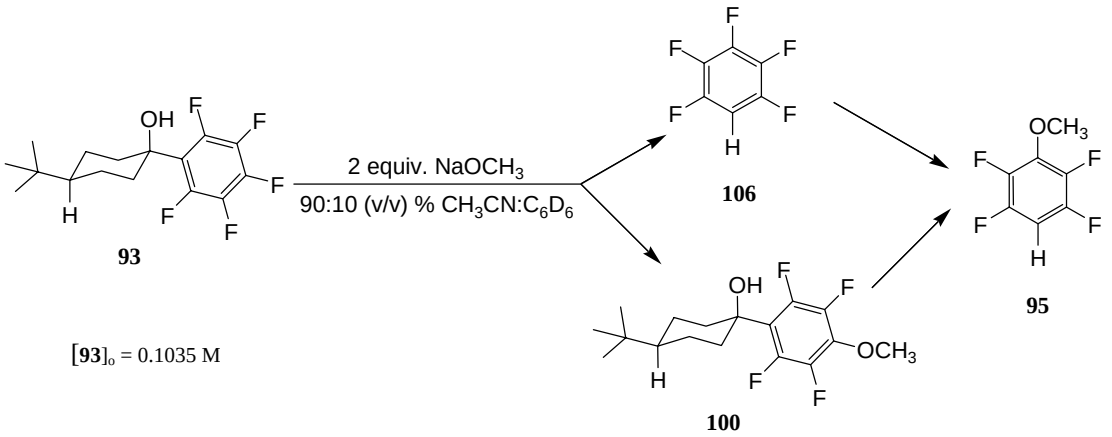

Table A.14. ^{19}F NMR Kinetic Data for Solvent Studies using **93** in 90:10 (v/v) % $CH_3CN:C_6D_6$ treated with 2 equivalents of Sodium Methoxide and monitored for 3 hours.

Scan No.	Time, min.	% **93** Remaining (avg. integrals)	% Formation of **106**	% Formation of **100**	% Formation of **95**
1	0	100 (3.563)	0	0	0
2	2.33	65.9 (1.913)	30.8 (0.893)	-	3.27 (0.095)
6	10.3	5.28 (0.113)	55.1 (1.181)	8.92 (0.191)	30.7 (0.657)
8	20.3	-	33.9 (0.777)	11.9 (0.272)	54.3 (1.244)
9	30.3	-	22.4 (0.484)	10.3 (0.221)	67.3 (1.451)
11	40.3	-	15.1 (0.293)	10.9 (0.211)	74.0 (1.434)
12	50.3	-	9.89 (0.233)	8.62 (0.203)	81.5 (1.919)
13	60.3	-	6.43 (0.149)	11.0 (0.254)	82.6 (1.913)
15	90.3	-	2.52 (0.051)	8.30 (0.168)	89.2 (1.805)
16	120.3	-	-	8.46 (0.179)	91.5 (1.936)
17	180.3	-	-	7.39 (0.178)	92.6 (2.230)

Note 1: There a +/- 1% error on all percentages reported in this table.
Note 2: Addition of fluorobenzene (2 µL) was used as a chemical shift reference (-113.26 ppm) and as an internal standard to calibrate peak integrations.

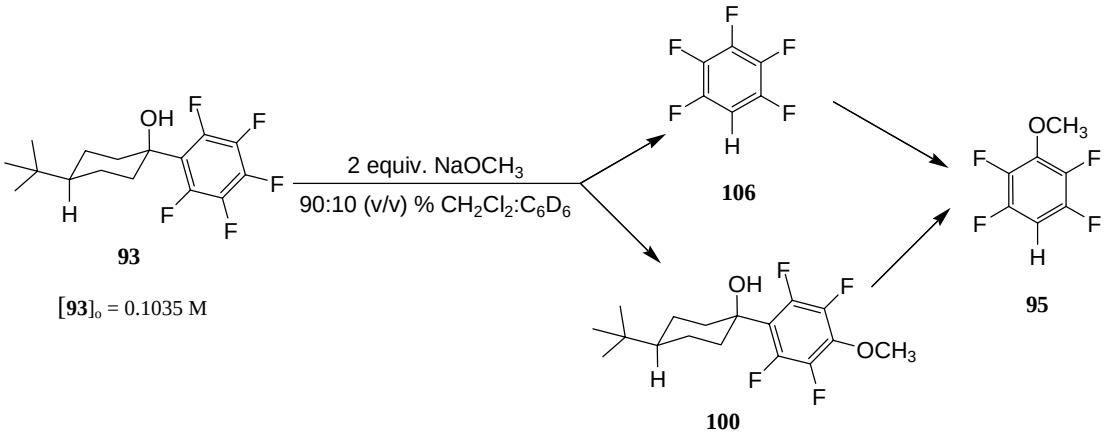

Table A.15. ^{19}F NMR Kinetic Data for Solvent Studies using **93** in 90:10 (v/v) % CH_2Cl_2:C_6D_6 treated with 2 equivalents of Sodium Methoxide and monitored for 3 hours.

Scan No.	Time, min.	% **93** Remaining (avg. integrals)	% Formation of **106**	% Formation of **100**	% Formation of **95**
1	0	100 (3.255)	0	0	0
2	2.25	100 (4.810)	-	-	-
6	10.3	96.4 (5.175)	2.38 (0.128)	-	1.25 (0.067)
7	20.3	94.3 (4.189)	4.03 (0.179)	-	1.62 (0.072)
8	30.3	89.7 (4.352)	5.36 (0.260)	-	4.93 (0.239)
9	40.3	90.3 (4.278)	6.80 (0.322)	-	2.89 (0.137)
10	50.3	87.3 (4.219)	8.73 (0.422)	-	3.95 (0.191)
11	60.3	85.4 (4.009)	9.86 (0.463)	-	4.73 (0.222)
14	90.3	78.9 (3.737)	12.6 (0.597)	1.60 (0.076)	6.94 (0.329)
15	120.3	73.3 (3.373)	15.7 (0.723)	1.69 (0.078)	9.30 (0.428)
16	180.3	61.0 (2.223)	23.7 (0.864)	3.10 (0.113)	12.2 (0.443)

Note 1: There a +/- 1% error on all percentages reported in this table.
Note 2: Addition of fluorobenzene (2 µL) was used as a chemical shift reference (-113.26 ppm) and as an internal standard to calibrate peak integrations.

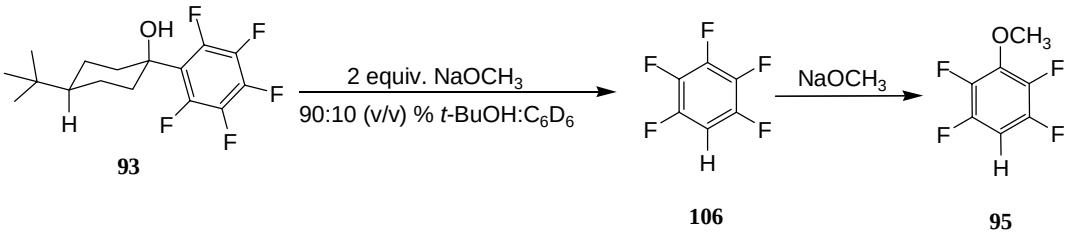

$[\mathbf{93}]_o$ = 0.1035 M

Table A.16. ^{19}F NMR Kinetic Data for Solvent Studies using **93** in 90:10 (v/v) % *t*-BuOH:C_6D_6 treated with 2 equivalents of Sodium Methoxide and monitored for 3 hours.

Scan No.	Time, min.	% **93** Remaining (avg. integrals)	% Formation of **106**	% Formation of **95**
1	0	100 (4.162)	0	0
2	2.08	100 (4.429)	-	-
6	10.1	97.1 (3.909)	2.90 (0.118)	-
7	20.1	93.8 (3.663)	5.04 (0.197)	1.15 (0.045)
8	30.1	90.7 (3.607)	7.89 (0.314)	1.46 (0.058)
9	40.1	87.9 (3.500)	10.5 (0.418)	1.61 (0.064)
10	50.1	88.0 (3.795)	9.51 (0.410)	2.48 (0.107)
11	60.1	84.8 (3.633)	12.5 (0.535)	2.71 (0.116)
14	90.1	78.1 (3.275)	19.1 (0.799)	2.79 (0.117)
15	120.1	72.5 (2.973)	23.3 (0.953)	4.20 (0.172)
16	180.1	58.6 (2.314)	33.7 (1.330)	7.79 (0.308)

Note 1: There a +/- 1% error on all percentages reported in this table.
Note 2: Addition of fluorobenzene (2 µL) was used as a chemical shift reference (-113.26 ppm) and as an internal standard to calibrate peak integrations.

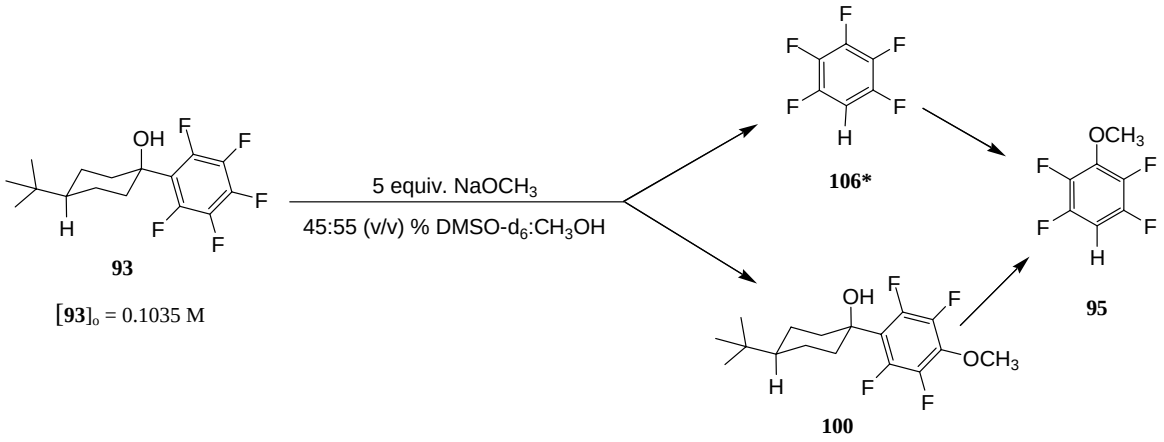

Table A.17. ^{19}F NMR Data for Rate Studies using **93** in 45:55 (v/v) % DMSO-d_6:CH_3OH
(See Figure 2.26 for linear plot of alcohol depletion).

Scan No.	Time, min. (~hour)	% **93** Remaining (avg. integrals)	% Formation of **100**	% Formation of **95**
1	0	100 (3.070)	0	0
2	7.43	96.6 (2.897)	3.40 (0.102)	-
7	32.6 (0.5)	84.8 (2.137)	15.2 (0.384)	-
13	63.2 (1.0)	69.5 (1.948)	27.2 (0.761)	3.32 (0.093)
19	125.3 (2.0)	44.3 (1.107)	48.4 (1.210)	7.28 (0.182)
25	187.5 (3.0)	35.3 (0.922)	54.7 (1.430)	9.95 (0.260)
31	249.5 (4.0)	24.5 (0.660)	64.4 (1.734)	11.1 (0.298)
36	311.7 (5.0)	19.4 (0.508)	68.4 (1.789)	12.2 (0.319)
42	373.9 (6.0)	14.1 (0.381)	72.7 (1.962)	13.2 (0.355)
48	436.0 (7.0)	10.9 (0.283)	78.3 (2.024)	14.7 (0.379)
54	498.2 (8.0)	7.55 (0.200)	77.7 (2.059)	14.7 (0.390)

*Formation of Pentaflurobenzene was not observed.
Note 1: There a +/- 1% error on all percentages reported in this table.
Note 2: Addition of fluorobenzene (2 µL) was used as a chemical shift reference (-113.26 ppm) and as an internal standard to calibrate peak integrations.

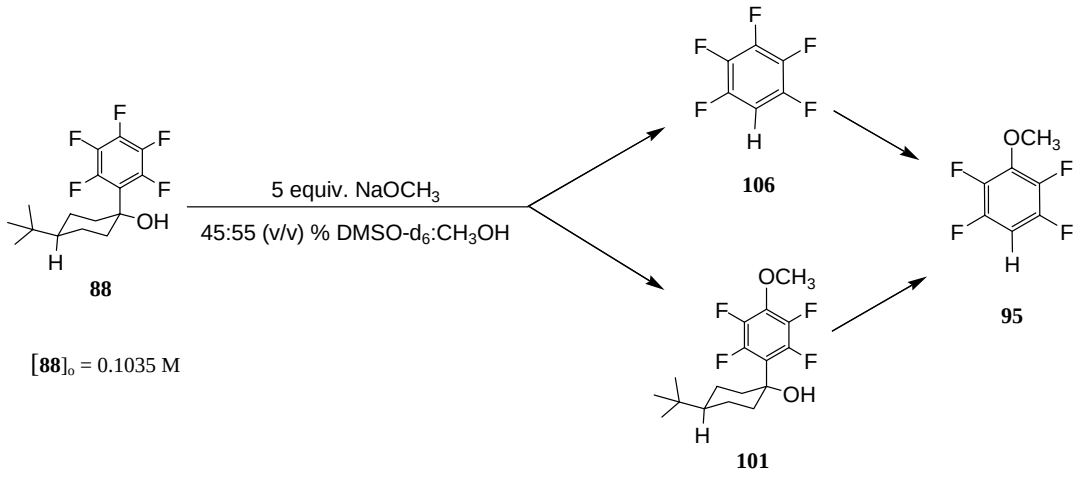

Table A.18. ^{19}F NMR Data for Rate Studies using **88** in 45:55 (v/v) % DMSO-d_6:CH_3OH
(See Figure 2.26 for linear plot of alcohol depletion).

Scan No.	Time, min. (~hour)	% **88** Remaining (avg. integrals)	% Formation of **106**	% Formation of **101**	% Formation of **95**
1	0	100 (3.906)	0	0	0
2	7.23	71.2 (1.888)	9.77 (0.259)	19.0 (0.504)	-
4	17.3 (0.3)	44.3 (1.168)	16.1 (0.424)	34.9 (0.920)	4.74 (0.125)
7	32.6 (0.5)	21.8 (0.574)	17.1 (0.450)	49.8 (1.314)	11.3 (0.298)
10	47.5 (0.8)	15.2 (0.417)	15.5 (0.426)	52.9 (1.449)	16.4 (0.448)
13	62.6 (1.0)	4.49 (0.115)	11.5 (0.295)	59.7 (1.530)	25.8 (0.622)

Note 1: There a +/- 1% error on all percentages reported in this table.
Note 2: Addition of fluorobenzene (2 µL) was used as a chemical shift reference (-113.26 ppm) and as an internal standard to calibrate peak integrations.

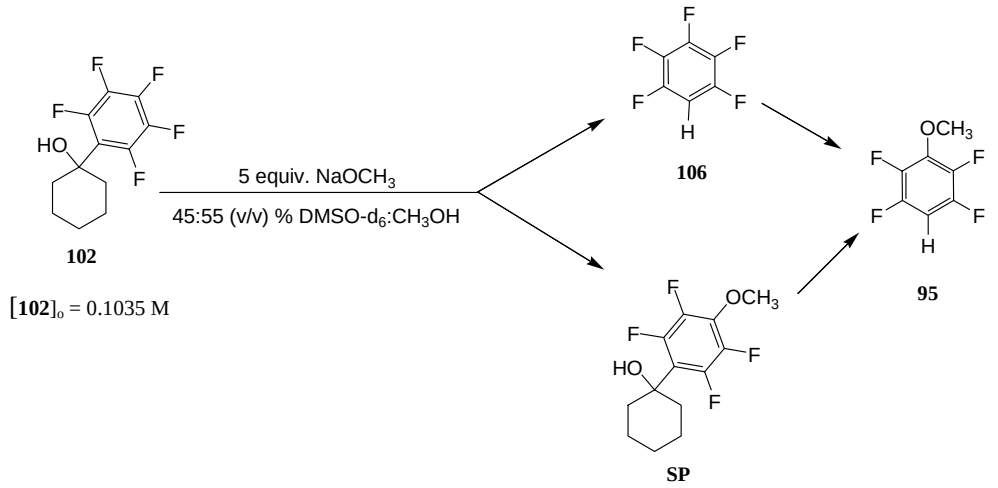

Table A.19. ^{19}F NMR Data for Rate Studies using **102** in 45:55 (v/v) % DMSO-d_6:CH_3OH
(See Figure 2.26 for linear plot of alcohol depletion).

Scan No.	Time, min. (~hour)	% **102** Remaining (avg. integrals)	% Formation of **106**	% Formation of **SP**	% Formation of **95**
1	0	100 (2.854)	0	0	0
2	7.47	91.3 (2.480)	3.35 (0.091)	5.34 (0.145)	-
7	33.0 (0.5)	70.5 (1.952)	6.32 (0.175)	19.0 (0.525)	4.19 (0.116)
13	63.2 (1.0)	49.2 (1.292)	7.16 (0.188)	33.0 (0.867)	10.7 (0.279)
19	125.4 (2.0)	27.0 (0.457)	4.90 (.083)	47.6 (0.807)	20.5 (0.348)
25	187.5 (3.0)	14.8 (0.386)	3.68 (0.096)	55.3 (1.443)	26.3 (0.686)
31	250.1 (4.0)	8.78 (0.224)	1.65 (0.042)	59.7 (1.524)	29.8 (0.761)
36	312.2 (5.0)	4.66 (0.112)	-	62.8 (1.509)	32.5 (0.781)
42	374.4 (6.0)	3.14 (0.080)	-	63.8 (1.627)	33.1 (0.844)

Note 1: There a +/- 1% error on all percentages reported in this table.
Note 2: Addition of fluorobenzene (2 µL) was used as a chemical shift reference (-113.26 ppm) and as an internal standard to calibrate peak integrations.

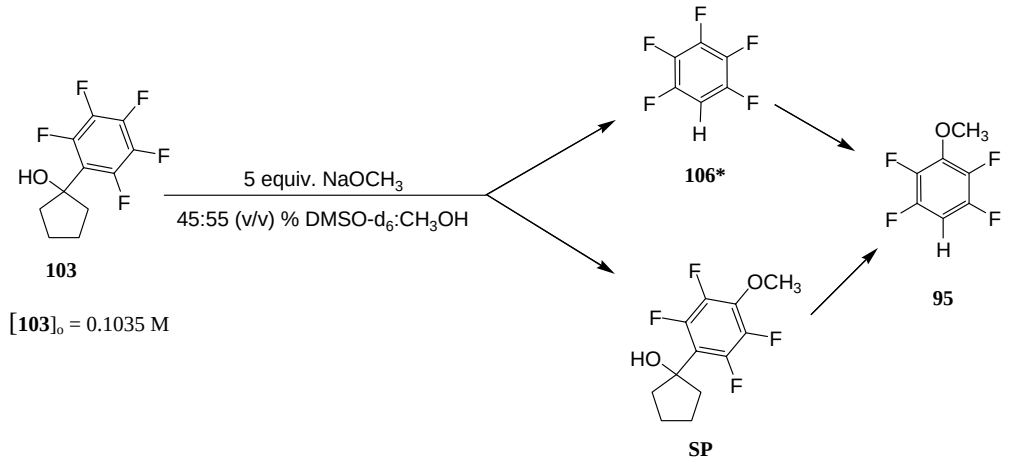

Table A.20. ^{19}F NMR Data for Rate Studies using **103** in 45:55 (v/v) % DMSO-d_6:CH_3OH
(See Figure 2.26 for linear plot of alcohol depletion).

Scan No.	Time, min. (~hour)	% **103** Remaining (avg. integrals)	% Formation of **SP**	% Formation of **95**
1	0	100 (2.567)	0	0
2	7.49	94.4 (2.397)	5.56 (0.141)	-
7	32.3 (0.5)	71.5 (1.923)	28.5 (0.765)	-
13	67.5 (1.0)	58.2 (1.433)	41.8 (1.028)	-
19	129.7 (2.0)	34.8 (0.845)	61.5 (1.495)	3.74 (0.091)
25	191.9 (3.0)	22.0 (0.527)	73.4 (1.756)	4.56 (0.109)
31	254.0 (4.0)	13.7 (0.349)	80.6 (2.053)	5.73 (0.146)
36	316.2 (5.0)	8.89 (0.239)	85.0 (2.285)	6.14 (0.165)
42	378.3 (6.0)	5.61 (0.143)	88.0 (2.245)	6.39 (0.163)
48	440.5 (7.0)	4.06 (0.101)	89.7 (2.233)	6.23 (0.155)

* Formation of Pentafluorobenzene was not observed.
Note 1: There a +/- 1% error on all percentages reported in this table.
Note 2: Addition of fluorobenzene (2 µL) was used as a chemical shift reference (-113.26

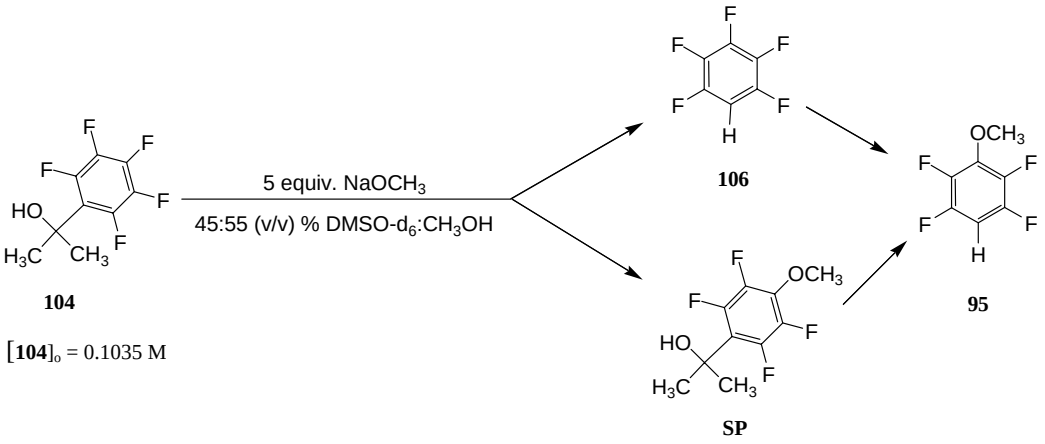

Table A.21. ^{19}F NMR Data for Rate Studies using **104** in 45:55 (v/v) % DMSO-d_6:CH_3OH
(See Figure 2.26 for linear plot of alcohol depletion).

Scan No.	Time, min. (~hour)	% **104** Remaining (avg. integrals)	% Formation of **106**	% Formation of **SP**	% Formation of **95**
1	0	100 (4.043)	0	0	0
2	7.36	85.9 (2.595)	9.77 (0.295)	4.30 (0.130)	-
7	32.5 (0.5)	55.1 (1.602)	15.8 (0.459)	14.5 (0.420)	8.33 (0.242)
13	62.7 (1.0)	34.7 (1.054)	17.1 (0.502)	24.6 (0.722)	23.6 (0.694)
19	124.9 (2.0)	12.2 (0.389)	25.4 (0.812)	27.0 (0.862)	35.4 (1.130)
25	187.0 (3.0)	7.23 (0.209)	5.82 (0.168)	34.9 (1.008)	52.1 (1.504)
31	249.2 (4.0)	3.21 (0.091)	3.57 (0.101)	35.7 (1.010)	57.5 (1.629)

Note 1: There a +/- 1% error on all percentages reported in this table.
Note 2: Addition of fluorobenzene (2 µL) was used as a chemical shift reference (-113.26 ppm) and as an internal standard to calibrate peak integrations.

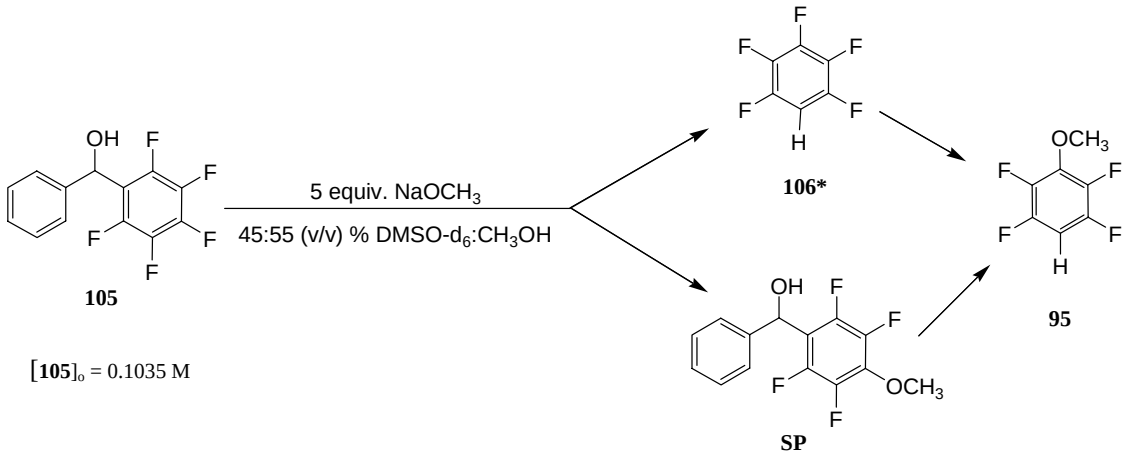

Table A.22. ^{19}F NMR Data for Rate Studies using **105** in 45:55 (v/v) % DMSO-d_6:CH3OH
(See Figure 2.26 for linear plot of alcohol depletion).

Scan No.	Time, min. (~hour)	% **105** Remaining (avg. integrals)	% Formation of **SP**	% Formation of **95**
1	0	100 (2.925)	0	0
2	8.31	93.1 (2.052)	6.90 (0.152)	-
7	33.5 (0.5)	68.2 (1.470)	27.6 (0.588)	3.47 (0.074)
13	63.6 (1.0)	50.5 (1.077)	46.1 (0.983)	3.33 (0.071)
19	125.8 (2.0)	29.7 (0.550)	65.6 (1.216)	4.75 (0.088)
25	188.0 (3.0)	18.0 (0.323)	76.4 (1.369)	5.58 (0.100)
31	250.1 (4.0)	7.41 (0.158)	88.7 (1.890)	3.89 (0.083)
36	312.3 (5.0)	5.83 (0.121)	89.6 (1.860)	4.53 (0.094)

* Formation of fluorobenzene was not observed.
Note 1: There a +/- 1% error on all percentages reported in this table.
Note 2: Addition of fluorobenzene (2 µL) was used as a chemical shift reference (-113.26 ppm) and as an internal standard to calibrate peak integrations.

APPENDIX B

LIST OF TABLES

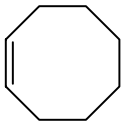

Cyclooctene (**115**)
C_8H_{14}
Mol. Wt. = 110.20

Table B.1. Observed Product Formation of Cyclooctene After Passage Through Modified Metal Liners.

Temperature Program: 60, hold for 2 min. to 270° C @ 20° C/min.

$ZnCl_2$	$CuCl_2$	$(Cp)W(CO)_3Cl$	$Br(CO)_5Mn$	$AgClO_4$	$ZrCl_4$	H_2PtCl_6	$RhCl_3$	$RuCl_3$
N. R.	S.M. 5.73 min.	S.M. 5.76 min	N. R.	S.M. 5.76 min.	N.R.	N.R.	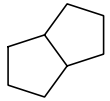 6.82 min. M = 110	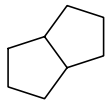 6.65 min. M = 110
	 5.99 min. M = 112	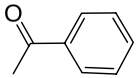 M = 120 7.27 min.		 5.99 min. M = 112			S.M. 7.17 min.	
	N.I. 9.66 min. M = 240			N.I. 7.75 min. M = 214			 7.41 min. M = 112	
	N.I. 10.1 min. M = 192							
	N.I. 11.9 min. M = 209							

S.M. = Starting Material **N.R**. = No Reaction Observed. **N.I.** = Structure Not Identified.

Table B.2. Observed Product Formation of 3-Carene After Passage Through Modified Metal Liners.

Temperature Program: 60, hold for 2 min. to 270° C @ 20° C/min.

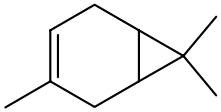

3-Carene (**116**)
$C_{10}H_{16}$
Mol. Wt. = 136.24

$ZnCl_2$	$CuCl_2$	$(Cp)W(CO)_3Cl$	$Br(CO)_5Mn$	$AgClO_4$	$ZrCl_4$	H_2PtCl_6	$RhCl_3$	$RuCl_3$
5.64 min M = 122				N.I. 6.47 min. M = 134	N.R.	N.R.		N.I. 7.69 min. M = 134
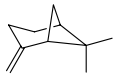 6.43 min M = 136			N.I. 6.84 min. M = 123	N.I. 6.55 min. M = 134				N.I. 7.80 min. M = 136
S.M. 6.70 min.	S.M. 6.80 min.	S.M. 6.84 min.	S.M. 7.10 min.	S.M. 6.81 min.			S. M. 8.11 min.	7.95 min. M = 134.
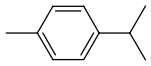 6.86 min. M = 134	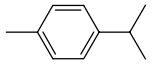 6.86 min. M = 134						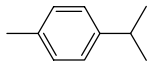 8.16 min. M = 134	S.M. 8.05 min.
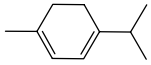 7.43 min M = 136		N.I. 8.86 min. M = 204		N.I. 8.75 min. M = 150			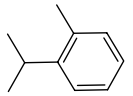 8.22 min. M = 134	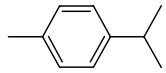 8.16 min. M = 134
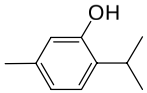 9.17 min M = 150								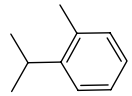 8.22 min. M = 136

S.M. = Starting Material **N.R**. = No Reaction Observed. **N.I.** = Structure Not Identified.

B.3. Observed Product Formation of β-Pinene After Passage Through Modified Metal Liners.

Temperature Program: 60, hold for 2 min. to 270° C @ 20° C/min.

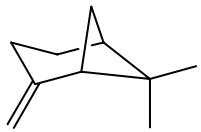

β-Pinene (**117**)
$C_{10}H_{16}$
Mol. Wt.: 136.24

$ZnCl_2$	$CuCl_2$	$(Cp)W(CO)_3Cl$	$Br(CO)_5Mn$	$AgClO_4$	$ZrCl_4$	H_2PtCl_6	$RhCl_3$	$RuCl_3$
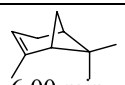 6.00 min M = 136	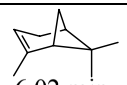 6.02 min M =136	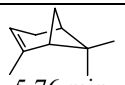 5.76 min M = 136	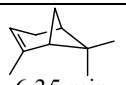 6.35 min M = 136	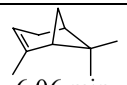 6.06 min M = 136		N.R.	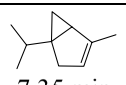 7.35 min M = 136	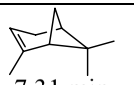 7.31 min M = 136
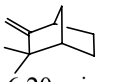 6.20 min M = 136	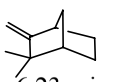 6.23 min M = 136	N.I. 6.08 min M = 136	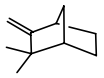 6.56 min M = 136	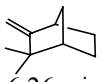 6.26 min M = 136	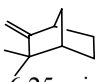 6.25 min M = 136		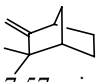 7.57 min M = 136	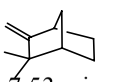 7.53 min M = 136
S.M. 6.47 min	S.M. 6.50 min	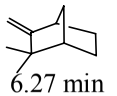 6.27 min M = 136	S.M. 6.82 min	S.M. 6.55 min	S.M. 6.40 min		S.M. 7.85 min	S.M. 7.80 min
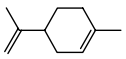 6.95 min. M = 136	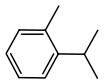 6.91 min M = 134	S.M. 6.55 min	N.I. 7.34 min M = 136	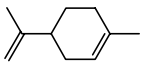 7.03 min M = 136	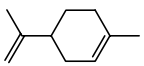 7.00 min M = 136		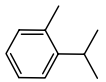 8.22 min M = 134	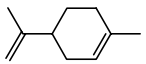 8.22 min M = 136
	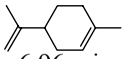 6.96 min M = 136	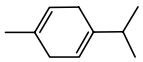 7.04 min M = 136			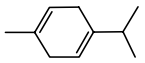 7.59 min M = 136		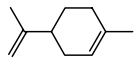 8.67 min M = 136	
	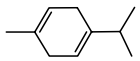 7.20 min M = 136							
	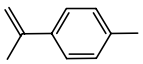 7.54 min M = 136							

S.M. = Starting Material

N.R. = No Reaction Observed.

N.I. = Structure Not Identified.

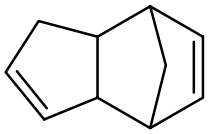

Dicyclopentadiene (**118**)
$C_{10}H_{12}$
Mol. Wt. 132.20

B.4. Observed Product Formation of Dicyclopentadiene After Passage Through Modified Metal Liners.

Temperature Program: 60, hold for 2 min. to 270° C @ 20° C/min.

$ZnCl_2$	$CuCl_2$	$(Cp)W(CO)_3Cl$	$Br(CO)_5Mn$	$AgClO_4$	$ZrCl_4$	H_2PtCl_6	$RhCl_3$	$RuCl_3$
N.R.	S.M. 7.03 min 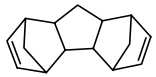 10.95 min M = 198 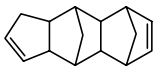 11.21 min M =198 N.I. 12.1 min M = 284	S.M. 7.07 min 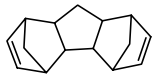 10.99 min M =198 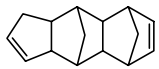 11.25 min M =198	S.M. 7.33 min 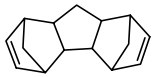 11.23 min M = 198 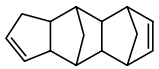 11.49 min M =198	S.M. 7.05 mn 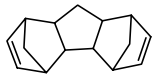 10.96 min M =198 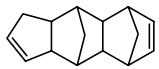 11.22 min M =198	S.M. 7.01 min N.I. 7.44 min M = 132 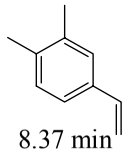 8.37 min M = 132 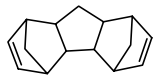 10.99 min M = 198 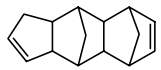 11.28 min M =198	N.R.	N.R.	N.R.

S.M. = Starting Material **N.R**. = No Reaction Observed. **N.I.** = Structure Not Identified.

B.5. Observed Product Formation of Cyclooctene Oxide After Passage Through Modified Metal Liners.
Temperature Program: 60, hold for 2 min. to 270° C @ 20° C/min.

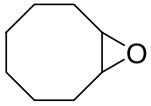 Cyclooctene Oxide (**120**) $C_8H_{14}O$ Mol. Wt.: 126.20	$ZnCl_2$	$CuCl_2$	$(Cp)W(CO)_3Cl$	$Br(CO)_5Mn$	$AgClO_4$	$ZrCl_4$	H_2PtCl_6	$RhCl_3$	$RuCl_3$
	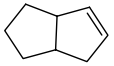 5.18 min M = 108	 4.33 min M = 96	N.I. 5.28 min M =108	N.I. 6.07 min M =108	 5.78 min M = 108	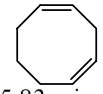 5.83 min M = 108	N.R.	N.R.	N.I. 8.59 min M = 120
	 5.30 min M = 108	 5.64 min M = 110	 5.78 min M =108	S.M. 8.21 min	S.M. 8.01 min	S.M. 6.58 min			N.I. 8.77 min M = 108
	N.I. 5.75 min M = 108	N.I. 7.42 min M = 126	7.38 M = 126			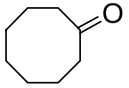 8.03 min M =126			S.M. 9.09 min
	N.I. 7.29 min M = 126	N.I. 7.71 min M = 126	7.59 min M = 108						
	N.I. 7.38 min M = 126	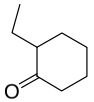 7.80 min M = 126	S.M. 7.38 min						
	N.I. 7.47 min M = 126	N.I. 8.17 min M = 160							

S.M. = Starting Material

N.R. = No Reaction Observe

N.I. = Structure Not Identified.

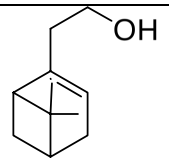

Nopol (**121**)
$C_{11}H_{18}O$
Mol. Wt.: 166.26

B.6. Observed Product Formation of Nopol After Passage Through Modified Metal Liners.

Temperature Program: 60, hold for 2 min. to 270° C @ 20° C/min.

$ZnCl_2$	$CuCl_2$	$(Cp)W(CO)_3Cl$	$Br(CO)_5Mn$	$AgClO_4$	$ZrCl_4$	H_2PtCl_6	$RhCl_3$	$RuCl_3$
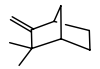 6.19 min M = 136	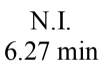 N.I. 6.27 min M = 134	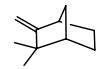 6.28 min M = 136	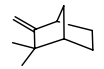 6.82 min M = 136	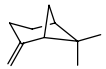 6.55 min M = 136	 6.20 min M =136	N/A	N/A	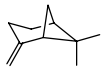 7.80 min M = 136
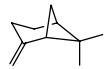 6.48 min M = 136	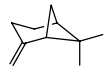 6.53 min M = 136	 7.14 M = 148	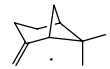 6.82 min M = 136		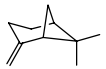 6.59 M = 136			N.I. 9.95 min M = 164
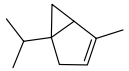 6.97 min M = 136	N.I. 9.15 min M = 168		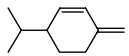 7.32 min M = 136		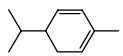 6.84 min M = 136			S.M. 10.44 min
		S.M. 9.16 min	S.M. 9.43 min	S.M. 9.17 min	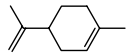 7.00 min M = 136			
					S.M. 8.73 min			

S.M. = Starting Material **N.R**. = No Reaction Observed. **N.I.** = Structure Not Identified.

B.7. Observed Product Formation of 4-*tert*-Butylcyclohexanol After Passage Through Modified Metal Liners.

Temperature Program: 60, hold for 2 min. to 270° C @ 20° C/min.

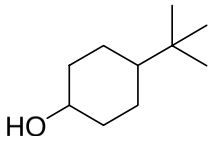

4-tert-Butylcyclohexanol
(**122**)
$C_{10}H_{20}$
Mol. Wt. 156.26

$ZnCl_2$	$CuCl_2$	$(Cp)W(CO)_3Cl$	$Br(CO)_5Mn$	$AgClO_4$	$ZrCl_4$	H_2PtCl_6	$RhCl_3$	$RuCl_3$
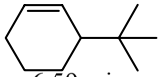 6.59 min M = 138		N.R.	N.R.	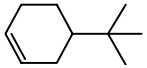 6.81 min M = 138		n/a	n/a	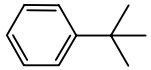 7.94 min M = 134
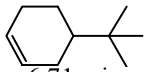 6.71 min M = 138	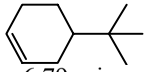 6.79 min. M = 138							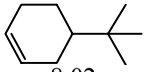 8.02 M = 138
S.M. 8.59 min	S.M. 8.55 min			S.M. 8.71 min				S.M.(*trans*) 9.85 min
				N.I. 11.7 min. M = 204				S.M. (*cis*) 9.96 min
					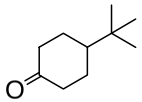 8.82 min M = 154			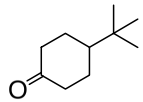 10.1 min M =154

S.M. = Starting Material **N.R**. = No Reaction Observed. **N.I.** = Structure Not Identified.

B.8. Observed Product Formation of 2-Phenylproprionaldehyde After Passage Through Modified Metal Liners.

Temperature Program: 60, hold for 2 min. to 270° C @ 20° C/min.

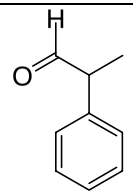

2-Phenylproprionaldehyde
(**123**)
$C_9H_{10}O$
Mol. Wt.: 134.17

S.M. = Starting Material

N.R. = No Reaction Observed.

N.I. = Structure Not Identified.

$ZnCl_2$	$CuCl_2$	$(Cp)W(CO)_3Cl$	$Br(CO)_5Mn$	$AgClO_4$	$ZrCl_4$	H_2PtCl_6	$RhCl_3$	$RuCl_3$
 5.57 min M = 104	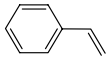 5.74 M = 104	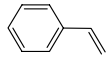 5.71 min M = 104	N.R.	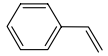 5.63 min M =104	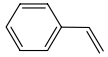 5.67 min M = 104	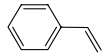 7.14 min M = 104	N/A	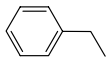 6.54 min M = 106
								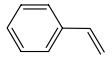 6.89 min M = 104
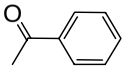 7.33 min M = 120	S.M 7.71 min	S.M. 7.71 min		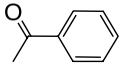 7.40 min M = 120	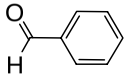 6.47 min M = 106	S.M. 9.18 min		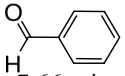 7.66 min M = 106
								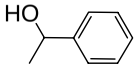 8.60 min M = 122
S.M. 7.66 min	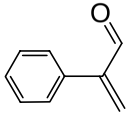 8.20 min M = 132	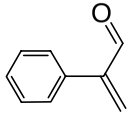 8.22 min M = 132		S.M. 7.73 min	S.M. 7.81 min	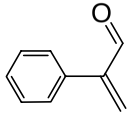 9.64 min M =132		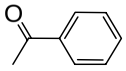 8.67 min M = 120
N.I. 8.22 min M = 134	N.I. 8.49 min M = 168			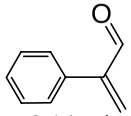 8.14 min M = 132	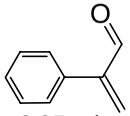 8.27 min M = 132			S.M. 8.99 min

B.9. Observed Product Formation of 2,4,6-Trimethoxybenzaldehyde After Passage Through Modified Metal Liners.

Temperature Program: 60, hold for 2 min. to 270° C @ 20° C/min.

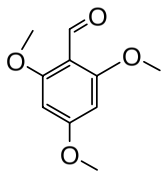 2,4,6-Trimethoxybenzaldehyde (**124**) $C_{10}H_{12}O_4$ Mol. Wt. = 196.20	$ZnCl_2$	$CuCl_2$	$(Cp)W(CO)_3Cl$	$Br(CO)_5Mn$	$AgClO_4$	$ZrCl_4$	H_2PtCl_6	$RhCl_3$	$RuCl_3$
	N.R.	N.R.	N.R.	N.R.	N.R.	N.R.	N.R.	N.R.	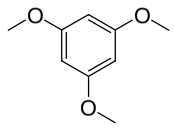 11.21 min M = 168 N.I. 11.91 min M = 221 N.I. 12.33 min. M = 194

S.M. = Starting Material **N.R**. = No Reaction Observed. **N.I.** = Structure Not Identified.

B.10. Observed Product Formation of 4-Pentenoic Acid After Passage Through Modified Metal Liners.

Temperature Program: 60, hold for 2 min. to 270° C @ 20° C/min.

4-Propenoic Acid (**125**) $C_5H_8O_2$ Mol. Wt. 100.12	$ZnCl_2$	$CuCl_2$	$(Cp)W(CO)_3Cl$	$Br(CO)_5Mn$	$AgClO_4$	$ZrCl_4$	H_2PtCl_6	$RhCl_3$	$RuCl_3$
	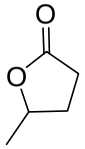 6.53 min M =100	S.M. 5.55 min N.I. 8.34 min M =134	N.R.	N.R.	N.R.	N.R.	N.R.	N.R.	N.R.

S.M. = Starting Material **N.R**. = No Reaction Observed. **N.I.** = Structure Not Identified.

B.11.Observed Product Formation of Methyl Mandelate After Passage Through Modified Metal Liners.

Temperature Program: 60, hold for 2 min. to 270° C @ 20° C/min.

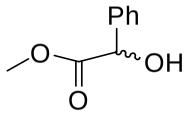

Methyl mandelate
(**126**)
$C_9H_{10}O_3$
Mol. Wt.: 166.18

$ZnCl_2$	$CuCl_2$	$(Cp)W(CO)_3Cl$	$Br(CO)_5Mn$	$AgClO_4$	$ZrCl_4$	H_2PtCl_6	$RhCl_3$	$RuCl_3$
N.R.	N.R.	N.R.	N.R.	N.R.	N.R.	N.R.	N.R.	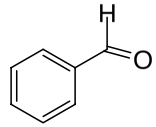 7.60 min M = 106 S.M. 10.4 min

S.M. = Starting Material **N.R**. = No Reaction Observed. **N.I.** = Structure Not Identified.

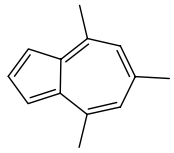

4,6,8–Trimethylazulene
(**119**)
$C_{13}H_{14}$
Mol. Wt. = 170.25

B.12. Observed Product Formation of 4,6,8-Trimethylazulene After Passage Through Modified Metal Liners.

Temperature Program: 60, hold for 2 min. to 270° C @ 20° C/min.

$ZnCl_2$	$CuCl_2$	$(Cp)W(CO)_3Cl$	$Br(CO)_5Mn$	$AgClO_4$	$ZrCl_4$	H_2PtCl_6	$RhCl_3$	$RuCl_3$

No reactivity was observed on any liner.

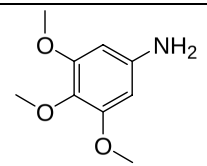

3,4,5-Trimethoxyaniline
(**127**)
$C_9H_{13}NO_3$
Mol. Wt. = 183.20

B.13. Observed Product Formation of 3,4,5-Trimethoxyaniline After Passage Through Modified Metal Liners.

Temperature Program: 60, hold for 2 min. to 270° C @ 20° C/min.

$ZnCl_2$	$CuCl_2$	$(Cp)W(CO)_3Cl$	$Br(CO)_5Mn$	$AgClO_4$	$ZrCl_4$	H_2PtCl_6	$RhCl_3$	$RuCl_3$

No reactivity was observed on any liner.

REFERENCES

1. Vollhardt, K. P. C.; Schore, N. E. *Organic Chemistry: Structure and Function;* W.H. Freeman and Co.: New York, **2003** .

2. Smith, M.; March, J. *March's Advanced Organic Chemistry: Reactions, Mechanisms, and Structure;* Wiley: New York, **2001**.

3. Wan, P.; Muralidharan, S. *J. Am. Chem. Soc.* **1988**, *110*, 4336-4345.

4. Zucco, C.; Lima, C. F.; Rezende, M. C.; Vianna, J. F.; Nome, F. *J. Org. Chem.* **1987**, *52*, 5356-5359.

5. Scharlin, P. *Acta Chemica Scandinavica, Series A: Physical and Inorganic Chemistry* **1987**, *A41*, 480-483.

6. Grob, C. A. *Angew. Chem, Int. Ed. Eng.* **1969**, *8*, 535-546.

7. Bordwell, F. G.; Matthews, W. S.; Vanier, N. R. *J. Am. Chem. Soc.* **1975**, *97*, 442-443.

8. Bordwell, F. G.; Algrim, D. J. *J. Am. Chem. Soc.* **1988**, *110*, 2964-2968.

9. Selikson, S. J.; Watt, D. S. *J. Org. Chem.* **1975**, *40*, 267-268.

10. Ogura, K.; Shimamura, Y.; Fujita, M. *J. Org. Chem.* **1991**, *56*, 2920-2922.

11. Bunnett, J. F.; Hrutfiord, B. F. *J. Org. Chem.* **1962**, *27*, 4152-4156.

12. Adams, R. *Org. React.* **1942**, *10*, 187.

13. Bordwell, F. G.; Bares, J. E.; Bartmess, J. E.; McCollum, G. J.; Van der Puy, M.; Vanier, N. R.; Matthews, W. S. *J. Org. Chem.* **1977**, *42*, 321-325.

14. Mullay, J. *J. Am. Chem. Soc.* **1985**, *107*, 7271-7275.

15. Benkeser, R. A.; Siklosi, M. P.; Mozdzen, E. C. *J. Am. Chem. Soc.* **1978**, *100*, 2134-2139.

16. Kemp, D. S.; Paul. K. *J. Am. Chem. Soc.* **1970**, *92*, 2553-2554.

17. Kemp, D. S.; Paul, K. G. *J. Am. Chem. Soc.* **1975**, *97*, 7305-7312.

18. Kemp, D. S.; Cox, D. D.; Paul, K. G. *J. Am. Chem. Soc.* **1975**, *97*, 7312-7318.

19. Buncel, E.; Venkatachalam, T. K.; Menon, B. C. *J. Org. Chem.* **1984**, *49*, 413-417.

20. Terrier, F.; Xie, H. Q.; Farrell, P. G. *J. Org. Chem.* **1990**, *55*, 2610-2616.

21. Wierenga, W.; Skulnick, H. I. *J. Org. Chem.* **1979**, *44*, 310-311.

22. Gordon, A. J.; Ford, R. A. *The Chemist's Companion: A Handbook of Practical Data, Techniques, and References;* John Wiley & Sons, Inc.: New York, **1972**.

23. Havens, S. J.; Hergenrother, P. M. *J. Org. Chem.* **1985**, *50*, 1763-1765.

24. Gustafson, D. H.; Erman, W. F. *J. Org. Chem.* **1965**, *30*, 1665-1666.

25. Weygand, F.; Daniel, H. *Chem. Ber.* **1961**, *94*, 1688-1692.

26. Weygand, F.; Daniel, H. *Chem. Ber.* **1961**, *94*, 3145-3146.

27. Eisele, W.; Grob, C. A.; Renk, E. *Tetrahedron Lett.* **1963**, 75-76.

28. McCreary, M. D.; Lewis, D. W.; Wernick, D. L.; Whitesides, G. M. *J. Am. Chem. Soc.* **1974**, *96*, 1038-1054.

29. Arnett, E. M.; Small, L. E.; McIver, R. T., Jr.; Miller, J. S. *J. Org. Chem.* **1978**, *43*, 815-817.

30. Artamkina, G. A.; Beletskaya, I. P. *Usp. Khim.* **1987**, *56*, 1717-1752.

31. Zook, H. D.; March, J.; Smith, D. F. *J. Am. Chem. Soc.* **1959**, *81*, 1617-1620.

32. Exner, J. H.; Steiner, E. C. *J. Am. Chem. Soc.* **1974**, *96*, 1782-1787.

33. Lomas, J. S.; Dubois, J. E. *J. Org. Chem.* **1984**, *49*, 2067-2069.

34.Garner, C. M.; Terech, P.; Allegraud, J.; Mistrot, B.; Nguyen, P.; de Geyer, A.; Rivera, D. *J. Chem. Soc., Faraday Trans.* **1998**, *94*, 2173-2179.

35. Garner, C. M. *Techniques and Experiments for Advanced Organic Laboratory;* John Wiley & Sons, Inc.: New York, **1997**.

36. Kokes, R. J.; Tobin, H., Jr.; Emmett, P. H. *J. Am. Chem. Soc.* **1955**, *77*, 5860-5862.

37. Hall, W. K.; Emmett, P. H. *J. Am. Chem. Soc.* **1957**, *79*, 2091-2093.

38. Schiffino, R. S.; Merrill, R. P. *J. Phys. Chem.* **1993**, *97*, 6425-6435.

39. Skrdla, P. J.; Robertson, R. T. *J. Mol. Catal. A:* **2003**, *194*, 255-265.